The Circadian Control of Host Response and Parasite Growth in a Mouse Model of Malaria

Priscilla Carvalho Cabral

Department of Microbiology & Immunology

McGill University, Montreal

August 2023

A thesis submitted to McGill University in partial fulfillment of the requirements of the degree of Doctor of Philosophy.

"A vida me ensinou a nunca desistir

Nem ganhar, nem perder mas procurar evoluir

Podem me tirar tudo que tenho

Só não podem me tirar as coisas boas que eu já fiz pra quem eu amo

E eu sou feliz e canto e o universo é uma canção

E eu vou que vou

História, nossas histórias

Dias de luta, dias de gloria"

-Charlie Brown Jr (*in memoriam*)

Table of Contents

Abstract 5

Resumé 7

Acknowledgments 9

List of Figures and Tables 12

List of abbreviations 15

Contribution to original knowledge 23

Contribution of authors 25

Chapter 1: Introduction 27

1.1. Malaria 27

1.1.1. Malaria distribution and transmission 27

1.1.2. Malaria intra-erythrocytic cycle 30

1.1.3. Malaria paroxysms and immune responses 34

1.1.4. Innate immune response to *Plasmodium spp*. derived molecules 41

1.1.5. Linking malaria tissue-pathology and the immune system 47

1.1.6. Mouse models of malaria 49

1.1.7. Human vs murine models: Insights for malaria studies 51

1.2. Circadian Rhythms 54

1.2.1. The circadian clock 54

1.2.2. Circadian clock in immunity 56

1.2.3. Circadian misalignment and pathogenesis 59

1.2.4. Circadian clock in host-pathogen interactions 63

1.2.5. Circadian rhythms during *Plasmodium spp.* infection 65

1.3. Rationale and objectives of the thesis 69

Chapter 2: Circadian Control of Macrophage Response to *Plasmodium spp.*-Infected Erythrocytes 71

2.1. Abstract 72

2.2. Introduction 73

2.3. Materials and Methods 75

2.4. Results 82

2.5. Discussion 87

2.6. Acknowledgments 93

2.7. Figures 94

2.8. Supplementary Materials 111

Preface to Chapter 3 115

Chapter 3: Time of Day and Circadian Disruption Influence Host Response and Parasite Growth in a Mouse Model of Cerebral Malaria 118

3.1. Abstract 119

3.2. Introduction 120

3.3. Materials and Methods 123

3.4. Results 129

3.5. Discussion 136

3.6. Acknowledgements 142

3.7. Figures 143

3.8. Supplementary Materials 163

Chapter 4: General Discussion and Conclusions 175

4.1. Specific considerations 175

4.2. Working model, future directions and implications 190

4.3. Final Conclusion 199

References 201

Copyright 228

Abstract

Over the past years, circadian rhythms in immune responses have been widely reported, along with a recent discovery of an endogenous circadian clock. In the context of parasitic infections, 24-h oscillations in cell response can have major implications for disease progression and severity. One example is during malaria pathogenesis, where the synchronized rupture of infected red blood cells with *Plasmodium spp.* parasite leads to a pro-inflammatory response, characterized by fevers peaking as multiples of 24 h. Although rhythms in malaria fevers have been known since the 5th century BC, only recently mechanisms for rhythms in malaria have started to be further investigated. In my Ph.D. thesis, we have focused on identifying the role of circadian clocks and host circadian rhythms in the response against malaria.

In the first part of my Ph.D., we developed a model to simulate the synchronized encounter of ruptured *P. berghei* ANKA-infected red blood cells with macrophages. To assess the role of the macrophage's circadian clock in this response, cells were stimulated at 4 different time points over 24 h. We found that reactive oxygen species generation is affected by the time of stimulation, and that cytokine/chemokine response is rhythmic. We also detected changes at the cell proteome and phosphoproteome in response to our stimulation and dependent on time points.

In the second part of my Ph.D., after confirming that host circadian clocks are important in leading rhythms in response to malaria, we tested whether host rhythms can also play a role during mouse infection. By using a mouse model of experimental cerebral malaria, we infected mice at 4 different time points over 24 h (ZT 1, 7, 13, and 19) with *P. berghei* ANKA and evaluated host response and disease progression. Parasite growth was demonstrated to be strongly affected by time of infection, with impairments for ZT19-infected mice. Along with this finding and aligned

with our hypothesis, at ZT19, we detected a lower frequency of red blood cells, in particular immature forms.

Finally, in the third part of my Ph.D., after confirming that time and host circadian rhythms affected malaria pathogenesis, we explored the consequences of host circadian misalignment in the same model. As a result, impaired parasite growth and lack of parasite rhythmicity were seen in these mice. Furthermore, we showed that rhythms in parasite load are dependent of host plasma glucose: animals subjected to time-restricted feeding or sucrose administration displayed abolished parasite load rhythms.

Altogether, my Ph.D. work showed for the first time the rhythmic response of macrophages upon presentation of infected red blood cells, and that time of infection and circadian disruption affected parasite growth and disease progression in mice. This study highlighted parasite dependency on host circadian rhythms and proposes the latter as a potential new therapeutical tool to control malaria pathogenesis. A further understanding of the interaction between host clocks and the parasite can help to not only predict the peaks of malaria-immune responses but also control parasite growth.

Keywords: Malaria, circadian rhythms, macrophages, time of infection, circadian disruption, glucose

Resumé

Durant les dernières années, des rythmes circadiens de réponses immunitaires ont été largement rapportés, ainsi qu'une découverte récente d'une horloge circadienne endogène. Dans le cadre des infections parasitaires, les oscillations sur 24 h de la réponse des cellules immunitaires peuvent avoir des implications majeures sur la progression et la gravité de la maladie. Un exemple est durant la pathogenèse du paludisme, où la rupture synchronisée des globules rouges infectés avec le parasite *Plasmodium spp*. conduit à une réponse pro-inflammatoire caractérisée par des fièvres culminant en multiples de 24 h. Bien que les rythmes des fièvres paludéennes soient connus depuis le 5ème siècle avant JC, ce n'est que récemment que les mécanismes des rythmes du paludisme ont commencé à être plus étudiés. Au cours de mon doctorat, nous nous sommes concentrés sur l'identification du rôle des horloges circadiennes et des rythmes circadiens de l'hôte dans la réponse contre le paludisme.

Dans la première partie de mon étude, nous avons développé un modèle pour simuler la rencontre synchronisée de globules rouges infectés rompus avec des macrophages. Pour évaluer le rôle de l'horloge circadienne du macrophage dans cette réponse, les cellules ont été stimulées à 4 moments différents sur 24 h. Nous avons constaté que la génération d'espèces réactives de l'oxygène était affectée par le temps de stimulation et que la réponse cytokine/chimiokine était rythmique. Nous avons également détecté des changements au niveau du protéome cellulaire et phosphoprotéome en réponse à notre stimulation et en fonction des repères temporels.

Dans la deuxième partie de mon projet, après avoir confirmé que les horloges circadiennes de l'hôte étaient importantes pour diriger les rythmes de réponse au paludisme, nous avons testé si les rythmes de l'hôte peuvent aussi jouer un rôle lors de l'infection des souris. En utilisant un modèle murin de neuropaludisme, nous avons infecté des souris à 4 moments différents sur 24 h (ZT 1, 7,

13 et 19) et évalué la réponse de l'hôte et la progression de la maladie. Il a été démontré que la croissance du parasite était fortement affectée par le moment de l'infection, avec des déficiences pour les souris infectées à ZT19. Parallèlement à ce constat et en accord avec notre hypothèse, à ZT19, nous avons détecté une fréquence plus faible de globules rouges, en particulier des formes immatures.

Enfin, dans la troisième partie de mon étude, après avoir confirmé que le temps et les rythmes circadiens de l'hôte affectaient la pathogenèse du paludisme, nous avons exploré les conséquences du désalignement circadien de l'hôte dans le même modèle. En conséquence, une croissance parasitaire altérée et un manque de rythmicité parasitaire ont été observés chez ces souris. De plus, nous avons montré que les rythmes de la charge parasitaire dépendent du glucose plasmatique de l'hôte: les animaux soumis à une alimentation limitée dans le temps ou à une administration de sucrose présentaient une abolition des rythmes de charge parasitaire.

En conclusion, les travaux réalisés pendant mon doctorat ont montré pour la première fois la réponse rythmique des macrophages lors de la présentation de globules rouges infectés et que le moment de l'infection et la perturbation circadienne affectent la croissance du parasite et la progression de la maladie chez les souris. Cette étude a mis en évidence la dépendance du parasite aux rythmes circadiens de l'hôte et propose ce dernier comme un nouvel outil thérapeutique potentiel pour contrôler la pathogenèse du paludisme. Une meilleure compréhension de l'interaction entre les horloges de l'hôte et le parasite peut aider non seulement à prédire les pics de réponses immunitaires contre le paludisme, mais également à contrôler la croissance du parasite.

Mots-clés: Paludisme, rythmes circadiens, macrophages, moment de l'infection, perturbation circadienne, glucose

Acknowledgments

About 5.5 years ago, I turned a new chapter in my life, which was by far the biggest change (and challenge!) I have ever experienced. Moving abroad, diving into a new research field, starting a Ph.D! I know I could not have done without the immense support and sacrifice of so many involved.

First, I am truly grateful for the opportunity given to join the lab and conduct such an exciting project. So, for that, I thank my supervisors, Dr. Nicolas Cermakian and Dr. Martin Olivier for trusting me with this project, for all the guidance, discussions, feedbacks – by which have all made me grown as a person and as a researcher. Thank you, Nico, for allowing me to publish my first review article (and my first research article, soon to be published!).

Thank you to all members of the Cermakian and Olivier's lab for their friendship, help and feedbacks. Special thanks to Sophia Stegeman, who has become such a dear friend to me. It was such a great time sharing the bench with you, all the middle-of-the night time points and long hours at the imagining flow cytometer. Time flew by, and it meant a lot having your support and friendship. Special thanks to Tara Delorme and Shashank Srikanta for your friendship, feedbacks and help. You both made the lab a fun environment to work with! Thank you, Marie-Ève, for all your help at the confocal and great moments. I would also like to thank Caroline Martel for the help during my initial months of the Ph.D, by teaching me techniques, sharing protocols, giving me assistance. Thank you, Fiorella Vialard for all the discussions and protocol sharing.

Also, thank you to my both MIMM honours students (Shivali Sood and Joelle Weinerman) who contributed so much for this project! It was a pleasure having you as my mentee and I appreciate all the work you have put into it. I must also acknowledge all the Douglas Animal Facility staff, with special considerations to Guylaine Gadoury, Tara Thomson and Jessica Balbin,

for helping me so many times that I have lost count. I could not have done it without you. Special thanks to the Immunophenotyping Platform (MUHC) staff (Marie-Hélène Lacombe, Hélène and Ekaterina) for all your help, feedback and troubleshooting.

Thank you to all the members of my Ph.D. Advisory Committee (Dr. Petronela Ancuta and Dr. Momar Ndao) for your time, and all the guidance/feedback over the years.

Thank you to the whole MIMM Department for all the assistance, support and fellowships. To Fonds de Recherche du Québec - Santé (FRQS) and Faculty of Medicine (McGill) for the scholarship awards.

Thank you to Mervyn Mojica and Dr. Momar Ndao for giving me the opportunity to act for almost 2 years as the Student Representative of the Glen Facility Animal Care Committee (FACC) of the RI MUHC. I have learned so much and I had enjoyed being part of the team and contributing to the great work!

I must also thank from the bottom of my heart my husband, Mike, and my dear parents. You have all done incredible sacrifices to allow me to follow my dream and pursue this Ph.D. I will never be able to thank you enough and your support was everything to me. Mom and dad, you are my biggest inspirations, and I am the luckiest person to have such loving parents and strong pillar of support. I cannot thank you enough.

Thank you to all my dear friends and relatives who has always encouraged me to keep going. I must also thank my dog, Max, for being the most loving and affectionate dog I could have ever asked. He is not only my fur baby, but he is my emotional rock.

Lastly, but not least, thank you to all the mice and for their gigantic contribution to research. No research can be done without them, and science will always own them a great debt.

To wrap up, the road has been bumpy, but each and every one of you had a special role in my journey and this has helped me to become the person I am today. For that, I am grateful, and I dedicate this thesis to you all.

List of Figures and Tables

Chapter 1:

Table 1: Breakdown of malaria cases in 2021. 28

Figure 1: Intracellular signaling pathways triggered by Hz……45

Chapter 2:

Figure 1. Lysed infected RBCs, but not intact cells, leads to macrophage proinflammatory response..... 95

Figure 2. Circadian regulation of macrophage proinflammatory response. 98

Figure 3. Lysed infected RBCs leads to generation of reactive oxygen species in a time-dependent manner in macrophages. 100

Figure 4. Changes in proteome and phosphoproteome upon stimulation with lysed infected RBCs at different circadian time-points. 102

Table 1. Analysis of BMDM phosphoproteome following infected RBCs stimulation. 105

Figure 5. Enriched pathways on the proteome and phosphoproteome upon stimulation with lysed infected RBCs at different circadian time-points..... 107

Figure 6. Graphical summary of key pathways and their players detected at the proteome and phosphoproteome of macrophages stimulated with lysed infected RBCs in a time-dependent manner..... 108

Figure 7. Phosphorylation of ERK is not affected, in a time-dependent way, by lysed infected RBCs stimulation in macrophages. 109

Table S1. List of primers used on the RT-qPCR run of BMDM stimulated samples…….111

Figure S1. Proteome and phosphoproteome sample analysis……...…112

Figure S2. Phosphorylation status on BMDMs stimulated with lysed infected RBCs at 22 h or 34 h post-synchronization…….113

Figure S3. Phosphorylation of ERK measured after a time course stimulation of BMDMs with lysed infected RBCs…….114

Chapter 3:

Figure 1. Host survival and sickness behavior in response to *Plasmodium berghei ANKA* infection. 144

Figure 2. Host immune response to *Plasmodium berghei ANKA* is affected by the time of infection. 146

Figure 3. Parasite growth is affected by the time of infection. 147

Figure 4. Time-of-day variation in immune cells and erythrocyte subsets..... 150

Figure 5. ZT19-infected mice have fewer infected cells. 152

Figure 6. The spleen is a more parasitized target with a preference for reticulocyte invasion similar in both ZT7 and ZT19 groups. 153

Figure 7. Circadian disruption affects parasite growth and number of parasites per cell..... 156

Figure 8. Rhythms in blood parasite load and plasma glucose are disrupted in jet lag mice. ... 158

Figure 9. Rhythms in glucose and blood parasite load are disrupted following time-restricted feeding in infected mice. 160

Figure 10. Rhythms in glucose and blood parasite load are affected by sucrose administration in infected mice. 162

Figure S1. Blood-brain barrier integrity assessment……163

Figure S2. Flow cytometry gating strategy for erythrocyte subsets, and infected cells. 165

Figure S3. "Short" circadian disruption protocol does not affect host survival or parasite growth. 166

Figure S4. An acute circadian disruption protocol does not affect host survival or parasite growth. 168

Figure S5. Long-term circadian disruption protocol impacts parasite growth in Plasmodium chabaudi infected mice. 169

Figure S6. Long-term circadian disruption protocol does not affect host survival. 171

Figure S7. "Long-term" circadian disruption protocol does not affect host immune responses….. 172

Figure S8. Parasite growth, but not host response, is reduced in circadian clock mutant mice. 173

Chapter 4:

Figure 1. Working model under homeostatic conditions. 191

Figure 2. Working model under circadian disruption conditions. 192

List of abbreviations

AGPAT5: 1-Acylglycerol-3-Phosphate O-Acyltransferase 5

AKT: Protein kinase B

ASC: Apoptosis-associated speck-like protein containing a CARD

BMAL1: Bone and muscle ARNT-like 1

BMDM: Bone marrow-derived macrophages

CCGs: Clock-controlled genes

CCL5: C-C Motif chemokine ligand 5

CCR2: C-C chemokine receptor type 2

CCR5: C-C chemokine receptor type 5

CLOCK: Clock circadian regulator

Col1a1: Collagen Type I α 1

CR1: Complement receptor 1

CRY: Cryptochrome

CSAD: Cysteine Sulfinic Acid Decarboxylase

CT: Circadian time

CX3CR1: C-X3-C Motif chemokine receptor 1

CXCL1: C-X-C Motif chemokine ligand 1

CXCL10: C-X-C Motif ligand 10

CXCL11: C-X-C Motif ligand 11

CXCL12: C-X-C Motif chemokine 12

CXCL5: C-X-C Motif chemokine ligand 5

CXCL9: C-X-C Motif ligand 9

CXCR3: C-X-C Motif chemokine receptor 3

DAMPs: Damage-associate molecular patterns

DARC: Duffy antigen/receptor for chemokines

DD: Constant darkness

DNA: Deoxyribonucleic acid

DPBS: Dulbecco's phosphate-buffered saline

DTT: Dithiothreitol

EB: Evans blue

ECM: Experimental cerebral malaria

Epo: Erythropoietin

ERKs: Extracellular signal-regulated kinases

FSC: Forward scatter

GBγ: G protein subunit γ 14

GFP: Green fluorescent protein

GM-CSF: Granulocyte-macrophage colony-stimulating factor

GPI: Glycosylphosphatidylinositol

HRP: Horseadish peroxidase

HSCs: Hematopoeitic stem cells

Hsp70: Heat shock protein 70

HSPCs: Hematopoietic stem and progenitor cells

Hz: Haemozoin

IκBα: NFKB inhibitor α

ICAM-1: Intercellular adhesion molecule 1

IFN: Interferon

IFNγ: Interferon γ

IFNAR1: Interferon α and β receptor subunit 1

IL-1: Interleukin 1

IL-1β: Interleukin 1 β

IL-10: Interleukin 10

IL-12: Interleukin 12

IL-12p40: Interleukin 12 subunit β

IL-12p70: Interleukin-12p70

IL-13: Interleukin 13

IL-18: Interleukin 18

IL-27: Interleukin 27

IL-4: Interleukin 4

IL-6: Interleukin 6

IMAC: Immobilized metal affinity chromatography

iNOS: Inducible nitric oxide synthase

IPA: Ingenuity Pathway Analysis

iRBCs: *Plasmodium berghei ANKA*-infected red blood cells

IRF3: Interferon Regulatory Factor 3

Itgb5: Integrin β 5

JNK: c-Jun N-terminal kinase

KEGG: Kyoto encyclopedia of genes and genomes

KO: Knockout

KRAS: Kirsten rat sarcoma viral oncogene homolog

LC-MS: Liquid Chromatography with tandem mass spectrometry

LCCM: L cell conditioned medium

LD: Light-dark

LL: Constant light

LPS: *E. coli* lipopolysaccharide

Lyn: LYN proto-oncogene

MAHRP1: Membrane-associated histidine-rich protein 1

MAKI: Malaria acute kidney injury

MAP: Mitogen-activated protein

MAPK: MAP kinase pathway

Mapk3k20: Mixed lineage kinase 7

MAPKAPK-2: MAPK activated protein kinase 2

MCP-1/CCL2: Monocyte chemoattractant protein-1 / C-C Motif chemokine ligand 2

MDF10: Mouse Cytokine Proinflammatory Focused 10-Plex Discovery Assay Array

MHC: Major histocompatibility complex

MIP-1α/CCL3: Macrophage Inflammatory Protein-1 α / C-C Motif chemokine ligand 3

MIP-1β/CCL4: Macrophage Inflammatory Protein-1 β / C-C Motif chemokine ligand 4

MIP-2/CXCL2: Macrophage Inflammatory Protein-2 / Chemokine (C-X-C motif) ligand 2

MKK3: Mitogen-activated protein kinase kinase 3

MKK4: Mitogen-activated protein kinase kinase 4

MO-DCs: Monocyte-derived dendritic cells

MRI: Magnetic resonance imaging

mRNA: Messenger ribonucleic acid

MSP1: Merozoite surface protein 1

MSU: Monosodium urate

mTOR: Mammalian target of rapamycin

NADPH: Nicotinamide adenine dinucleotide phosphate

NF-κB: Nuclear factor κ-light-chain-enhancer of activated B cells

nHz: Native haemozoin

NK cells: Natural killer cells

NLR: Nod-like receptor

NLRP3: NLR family pyrin domain containing 3

NLRP4: NLR family pyrin domain containing 4

NO: Nitric Oxide

NOX: NADPH oxidase

NRF2: Nuclear factor erythroid 2-related factor 2

ns = Not significant

PbA: *Plasmodium berghei ANKA*

PBMCs: Peripheral blood nuclear cells

PBS: Phosphate-buffered saline

PECs: Peritoneal exudate cells

PER: Period

PFA: Paraformaldehyde

PfEMP1: *Plasmodium falciparum* erythrocyte membrane protein 1

PfHT: *Plasmodium* hexose transporter

PfNT1: *Plasmodium falciparum* nucleoside transporter 1

PI3K: Phosphoinositide 3-kinase

PKC: Protein kinase C

PMA: Phorbol myristate acetate

PMS-F: Phenylmethylsulfonyl fluoride

pSer: Serine phosphorylation

pThr: Threonine phosphorylation

pTyr: Tyr phosphorylation

Rap1a: Ras-related protein Rap-1a

RBCs: Red blood cells

RELA: V-Rel Avian Reticuloendotheliosis Viral Oncogene Homolog A

REML: Restricted maximum likehood

REV-ERB: Reverse erythroblastosis virus proteins

RIPA buffer: Radioimmunoprecipitation assay buffer

RLU/s: Relative light unis per second

RMCBS: Rapid Murine Coma and Behavior Scale

RNA-seq: RNA sequencing

RNA: Ribonucleic acid

ROCK2: Rho associated coiled-coil containing protein kinase 2

ROR: RAR-related orphan receptors

RORE: ROR response elements

ROS: Reactive oxygen species

RPMI: Roswell Park Memorial Institute

RT-qPCR: Reverse transcription quantitative polymerase chain reaction

SBP1: Skeleton-binding protein 1

SCN: Suprachiasmatic nuclei

SEM: Standard deviation error

sHz: Synthetic haemozoin

SiO2: Silicon dioxide

SMAC: Schizont membrane-associated cytoadherence protein

SOD: Superoxide dismutase

SPECT: Sporozoite microneme protein

SPECT2: Perforin-like protein 1

Src: Proto-oncogene c-Src

SSC: Side scatter

Syk: Spleen tyrosine kinase

TGFβ: Transforming growth factor-β

Th1: T helper 1 subtype

Th2: T helper 2 subtype

TLR-1-2: Toll-like receptor 1-2

TLR-2-6: Toll-like receptor 2-6

TLR-4: Toll-like receptor 4

TLR-9: Toll-like receptor 9

TLR: Toll-like receptor

TNFα: Tumor necrosis factor α

TNFRII: Soluble tumor necrosis factor receptor II

Vps15: Phosphoinositide-3-Kinase regulatory subunit 4

w/v: Weight/Volume

WHO: World Health Organization

WT: Wild type

ZT: *Zeitgeber*

Contribution to original knowledge

The key findings and achievements of this thesis are summarized below.

Chapter 2:

1. Development of a unique *ex-vivo* macrophage-*Plasmodium spp*-infected red blood cells stimulation model to study host circadian clocks and immune responses in a context of malaria.
2. Identification of rhythms in immune response (cytokine/chemokine and ROS) following macrophage stimulation with *Plasmodium spp*-infected red blood cells.
3. Discovery of macrophage's intracellular signaling pathways influenced by stimulation with *Plasmodium spp*-infected red blood cells in a circadian-dependent way.

Chapter 3:

1. Detection of time-of-infection effects on disease progression and parasite growth, in a mouse model of cerebral malaria.
2. Identification of time variations in erythrocyte abundance and their subsets (blood and spleen) in infected and non-infected mice.
3. Execution of different circadian disruption protocols to measure the effects on host response and disease progression.
4. Identification of chronic circadian disruption as a disruptive factor for parasite growth and rhythmicity.
5. Discovery of parasite load rhythmicity in the model of *Plasmodium berghei ANKA* infection.
6. Evaluation of host metabolism disruption and its effects on parasite rhythmicity.

Publications:

1. First author of a review article on circadian rhythms in immunity and parasitic infections, published in Parasite Immunology (2022).

   Carvalho Cabral, P., Tekade, K.; Stegeman, S.; Olivier, M.; Cermakian, N. The involvement of host circadian clocks in the regulation of the immune response to parasitic infections in mammals. Parasite Immunology. 44(3):e12903. (2022) doi: 10.1111/pim.12903

2. First author of a review article on circadian rhythms and parasitic infections, published in Frontiers in Cellular and Infection Microbiology (2019).

   Carvalho Cabral, P., Olivier, M., Cermakian, N. The Complex Interplay of Parasites, their Hosts and Circadian Clocks. Frontiers Cellular and Infection Microbiology. 12;9:425. (2019) doi: 10.3389/fcimb.2019.00425

3. First author of the manuscript "Circadian Control of Macrophage Response to *Plasmodium spp*.-Infected Erythrocytes". To be submitted in the fall 2023.

4. First author of the manuscript "Time of Day and Circadian Disruption Influence Host Response and Parasite Growth in a Mouse Model of Cerebral Malaria". To be submitted in the fall 2023.

Publication not part of the presented thesis:

1. First author, with shared co-authorship with Sophia Stegeman, of the manuscript "Macrophage's Circadian Rhythms Control Leishmaniasis Parasite Internalization". To be submitted in the fall 2023.

Contribution of authors

Chapter 2:

Priscilla Carvalho Cabral (P.C.C.) was responsible for the development and optimization of the model, including the generation of iRBCs, extraction and culture of cells, and stimulation of macrophages. The experimental design, execution of immunoassays, and data acquisition with analyses were carried out by P.C.C. Manuscript writing, editing and formatting were performed by P.C.C.

Protein quantification by multiplex-array was executed by Eve Technologies.

Acquisition of confocal images was performed with assistance from Marie-Ève Cloutier.

Shivali Sood provided assistance with immunoblotting troubleshooting.

Sophia Stegeman provided assistance with extraction and culture of cells.

Vincent Richard was responsible for protein sample processing and phospho enrichment, LC-MS/MS data acquisition and analysis. Additional analyses were performed by P.C.C.

Nicolas Cermakian participated in experimental discussions, funding acquisition, supervision, manuscript revision and writing. Martin Olivier participated in experimental discussions, supervision and manuscript revision.

Chapter 3:

P.C.C. was responsible for the all the experimental design and plan, as well as data acquisition and analyses. P.C.C. executed the infections, mouse manipulation, ECM assessment, protocol administration, tissue harvesting/blood sampling, microscopy analysis, flow cytometry staining, acquisition and analysis, bioluminescence assays. Manuscript writing, editing and formatting were performed by P.C.C.

Protein quantification by multiplex-array was executed by Eve Technologies.

Joelle Weinerman provided assistance by executing blood sampling/tissue harvesting, bioluminescence assays, ECM assessment and microscopy quantification.

Marie-Ève Cloutier perfused all mice for organs sequestration experiment.

Nicolas Cermakian participated in experimental discussions, funding acquisition, supervision, manuscript revision and writing. Martin Olivier participated in experimental discussions, supervision and manuscript revision.

Chapter 1: Introduction

1.1. Malaria

Malaria is a serious endemic disease, which is responsible for hundreds of millions of cases, and approximately 500 thousand deaths every year [1]. Malaria is caused by *Plasmodium spp.* parasite, and when inside the mammalian host, they are known to induce intense immune activation, which involves both the innate and adaptive branches of the immune system. As a direct consequence, morbidity and lethality are not uncommon to be found in malaria-affected individuals [2, 3]. Nevertheless, the understanding of malaria pathogenesis is strongly dependent on lab research and in particular, the use of murine models. As much as these models carry their own individual limitations and have an intrinsic lack of being a full representation of human pathogenesis [4], they are still strong allies, and much of the knowledge acquired through the years which helped the development of targeted therapies, are due to them [5-8]. Herein we will discuss malaria pathogenesis, immunity, and the use of murine models in detail.

1.1.1. Malaria distribution and transmission

Plasmodium spp. is a eukaryotic parasitic member of the *Apicomplexa* phylum and the causative agent of malaria disease. Only in 2021, the parasite was responsible for 247 million cases of malaria in 84 countries, according to the most updated report issued in 2022 by the World Health Organization [1]. The yearly tracking of the disease progression indicates that malaria cases have been increasing since 2016, despite data collection from the period of 2020-2021 faced service disruption during the COVID-19 pandemic. The cases number increase came mostly from

countries in the African Region displaying 234 million cases in 2021, where 4 countries were responsible for almost half of all cases: Nigeria (26.6%), the Democratic Republic of the Congo (12.3%), Uganda (5.1%) and Mozambique (4.1%), and accounted for just over half of malaria deaths globally. Despite the increase in cases, malaria death numbers have reduced since 2000. The breakdown of endemic regions in 2021, according to the WHO Report 2022, is demonstrated in Table 1.

Table 1: Breakdown of malaria cases in 2021.

Source: World Health Organization, World Malaria Report 2022.

WHO Region	Number of cases in 2021	Countries with the majority of cases
African	234 million	Nigeria Democratic Republic of the Congo
South-East Asia	5.4 million	India Indonesia
Eastern Mediterranean	6.2 million	Sudan Somalia
Western Pacific Region	1.4 million	Papua New Guinea Solomon Island
Americas	0.6 million	Bolivarian Republic of Venezuela Brazil

The human malaria disease can be caused by one of 5 *Plasmodium spp.* species which are all transmitted through the bite of the female *Anopheles* mosquito. Notably, mixed infections are not uncommon in endemic areas [9]. Nevertheless, epidemiological and evolutionary studies report species distribution around the globe as being dependent on parasite tropism and ethnicity of the

individual. For instance, from the pool of species that are pathogenic to humans, given the parasite's preference for tropical and temperate areas, *Plasmodium vivax* is more often found in Southeast Asia, Ethiopia, and South America. Moreover, parasite invasion of host blood cells requires Duffy antigen expression, which is limited in African populations [10]. Importantly, the majority of malaria mortality cases are attributed to *Plasmodium falciparum* as it causes severe complications, especially in young children, and has a wide distribution in the African continent. Milder infections are found with *Plasmodium ovale*, still with approximately an 8-time-fold preference for infecting young children as opposed to adults, but fever episodes are low and most infections carry as asymptomatic [11]. Still, on the mild severity side, *Plasmodium malarie* is known to cause a less virulent pathology but reports indicated that in the long term, chronic infections can occur with reoccurrence after decades of exposure. In older children, chronic nephrotic syndrome has been reported [12]. The last *Plasmodium spp.* species known to be infectious to humans is *Plasmodium knowlesi.* Human infection with this species requires transmission from a mosquito that had previously been fed from an infected rhesus monkey. Although this species has a limited distribution around the globe (initially identified in the Malaysian Borneo), there are recent reports on disease migration to other regions surrounding Singapore, Cambodia, and more [13].

The malaria transmission cycle initiates with *Anopheles* bite and inoculation of sporozoites form of the parasite. This stage form enters the bloodstream and establishes infection within hepatocytes. Parasite entrance in these cells requires a sophisticated mechanism evading immune cells, more specifically liver macrophages, also denominated Kupffer cells. Several sporozoites proteins, such as sporozoite microneme protein (SPECT) and perforin-like protein 1 (SPECT2) play a role in such process, yet not all of them have their functionally well understood [14]. Within

the liver, parasite maturation occurs in a process that takes 2-10 days, culminating in the release of approximately 30,000-40,000 merozoites per hepatocyte. Importantly, infections with *Plasmodium vivax* and/or *Plasmodium ovale* are known to produce dormant forms (hypnozoites) in the liver, which could lead to infection recurrences years later [10]. Nevertheless, merozoites, the newly produced parasite stage form, egress the liver and proceed to infect erythrocytes (commonly referred to as red blood cells) in a multi-step entry process, which culminates with the intra-erythrocyte stage of the disease.

1.1.2. Malaria intra-erythrocytic cycle

Red blood cells are the final host target cells in this disease. The cycle begins with parasite binding to the surface of erythrocytes which occurs in a reversible and low-affinity process involving merozoite proteins, including the merozoite surface protein 1 (MSP1). After this connection, the apical end of the merozoite starts reorientation to allow closer proximity to erythrocyte's cell surface. This binding to receptors triggers the formation of a tight junction and allows the parasites to enter. Once inside the erythrocytes, they will reside in the parasitophorus vacuole, where parasites lie and stay protected from intracellular proteases [15].

Importantly, the entry mechanisms and proteins involved vary across *Plasmodium spp.* species, as well as the parasite's preference for cell type to invade [16]. One example is through host expression of a glycoprotein known as Duffy antigen/receptor for chemokines (DARC) in the surface of erythrocytes. Notably, individuals who harbor a genetic mutation that lacks DARC expression are known to be resistant to infections with *Plasmodium vivax* and *Plasmodium knowlesi* [17, 18]. As another example, *Plasmodium falciparum* is known to use the ABO system to establish invasion. A study has shown a 3-fold relative risk of severe malaria for individuals of

blood group A compared to those from blood group O [17]. Moreover, *Plasmodium falciparum* seems to be dependent on the expression of the complement regulatory protein CD55 on the surface of red blood cells, as CD55-knockdown showed to reduce by half the parasites' capacity to invade cells [19].

As for the species divergencies in cell invasion preference, in the bloodstream, 2 major subtypes of erythrocytes are found: mature and immature (reticulocytes) forms. It is known that *Plasmodium vivax*, for instance, only invades immature forms. Since these cell types are found in very low frequencies (about 1% in human blood), the parasitemia (or rate of infection) does not reach high levels as compared to *Plasmodium falciparum* invasion, as the latter does not display any cell preference [20].

The moment of red blood cell invasion has been a target for vaccine design to the extensive research done in the topic. Unfortunately, to date, there is not a single malaria vaccine available to the public, despite attempts that began in mid-1980 [21]. Moreover, targeting living freely parasites in the bloodstream is a real challenge. The average time of merozoites in the blood stream, after red blood cells burst until new cell invasion is approximately 38 seconds, according to a kinetic study conducted with *Plasmodium falciparum* parasite [22].

After erythrocyte invasion, the parasite starts an asexual replication cycle in a highly metabolic demanding process. To be successful in such a maturation stage, parasites rely exclusively on host nutrients, given their inability to synthesize amino acids [23]. Initially, the digestion of haemoglobin available inside red blood cells confers a rapid source of amino acids. However, some essential amino acids, such as isoleucine, cannot be obtained through this route [24]. Additionally, the digestion of haemoglobin generates an unstable heme crystal, called hemozoin. In the case of isoleucine uptake, a 2007 study demonstrated that *Plasmodium*

falciparum-infected red blood cells are more permeable to extracellular isoleucine in comparison to not infected cells, and its uptake happens rapidly in a process that takes approximately 15 seconds [25]. Moreover, the uptake of host purines in *Plasmodium falciparum*-infected red blood cells requires a specialized transportation system. A purine transporter, identified as PfNT1 (*Plasmodium falciparum* nucleoside transporter 1) has been discovered and shown that maximal expression levels are found at the peak of parasite replication, as nucleic acid utilization is most needed [26]. Moreover, recently, the role of RhopH2 (a parasite protein synthesized at late replication stages) in shifting the metabolic state of red blood cells and nutrients uptake has been shown in a metabolomic study [27]. Over the years, more evidence into "new permeability pathways" on *Plasmodium spp.* infected red blood cells have been presented and it is now known that several transportation processes take place and are parasite controlled. A few examples can be highlighted: calcium and potassium influx, lactate, folate, phosphate, and ATP/ADP transport [28].

Along with many essential nutrients, host glucose uptake by internalized parasites represents one of the most important events to assure parasite growth and survival inside red blood cells [29], as it represents their main energy source. It is currently known that glucose entry is mediated by GLUT transporters expressed on the surface of cells. Within the cell, glucose reaches the parasite through the *Plasmodium* hexose transporter (PfHT). Interestingly, the latter has been suggested as a potential therapeutical target [30] after a study where inhibition of PfHT suppressed *P. falciparum* growth *in vitro* and, by using mouse strain *Plasmodium berghei* model, the same treatment induced a reduction of about 40% of the parasitemia when compared to untreated infected mice [31]. This highly energy-active replication culminates in different parasite maturation forms. Initially, asexual development leads to the generation of delicate parasite forms (commonly referred to as "ring forms"). Further maturation culminates into larger amoeboid

structures, now denominated “trophozoites”. The more mature stage is reached when a multinucleate parasitic form, called “schizonts”, is formed. At this stage, the red blood cell is found enlarged, containing 8 to 24 parasites. This developmental process is designated “schizogony”, taking 24 h to be completed. For instance, the human pathogenic species *Plasmodium knowlesi* displays a 24 h replication cycle, whereas *Plasmodium falciparum* and *Plasmodium vivax* take 48 h to complete the cycle. A longer developmental cycle is found in patients infected with *Plasmodium malariae*, which requires 72 h for its completion. Importantly, the 24 h feature is not present in all *Plasmodium spp.* species, although the ones that do not represent the minority. One example is *Plasmodium ovale* with a replication cycle of 50 hours [32], being then classified as an “asynchronous parasite”. At the end of the replication cycle, cell burst and the release of “merozoites” in the bloodstream is an immediate event. This step will allow parasites to continuously invade neighbouring cells and restart the intraerythrocytic cycle.

Notably, at some point during schizogony, a portion of parasites undergo sexual development in a process to form male and female gametocytes, which are the infectious form of the vector (*Anopheles*). Although the molecular events responsible for determining the timing and the parasites that will commit through this process are unclear, it is known that this a relatively long journey (e.g. 11 days needed in case of *Plasmodium falciparum* infections), and these forms are kept sequestered in the bone-marrow to avoid splenic elimination, as demonstrated by a study conducted with *post-mortem* human samples. More specifically, the study showed that the early gametocyte stages (measured by young gametocyte markers) were enriched in the bone-marrow compartment whereas late stages were distributed in several peripheral tissues. Moreover, these forms are shown to be located in the extra-vascular space of the bone marrow, which makes them hardly accessible to local macrophages protecting them from immune elimination [33]. At the end

of the maturation step, these forms return to the bloodstream and wait for the moment by a blood meal is taken by the vector. After ingestion of infected blood, male and female gametocytes will produce an oocyst in the mosquito's mid-gut within 7-10 days, culminating in the release of sporozoites forms which will migrate to its salivary gland [34]. The inoculation of these forms in a mammalian host will complete *Plasmodium spp.* transmission cycle.

The intra-erythrocyte stage of the disease is accompanied by intense immune responses and a unique synchrony feature on parasite maturation, suggesting a 24 h circadian component involved. The latter involves the multiple parasite replication cycles of 24 h with the subsequent red blood cell burst and the release of merozoites into the bloodstream. Continuous rounds of red blood cell invasion by merozoites culminate in an increased frequency of infected cells in the blood stream and generalized cell lysis. Altogether these events promote an anemic state in the host. Furthermore, the capture of intact and lysed infected red blood cells by phagocytes is known to trigger intense pro-inflammatory responses, which contribute to the severity of the disease [35]. Lastly, infected red blood cells sequestration (via receptor binding) in the microvessel of organs such as the spleen, brain, lung, kidney and, more, can cause important tissue damage [14].

Altogether, malaria severity is directly associated with the host response to *Plasmodium spp.* parasite at the level of its intra-erythrocytic cycle and, interestingly, the 24 h replication cycle is responsible for host symptoms to be highly rhythmic. This classical process is defined as "malaria paroxysms" [36] and it involves rhythmic fevers with period of 24 h or multiples, and high levels of pro-inflammatory cytokines in the bloodstream.

1.1.3. Malaria paroxysms and immune responses

As an ancient disease, malaria periodic fevers have been reported by physicians in every civilized society from China 2700 BC up to the 19th century with the first detailed reports from Hippocrates in the 5th century BC [37]. Related to this, in 1992, a study showed that in *Plasmodium vivax*-infected patients, the appearance of malaria fevers is normally accompanied by an onset of chill sensation, starting a couple of minutes before the rise in temperature. Interestingly, levels of blood tumor necrosis factor alpha (TNFα) rise and fall closely with the dynamics of temperature. In fact, high protein levels are detected 30-60 minutes prior to fevers [38]. Similarly, in *Plasmodium falciparum*-infected children, the link between fevers, TNFα and schizont burst was shown a couple of years before Karunaweera's *Plasmodium vivax* report. In 1989, Kwiatkowski D and cols, observed significantly higher TNFα levels in the bloodstream of acute malaria patients, as opposed to healthy adults. When mononuclear cells were isolated from the blood of these patients and stimulated *in vitro* with endotoxin, the authors also observed an increased in TNFα production. Interestingly, when these mononuclear cells were incubated with *Plasmodium falciparum*-infected red blood cells and levels of TNFα was tracked over time, the protein peaked 48 h after culture consistently with schizont rupture moment [39].

Importantly, during paroxysms, the dynamics of inflammation are not only restricted to fluctuations in the levels of TNFα, as still in 1992, levels of interleukin 6 (IL-6) have shown to be rhythmicity expressed with high levels 1-4 hours after paroxysms [38]. Moreover, a study showed a positive correlation between the intensity of paroxysmal symptoms in *Plasmodium vivax*-affected patients and levels of circulating proteins such as IL-10, IL-6 and soluble tumor necrosis factor receptor II (sTNFRII) [40]. Furthermore, high cytokine levels can be used as predictors for malaria severity [41].

In this disease, secretion of proinflammatory proteins is a result of phagocyte's recognition of infected red blood cells (intact or lysed) and/or plasmodium-derived molecules. Nonetheless, innate immunity plays a crucial role in the host response against the infection and contributes to severe pathology and death, as an attempt to control parasite growth [42]. More specifically, circulating monocytes are one of the first cell types to encounter infected red blood cells and merozoites. Not only do these cells contribute to the large production of pro-inflammatory cytokines and chemokines, but they are also important in limiting parasitemia by engulfing infected cells. This phagocytic process mainly occurs through opsonization, via antibody or complement receptor binding (e.g. complement receptor 1) [35]. Importantly, opsonization by antibodies requires FcγRs expression by monocytes and, as reports have shown that the level of this receptor varies between cell subpopulations and, that polymorphisms are found across individuals, the efficacy of this response is variable. As one example, in a study with 182 children infected with *Plasmodium falciparum*, it was found that individuals with FcγRIIa-Arg/Arg131 genotype were significantly less likely to be in the high-risk density parasitemia group [43].

Following phagocytosis, monocytes can become activated by distinct intracellular routes dependent on the nature of the material engulfed and the activation of pattern recognition receptors. As of note, phagocytosis of *Plasmodium*-derived products, such as haemozoin, is known to trigger MyD88/NF-κB pathway in a NLRP3-dependent way, whereas parasite DNA triggers the same pathway via different upstream mediators such as toll-like receptor 9 (TLR-9). Notably, MyD88/NF-κB pathway can also be induced by parasite surface proteins such as glycosylphosphatidylinositol (GPI) anchor protein via several toll-like receptors (TLR1-2, TRL4, and TLR2-TLR6) [2]. Nevertheless, the engagement of such proteins and their corresponding

phagocyte intracellular sensors culminates in one single outcome: cellular activation and a switch to a pro-inflammatory state.

It is important to mention that although circulating monocytes play an important role in the acute proinflammatory phase of the disease, several other circulating cells take an active seat as well. As an example, in the last couple of years, increased importance has been given to natural killer (NK) cells, especially in the context of repeated exposure to *Plasmodium spp.* and as potential therapeutical targets. NK cells are important producers of IFNγ, a cytokine crucial for leukocyte recruitment, and they are cytotoxic cells (mechanism through degranulation and release of granzyme B) in the presence of infected red blood cells [3]. Recently, a cohort with 264 children in Uganda detected a subset of NK cells ($CD56^-$) which was shown to be increased in children repeatedly exposed to malaria [44]. Further analysis demonstrated that these cells are epigenetically distinct and express reduced levels of several surface proteins including FcRγ, NKG2A, and more. As for its function, greater production of IFNγ and degranulation was observed within these cells. The study then concluded that repeated exposure to malaria infection leads to the expansion of a specific subset of NK cells which is highly functional. Furthermore, the presence of this subset is associated with a higher chance of asymptomatic infections in case of re-encounters [44]. The striking findings in this study have shone light on the potential protective role of NK cells in the context of malaria re-infections, which is particularly relevant given the host's inability to sustain long-term memory protection against malaria. It does also make one think about whether artificial polarization towards NK $CD56^-$ could have the potential to become a future prophylactic tool.

Without any doubt, patrolling innate immune cells are essential to govern responses against malaria parasites and infected cells, as first responders. However, many studies have also

demonstrated the contribution of tissue-resident cells, including macrophages and dendritic cells. Notably, one of the most important tissue resident populations involved in malaria pathology is located in the spleen. This organ is responsible for red blood cell clearance when biophysical anomalies are detected (shape, size, deformities), being classified as the "largest filter of red blood cells" in the body [45]. It is well known that during malaria pathogenesis, enlargement of the spleen (or splenomegaly) is a common outcome. This is the result of immune cell expansion in the red and white pulp [46]. *Post-mortem* analysis of spleen samples of patients infected with *Plasmodium falciparum* has indicated a significant higher number of $CD68^+$ macrophages in the red pulp. Moreover, microscopic analysis of these cells allowed visualization of internalized haemozoin, an event that conferred macroscopic changes in the color of the spleen (more towards a brown dark pigmentation) [47].

Importantly, for more in-depth investigations, most studies relied on the use of animal models as evaluation of tissue-resident cells often requires invasive procedures, which are hardly ethically approved to be run in humans. Therefore, through the use of a mouse model of malaria, researchers have identified a subset of tissue-resident macrophages as $CD169^+$ cells which are present in tissues such as the spleen, lungs, and kidneys [48]. These cells are shown to be important in parasite clearance as their absence (through the use of a CD169-DTR transgenic mouse line) lead to an increase in systemic parasite burden. As these cells are also crucial in controlling the intensity of inflammatory responses, accumulation of leukocytes in the brain blood vessels with consequent neurological impairment was also observed. The modulatory effects in inflammation were due secretion of anti-inflammatory interleukin 10 (IL-10) cytokine by which these cells have shown to be major producers. Upon specific cell ablation, reduced levels of IL-10 were found in comparison to the control group, while levels of TNFα were significantly increased – events which

together contribute to a dysregulated inflammatory response [48]. Similarly, by using confocal intravital microscopy, a rapid phagocytic activity of infected red blood cells was seen by splenic dendritic cells after 15 minutes of intravenous infection [49].

Contrary to immune suppressive activities, innate resident tissue cells are well known to take proinflammatory active roles in this disease and, unfortunately, in most cases, culminate with deleterious systemic effects. Still using a mouse model of malaria, Hirako IC and cols, identified a highly efficient phagocytic population of monocyte-derived dendric cells (MO-DCs) in the spleen of infected mice. As dendritic cells are known for their capacity to induce adaptive immunity through antigen presentation [50], not surprisingly these cells were also found to be cross-presenters and important activators of $CD8^+$ T cells lymphocytes in the spleen. However, very interestingly, these cells were detected 5 days after infection in the brain of these mice in a migratory process dependent on chemokine receptors CCR2 and CCR5 [51]. Although innate immune responses contribute greatly to malaria pathogenesis and symptomatology, cellular and humoral adaptive immunity have major impacts as the infection progresses, as well as its capacity to influence immune responses in second malaria encounters. Related to this, re-stimulation of $CD4^+$ T lymphocytes from children who were previously exposed to malaria showed that the pattern of cytokine production was dependent on the prior exposure to malaria. In other words, levels of IFNγ and IL-10 were at higher frequencies among children that had high exposure (equal or more than 2 occasions) in comparison to children who had less than 2 encounters, showing that polarization and the shape of the immune response are influenced by repeated infections [52], although long-term adaptive protective immunity is not acquired through infections.

During the course of the infection, $CD4^+$ T lymphocytes can polarize towards a specific subtype depending on the nature of the antigen that is being presented during the antigen

presentation. In malaria, dendritic cells can polarize $CD4^+$ T lymphocytes towards T helper 1 subtype (Th1) in the presence of IL-12 cytokine [53]. As a result, Th1 cells act as important IFNγ producers which have been shown to have a protective role by impairing parasite growth. Nevertheless, contrasting roles of $CD4^+$ T cells in malaria pathogenesis have been also reported and often referred to as "pathogenic $CD4^+$ T cells", given their association in mouse models of experimental cerebral malaria [54].

Nevertheless, aligned with the findings observed in the 2014 Jagannathan human study, a mouse model study has demonstrated the role of IFNγ restoring protective $CD4^+$ T cells immunity during a secondary *Plasmodium spp*. infection [55]. Moreover, regulatory $CD4^+$ $Fopx3^+$ T lymphocytes were shown to suppress inflammatory response through the secretion of anti-inflammatory proteins such as IL-10 and TGFβ although the animal models of malaria have shown contrasting results [56]. *Plasmodium vivax* and *Plasmodium falciparum*-infected patients commonly harbor elevated numbers of these cells, indicating that this subtype plays a role during pathogenesis and such participation is not species-specific [57].

In the context of malaria, the cytotoxic activity of $CD8^+$ T cells has been importantly demonstrated, mostly in the cerebral pathology. A recent study with *post-mortem* samples has detected a remarkable interaction between $CD8^+$ T cells engaged with or adjacent to the wall of $CD31^+$ cerebrovasculature [58]. This observation suggested direct interaction between $CD8^+$ T cells and brain endothelial cells, as extracellular release of granzyme B by $CD8^+$ T cells [58] was detected in brain images. These observations corroborate many findings using mouse models of experimental cerebral malaria, showing brain endothelial antigen cross-presentation to $CD8^+$ T cells [48, 59, 60]. Furthermore, $CD8^+$ T cells can be activated by parasitized erythroblasts presenting antigens via MHC class I [61].

Although each immune cell type has individual roles during the course of malaria and not all of them are proinflammatory, altogether they build a complex immune network that often culminates in deleterious effects in the host, such as acute lung injury [62, 63], cerebral malaria [64, 65], renal failure, systemic cytokine storms, acidosis and more [66]

1.1.4. Innate immune response to *Plasmodium spp*. derived molecules

Heme dimerization is a process regulated by *Plasmodium spp*. that occurs during its intra-erythrocytic cycle as an attempt to stabilize unstable heme generated from haemoglobin digestion. As a result, a dark-brown insoluble crystal, called haemozoin (Hz), is formed. Hz engulfment by phagocytes triggers many immune signaling pathways that lead to cytokine/chemokine release, NO and ROS induction, and more events which will be detailed discussed in this section.

Immunomodulatory effects of *Plasmodium spp.* antigen products, including Hz, have been reported decades ago. In 1996, patients with severe malaria had their blood collected and leukocytes were stimulated for 2 hours *in vitro* with *Plasmodium falciparum* ring-stage antigens. As a result, a strong induction of IL-6 was detected [67]. In a similar study, 4 hours of incubation of human leukocytes with *Plasmodium falciparum* antigens led to increased levels of TNFα and IL-6. In mice, peritoneal inflammatory macrophages stimulated with *Plasmodium vinckei* erythrocyte antigens (60% parasitemia) also led to increased levels of both of these pro-inflammatory cytokines [68].

Furthermore, nitric oxide (NO) generation was detected upon a synergic effect of sHz (synthetic) and nHz (native) with IFNγ, in murine macrophages [69]. This observation was accompanied by an increase in inducible NOS (iNOS) mRNA and protein levels. The study also showed a rapid activation of MAP kinase (MAPK) pathway (by ERK1/2 phosphorylation) in

response to sHz alone or in combination with IFNγ [69]. In another study, despite phosphorylation of p38 MAPK within 24 hours after nHz phagocytosis ERK1/2 phosphorylation was not seen [70].

The discrepancies in the results between these 2 studies could be attributed to the nature of Hz used (native vs synthetic) and their potential to induce intracell signaling responses. As demonstrated by Parroche et al., the proinflammatory response of innate immune cells against nHz, such as dendritic cells, is believed to be due (at least partially) to the presence of malarial DNA which engages cells through TLR9/MyD88 pathway, as $TLR9^{-/-}$ and $MyD88^{-/-}$ mice failed to produce IL-12p40 in response to nHz. Similarly, nuclease digestion of nHz abolishes its proinflammatory capacity by preventing TLR binding, which further confirms that nHz carries DNA contaminants [71]. Moreover, it was later shown that sHz, when coated with *Plasmodium spp.* genomic DNA, modulates the TLR9 translocation to cellular phagosome [72].

Jaramillo et al., showed that sHz stimulation induced NF-κB binding to iNOS promoter [69]. Moreover, the activation of chemokines MCP-1 (CCL2), MIP-1α (CCL3), MIP-1β (CCL4), and MIP-2 (CXCL2) via direct binding of NF-κB to MCP-1 promoter was also showed [73]. With respect to NF-κB signaling pathway, IκBα phosphorylation was rapidly detected and showed to be dependent of MAPK signaling [73]. Aligned with this, phosphorylation of IκBα and translocation of p65 and p50 NF-κB subunits was also detected after phagocytosis of nHz by human monocytes, as well as increased secretion of IL-1β, TNFα and MIPα [74].

Notably, the role of sHz in cytokine and chemokine response has also been demonstrated *in vivo*. For instance, intraperitoneal injections of sHz resulted in induction of IL-1β, IL-6, MIP-1α, MIP-1β, and MIP-2. Interestingly, the same chemokines were also detected in high levels in the liver of mice upon intravenous injection of sHz. Therefore, the results showed Hz capacity to induce a proinflammatory response at the local and systemic levels [75]. Activation of NLRP3

inflammasome complex was shown to be of the utmost importance in phagocyte's response to sHz. This complex is well-known to be generated through phagocyte's engulfment of aluminum salts (alum) or inorganic crystals such as silicon dioxide (SiO2)/silica, monosodium urate (MSU), and calcium pyrophosphate dihydrate. This multi-step process requires phagocytosis, ROS generation, lysosomal destabilization/rupture, activation of downstream molecules such as caspase-1, and more [76].

Studies with sHz detected similarities in the intracellular response of haemozoin, given its crystal structure and inorganic compounds. In one study, when compared to monosodium urate (MSU) crystal, PMA-differentiated human monocytic cell line (THP-1) stimulated with 200 μg/mL of sHz induced IL-1β secretion at similar levels as cells stimulated with 100 μg/mL of MSU. Furthermore, sHz stimulation of bone-marrow-derived macrophages (BMDM) from $NLRP3^{-/-}$, $ASC^{-/-}$ or $NLRP4^{-/-}$ transgenic mice, induced caspase-1 cleavage in an NLRP3 and ASC, but not NLRC4, dependent manner [77]. Moreover, ROS generation was confirmed with sHz-stimulated macrophages. Nevertheless, activation of ERK1/2 by sHz does not seem to be triggered by ROS whereas NF-κB translocation, in the presence of Hz, was strongly impaired when the antioxidant enzyme SOD was administered. In addition, chemokine response and IL-1β production to sHz is also potassium efflux and ROS-dependent [73]. On the other hand, despite cathepsin B release, lysosomal integrity was maintained upon Hz engulfment whereas morphological deformities were seen in control samples (silica-treated cells) [77]. This suggests that although some aspects of the mechanism used by Hz to trigger NLRP3 inflammasome activation are similar to what was observed with inorganic crystals, Hz might still use different mediators which have not yet been fully identified.

It is, however, known that Spleen Tyrosine Kinase (Syk) and Scr family kinase member Lyn interact in an upstream signaling event to promote NLRP3 inflammasome activation and consequent release of IL-1β upon Hz phagocytosis. As Hz cellular response involves cathepsin release without promoting lysosomal deformity and a similar phenotype has been shown to be under the control of Syk in B cells [78], the authors hypothesized that NLRP3 inflammasome route of activation in Hz stimulation models could be resultant of Syk activation. Aligned with this hypothesis, the authors identified phosphorylation of Syk upon sHz addition, but this phenotype was absent in MSU-treated cells. This corroborates with the divergencies previously observed for NLRP3 inflammasome complex activation by inorganic crystals versus Hz, whereas the latest seem to use an exclusive activation route. Furthermore, as Syk phosphorylation and IL-1β secretion mediated by sHz was absent in $Lyn^{-/-}$ macrophages, the authors concluded that Lyn-Syk pathway is needed for such response. Notably, MSU-treated cell's capacity to produce IL-1β was not affected by the absence of Lyn [77].

In association with the Lyn-Syk pathway, Hz response requires Protein Kinase C activation. In phagocytes, PKC plays important roles such as modulation of complement receptor type I (CR1) expression, being particularly important during phagocytosis, and activation of NADPH oxidase controlling ROS generation [79]. That being said, the measurement of the level of PKC activation and PKC-dependent protein phosphorylation in Hz response is particularly relevant. Increased phosphorylation of PKC substrates was seen in PMA-differentiated THP-1 cells and BMDM stimulated with sHz. Interestingly, upon administration of a PKC inhibitor (GÖ6850), ROS generation and IL-1β maturation were compromised [80].

Altogether, over the years these results demonstrated that, in phagocytes, sHz activates NLPR3 inflammasome complex with IL-1β secretion, by triggering intracellular mechanisms that

require phagocytosis, activation of Lyn and Syk pathway, PKC activation, and ROS generation. Moreover, in this model, cellular activation with consequent cytokine/chemokine production requires MAPK and NF-κB signaling pathways. The summary of intracellular networks and components involved in the Hz-macrophages response, and which have been extensively discussed in this chapter are illustrated in Figure 1.

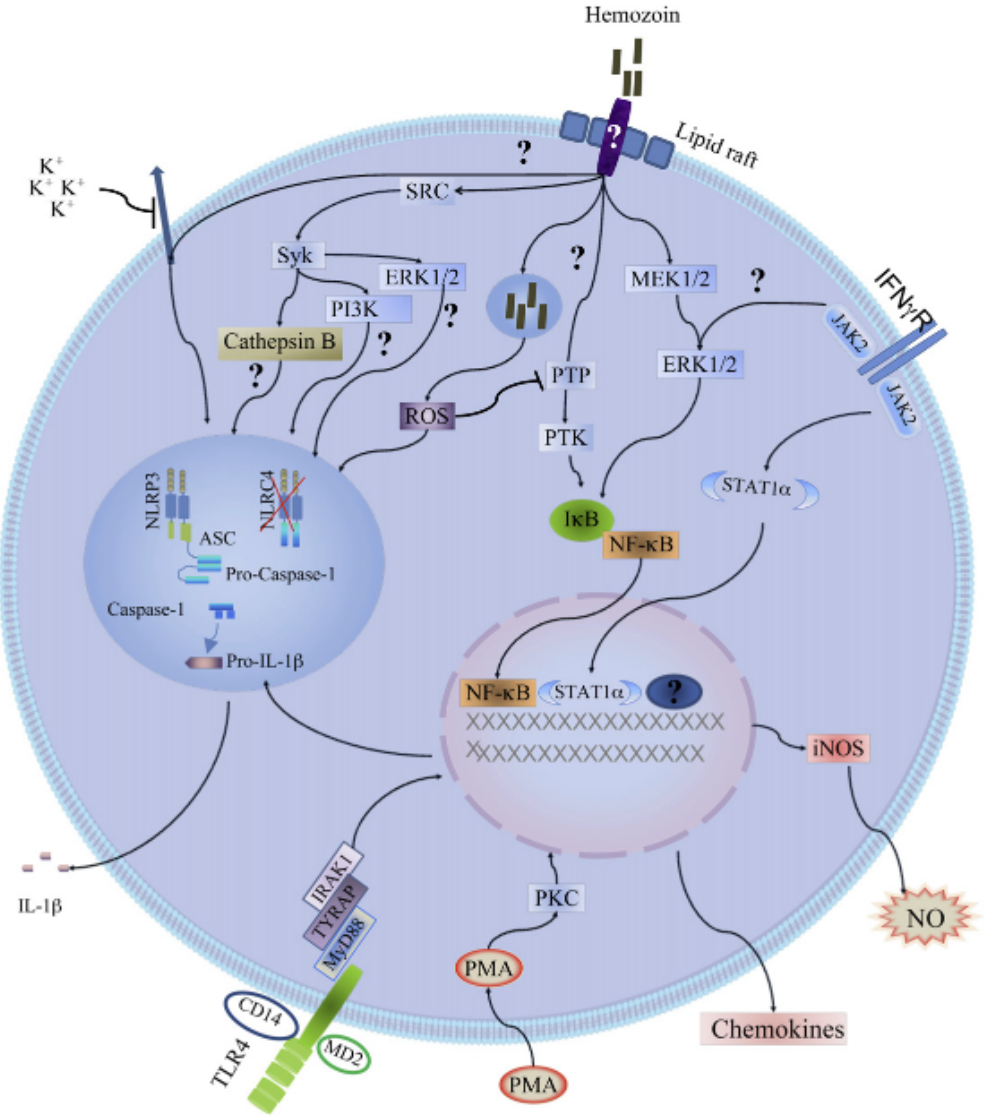

Figure 1: Intracellular signaling pathways triggered by Hz.

Source: Shio MT et al., 2010

Although important knowledge has been presented over the years as per the intracellular mechanisms governing Hz cell activation, most of the studies were conducted using purified synthetic haemozoin (sHz) whereas in *Plasmodium spp.*-infected mammals, Hz is often found in association with damage-associate molecular patterns (DAMPs), such as parasitic DNA. This association has been reported to trigger a diverse range of intracellular pathways [81] and add complexity to our further understanding of the key players involved. Furthermore, it is important to remind that, during malaria pathogenesis, the burst of infected red blood cells culminates with the release of many other molecules which are immune response activators, including free heme, merozoites, and more. For instance, a study reported an increase in CD40 expression and TNFα release in BMDMs, upon cell presentation with isolated sub-micron particles collected from a *Plasmodium berghei ANKA*-infected mouse at day 7 post-infection. Importantly, the particles did not contain measurable levels of Hz. Nevertheless, as platelets are known to be one of the major sources of microparticle release under homeostatic conditions, the authors conducted a phenotypic analysis to determine if their immunogenic microparticles were platelet derived. Interestingly, they found that the microparticles did not co-express CD41, indicating that platelets were not their source. In fact, their phenotypic profile showed increased frequencies of $Ter119^{+}$ and $CD45^{+}$ flow cytometric events, indicating red blood cells-derived and leukocyte-derived material, respectively.

The role of *Plasmodium spp*.-derived inflammatory molecules was also investigated in a study where dendritic cells stimulated with *Plasmodium yoelli*-infected lysed red blood cells, led to cell maturation but only when the infected material was presented in lysed form, not as intact cells [82]. Similarly, macrophage failed to respond to live and intact *Plasmodium berghei ANKA* infected red blood cells [83]. Despite this, phagocytosis of intact *Plasmodium falciparum*-infected red blood cells by human macrophages has been detected in a recent study [84].

Importantly, deleterious effects of long-term exposure to *Plasmodium spp.*-derived molecules, including Hz, have been reported. As Hz can persist for long periods of time in phagocytes (neutrophils, monocytes, and resident macrophages), some studies have shown that impairments in the cell function can be observed, especially in the cell's ability to respond to new challenges. Hz seems to impair cell function by generating intracellular reactive oxygen species (ROS) which suppress PKC. Given that PKC controls Complement Receptor of type I (CR1), further impairments in the phagocytic capacity of cells can be observed [79]. However, such impairments might not be an exclusively mediated effect by PKC. Another study reported cytosolic NADPH-oxidase (NOX) inhibition following Hz stimulation of human monocytes in the first 12 hours of Hz engulfment by a PKC-independent pathway. After 12 hours, phosphorylation of PKC 47kDa was found impaired in these cells, suggesting that long-term exposure to Hz leads to suppression of both PKC and NOX, events that could contribute to impairments in Hz-phagocytosed cells' function, therefore, the inability of Hz-phagocyted cells to respond to future infection challenges [85]. Such an event is known as the "phagocyte deactivation process" which is marked by a partial or complete unresponsiveness to an activating stimulus [86]. Similarly, intracellular pathogens such as *Histoplasma capsulatum* have been also shown to suppress PKC activity which allows long-term survival within phagocytes [87].

1.1.5. Linking malaria tissue-pathology and the immune system

During malaria pathogenesis, an immune activation is an early event, and it is responsible to start an entire cascade of events with multi-organ damage as the endpoint. For instance, IFNγ was shown to be involved in the development of cerebral malaria, as in humans *IFNAR1* gene, variants are protective. Similarly, $IFN^{-/-}$ mice demonstrated increased protection to experimental

cerebral malaria (or ECM) and reduced number of mononuclear cells in the brain microvasculature [88]. Moreover, during ECM, cerebral pathology occurs through cross-presentation of *Plasmodium Berghei ANKA* antigens by brain endothelial cells to $CD8^+$ T cells with further cellular activation and cytotoxic activity. Although brain leukocytes can cross-present parasite antigens, the contribution of these cells was about one tenth when compared to brain microvessels cross-presentation capacity. Interestingly, in this model, 90% of the T cells found in the brain were $\alpha\beta$ $CD8^+$ T cells [89] but the neurological impairments are not only dependent on $CD8^+$ T cells accumulation in the brain; anti-malarial drug administration a day prior to the development of cerebral pathology prevented mice from neurological damage without affecting $CD8^+$ T cells accumulation in the brain [60]. Moreover, parasite biomass (accumulation in tissue microvasculature) was associated with the onset of ECM [90], and reduced upon anti-malarial administration as well as the cross-presentation phenomenon [60].

As for the mechanisms driving $CD8^+$ T cells recruitment to the brain, initial priming of cells in the spleen is a necessary step in this disease, followed by a CXCR3 expression-dependent migratory process, given that CXCR3 ligands CXCL9, CXCL10, and CXCL11 are the most upregulated chemokines in the brain of ECM affected mice [91]. Moreover, studies in the field have shown that chemotaxis of $CD8^+$ T cells to the brain relies on $CD4^+$ T cells chemotactic capacity in the spleen, and such control is linked to IFNγ responsiveness and T-bet expression of splenic $CD4^+$ T cells [92].

Acute lung injury is another malaria's clinical manifestations [62] where activated $CD8^+$ T cells migrate to the lungs and promote tissue destruction (characterized by edema, loss of wall integrity, intra-alveolar erythrocyte extravasation, and more), while lung endothelial cells cross-present parasite antigens to $CD8^+$ T cells via major histocompatibility complex (MHC) class I

(MHC I) or class II (MHC II), and IFNγ [62]. In summary, this study showed that malaria lung injury was mechanistically similar to ECM.

1.1.6. Mouse models of malaria

Malaria mouse models are important tools to investigate disease pathogenesis and host responses to novel therapeutic approaches. Various murine malaria species have been isolated, and their pathogenesis widely studied. Similar to human parasites, each murine species has unique properties, and different levels of disease magnitude. *Plasmodium berghei* and *Plasmodium vinckei,* and some strains of *Plasmodium chabaudi* and *Plasmodium yoelli,* cause lethal infections. On the other hand, *Plasmodium yoell* 17x, *Plasmodium chabaudi adami* and *Plasmodium vinckei petterei* induces chronic parasitemia which can be cleared after an initial acute phase [93]. Thus, the choice of the model should be aligned with the study's research questions.

Importantly, the differences in pathogenesis and lethality are most of the time a direct result of the type of host immune response the pathogen can induce. As an example, although *Plasmodium yoelli nigeriensis* N67 and *Plasmodium yoelli nigeriensis* N67C strains are isogenic and share a very similar genome sequence, parasitemia levels and host susceptibility are very different. Of note, immune responses were shown to be very different between them, with splenomegaly being observed only in mice infected with N67 strain, along with elevated IFN-I responses, and increased phagocytic capacity of dendritic cells and macrophages [94]. *Plasmodium berghei ANKA* is the model of choice to study cerebral malaria, given the similarities with the human cerebral pathogenesis, as well as a good model to study malaria multi-organ damage. The model is commonly called "experimental cerebral malaria" or ECM.

Importantly, *Plasmodium berghei ANKA* virulence also relies on the mouse strain used, as in order to obtain a similar pathogenesis as seen in human cerebral malaria, infections must be performed with C57BL/6 or DBA/1 mouse strains [95]. Balb/c or DBA/2 fails to develop ECM and succumbs to the infection in later days due to hyperparasitemia and anemia. When infections are performed in C57BL/6, almost 100% mortality was observed within 12 days post-infection [91].

Striking, the same mouse strains but obtained via different vendors can also have an impact on malaria pathogenesis. Comparisons between C57BL/6 from Taconic Biosciences and Charles River Laboratories have resulted in increased parasitemia, parasite burden, liver injury, and morbidity for Charles River-infected mice with *Plasmodium yoelli* 17XNL [96].

Furthermore, similar to what is observed with human *Plasmodium spp.* parasites, preference for invasion of different subsets of erythrocytes is found with murine parasites. For instance, *Plasmodium berghei ANKA* is known to have a strong preference for reticulocytes [97] whereas *Plasmodium chabaudi AS* displays a preference for normocytes (mature erythrocytes). This preference impacts the level of parasitemia observed as it follows cell subset abundance [98].

Not surprisingly, as one of the main characteristics of malaria, the intraerythrocytic cycle synchrony is a variable feature among murine *Plasmodium spp.* species. Of all rodent species, *Plasmodium chabaudi* is the only one recognized as "synchronous", harboring a 24-h replication cycle, although several others are acknowledged as "partially synchronous" such as *Plasmodium yoelli* with an 18-h replication period, and *Plasmodium berghei* with approximately 22-h [32]. In addition to that, *in vitro* synchronization of *Plasmodium berghei* cultures has been already reported [99].

In summary, mouse models of malaria are great allies for studying this disease and they have been so for the past 20 years. As the development of the disease occurs at a fast pace and with similar progression steps, murine models allow research to evolve considerably, but still, many mechanisms and questions remain unaddressed.

1.1.7. Human vs murine models: Insights for malaria studies

During *Plasmodium falciparum* infections, it is known that the export of parasite proteins to the surface of erythrocytes is an active process. Among them, *Plasmodium falciparum* erythrocyte membrane protein 1 (PfEMP1), upon the control of a skeleton-binding protein 1 (SBP1), binds to the adhesion molecules (more specifically, CD36) at the surface of vascular endothelium cells [100], such as brain endothelial cells. As a result, infected cells are sequestered into the microvessels, and are now protected from splenic and phagocyte clearance. Importantly, as platelets and monocytes also express CD36, sequestration is not exclusive to endothelial cells. This contributes to the formation of cellular agglomerates and vessel clogging, thus driving malaria pathogenesis [101]. To study the pathogenesis behind cerebral malaria, the *Plasmodium berghei ANKA* (PbA) mouse model of ECM is commonly used as it partially recapitulates the symptoms experienced by patients under cerebral malaria, as well as the inflammatory response generated 7-14 days after infection. However, some of the mechanisms are not conserved in human and mouse pathogenesis. For example, PfEMP1 expression is restricted to *Plasmodium falciparum*, as specific domains that mediate CD36 binding are not present in PbA. Despite this, sequestration still occurs in PbA. One protein shown to be involved in sequestration in PbA is an orthologue of PfEMP1: a protein named schizont membrane-associated cytoadherence protein (SMAC) that promotes sequestration through a CD36-dependent manner, without direct binding. Furthermore, SMAC

protein translocation to the surface has not been observed [102]. Recently, in PbA, two orthologues of PfSBP1 and PfMAHRP1(*Plasmodium falciparum* membrane-associated histidine-rich protein 1), named SBP1 and MAHRP1 respectively, have been identified and shown to be involved in erythrocyte sequestration dependent on CD36 [103].

Nevertheless, the sequestration event is one of the most divergent points observed in cerebral malaria of human versus mouse models. Despite orthologues have been identified and so were mechanistical similarities, PbA studies have demonstrated that sequestration still happens at the peripheral level, more specifically in the liver, spleen, kidneys, and adipose tissue, whereas there is little or no sequestration in the brain vessels [8]. Moreover, in a mouse model of malaria acute kidney injury (MAKI), mice infected with SBP-1$^{-/-}$ *Plasmodium berghei* NK65 parasites, despite presenting fewer sequestration events, acute tubular and glomerular injury was still detected [104].

Notably, sequestration is one of the hallmarks of human cerebral malaria. In a cohort of 65 *Plasmodium falciparum*-infected patients (37 with cerebral malaria, and 28 without) binding between infected red blood cells and endothelial cells was detected with significantly more sequestration in the cerebellum, in cerebral malaria patients compared to the other group [105]. Interestingly, when parasite burden in the brain and in the blood was evaluated immediately before death, the authors observed that patients with undetectable parasites in the brain had significantly longer time to death than the rest of the group. For the remaining 48 patients (combining both groups), parasite burden in the brain was significantly higher than in the blood, indicating that increased parasite burden is associated with fatal outcomes. Moreover, a lack of significantly differences was found in blood parasitemia between the 2 groups, suggesting that blood parasite load cannot be used as a guide for tissue sequestration and cerebral [105]. In contrast, death

associated with cerebral malaria in PbA is not dependent on sequestration as $CD36^{-/-}$ mice developed the cerebral pathology similar to wild-type mice 5-10 days post-infection [106]. Although the pathogenesis of cerebral malaria is distinct between humans and mouse models, tissue sequestration in both scenarios seem to involve the late-stage forms of infected red blood cells. For instance, in human cerebral malaria, a brain sequestration analysis revealed attachment of infected red blood cells containing mid-trophozoites or schizonts [105], whereas in PbA, schizonts infected cells are the main forms involved in the attachment [8].

Despite differences between humans and mice, many authors still support PbA model choice as an adequate tool for malaria research [103]. Indeed, between 1990-2005, over ten times more murine studies with ECM (rather than human cerebral malaria) have been conducted yearly [107]. Furthermore, the ECM model allows testing different intervention treatments, e.g. 48 different potential therapeutical interventions have been reported in 45 ECM studies over the course of 22 years [107]. Moreover, both human and mouse ECM shares the common inflammatory component. As an example, a 2019 study showed that malaria severity and death in a cohort of 122 patients are correlated with the frequency of various monocytes subtypes and plasma levels of cytokines/chemokines IL-1β, IL-6, IL-10, CXCL10, and at the mRNA level, *Ccr2* and *Cx3cr1* [108].

Lastly, the pathogenesis resemblance between mice and humans allows additional exploration of many malaria-related features, including the long-term known rhythmicity aspect of the parasite, and potentially, whether host circadian rhythms also play a role in this disease.

1.2. Circadian Rhythms

Circadian rhythms are defined as biological oscillations with a 24 h period which persist in the absence of environmental cues [109]. They are controlled by endogenous circadian clocks: a central lock in the suprachiasmatic nucleus and peripheral clocks distributed in the body, and are regulated by a complex network of clock proteins and regulators [110]. Notably, circadian rhythms control various physiological processes including body temperature, hormonal secretion, immune responses, and more, and are particularly relevant in the context of infectious diseases and inflammatory disorders [111]. In Chapter 1.2 the most relevant studies in the field of chronobiology will be presented and discussed in the context of immunity, rhythms in malaria and, the negative effects of circadian misalignment in disease.

1.2.1. The circadian clock

Twenty-four hours circadian oscillations are aligned with Earth rotation and are known to be present in a variety of living organisms. With the help of extensive genetic studies using *Drosophila melanogaster*, the understanding of how circadian clocks function advanced considerably. In the 1990s, a mutation in mice was found to affect the mammalian circadian clock. The gene was denominated "*Clock*" and homozygous animals demonstrated altered circadian rhythms with a long period (assessed by behavioral locomotor activity) in constant darkness [112]. The phenotype observed aligned with findings from previous *Drosophila melanogaster* studies, where mutations in *per* resulted in altered periods and arrhythmicity [113, 114]. Interestingly, around that period, the existence of circadian rhythms in prokaryotes was uncertain, further contradicted by studies with cyanobacteria [115].

In mammals, circadian rhythms are controlled by a master pacemaker, denominated "central clock", located in the suprachiasmatic nuclei (SCN) of the hypothalamus. The neurons at the master clock play a crucial role in transmitting environmental light information captured through the retina to peripheral tissues [116]. This allows the peripheral tissues to be synchronized with day/night cycles [117]. Light, in this case, acts as an important environmental cue by which systems can synchronize to or entrain, and it is commonly referred to as a "*Zeitgeber*", a German terminology meaning "time giver" [118]. Synchronization of peripheral tissues can occur through a variety of molecules and entraining signals, such as autonomic innervation, body temperature, hormones (e.g. glucocorticoids), and feeding behavior [110]. These signals are then captured by commonly called cell-autonomous "peripheral clocks" which are endogenous circadian clocks located within various tissues around the body. Basic cellular functions are controlled by these endogenous clocks, but they still rely on synchronization inputs from the SCN to assure proper circadian phase alignment. Importantly, *ex-vivo* cultures of tissue explants (e.g. liver) can sustain circadian rhythms (phase and period), which are dictated by the local oscillators. However, the lack of a "synchronizer" input from the SCN, will in a matter of days/weeks, result in arrhythmicity (as a result of rhythms desynchronization), demonstrating the importance of both clocks (central and peripheral) for proper circadian functionality [119].

As briefly mentioned above, the circadian clock is an intracellular network responsible for generating circadian rhythms which are under the control of "clock genes/proteins". Through a transcriptional-translational feedback loop model, core components CLOCK and BMAL1 together heterodimerize and transcriptionally activate a family of *Period* genes *Per1, Per2, Per3* and *Cryptochromes Cry1, Cry2* through direct binding at E-box elements. Degradation of PER and CRY proteins in the cytosol induces these proteins to translocate back to the nucleus to inhibit

their transcription, by suppressing the activity of CLOCK/BMAL1 heterodimer [120]. This process will restart another circadian cycle. In a parallel loop, heterodimers CLOCK/BMAL1 activate REV-ERB (α, β), which in the nuclei binds to the ROR (RAR-related orphan receptors) response elements (ROREs) in the promoter of *Bmal1*, regulating its expression [121]. Importantly, as the network involves complex series of events ranging from transcription, translation, protein-protein interaction, phosphorylation, and degradation, the amount of time it takes for such a process to be executed each day is approximately 24 hours. Thus, an endogenous rhythm of a period close to 24 h is generated, and consequently, these rhythms affect intracellular processes in a rhythmic fashion [118]. As many downstream genes are dependent on clock proteins transcriptional activation, their rhythmic expression results in their rhythmic induction. These downstream genes are referred to as clock-controlled genes (CCGs) [122]. CCGs have been extensively identified in the past decades [123], with several directly involved in cellular activation and immune responses [124].

1.2.2. Circadian clock in immunity

Circadian rhythms in immunity have been repeatedly reported in human and animal models [125]. Some studies have shown stronger immune responses during the active phase with an increased number of immune cells in protective barriers (local immunity) such as the skin [126]. According to these studies, in peripheral tissues, a greater frequency of immune cells and their responsiveness during the active phase seems to be counterbalanced by a larger number of these cells in the bloodstream [127] or lymph nodes [128] during the dark phase, demonstrating the 24 h migratory pattern of immune cells. On the other hand, others have shown higher immune responses at different times of the day. For instance, the peak of phagocytic activity of

macrophages was at the transition between night and daytime, at circadian time 0 (CT0, dawn) [129].

Rhythms in immunity, including the egress of hematopoietic stem cells (HSCs) and their progenitors from the bone marrow, are controlled by the central clock. Through adrenergic neural signals, the SCN modulated the regulation of CXCL12, an important chemokine involved in HSCs migration. Moreover, environmental cues, such as light, showed to be an important factor in controlling the circadian fluctuations in HSCs and their progenitors where abolished rhythms at constant light (LL) were observed. However, rhythms were kept synchronous during constant darkness (DD), confirming that these rhythms can be defined as "circadian" as they persisted during mouse free-running [130] – based on the well-known and accepted criteria used to categorize circadian rhythms [109]. Similarly, in humans, circadian fluctuations of HSCs and progenitors were detected but with an "inverted" light-dark pattern given the diurnal and nocturnal phenotype of humans and rodents, respectively [131]. Furthermore, a migratory profile of monocytes in the blood and spleen was also detected in rodents [132] as well as the leukocyte rolling capacity significantly increased at the beginning of the active phase (ZT13) [127]. Along with chemokine gradients, oscillations in immune cell migration have been shown to also be dependent rhythmic expression of adhesion molecules such as ICAM-1 [127].

Given the existence of daily fluctuations in the number of cells and their migration, it is logical then to expect rhythms in immune responses in response to pathogens. One of the first pieces of evidence demonstrating an effect of time-of-day in host response immunity was a study conducted in 1960 using mice exposed to intraperitoneal injections of *E. coli* lipopolysaccharide (LPS) endotoxin. As a result, a rhythm in mortality was observed [133]. After that, LPS became a popular model to access rhythms in immune responses although contrasting results have been

presented over the years. A study confirmed the significantly reduced survival when LPS was injected at ZT12 as opposed to ZT0 [134]. On the other hand, a rhythm in mortality to LPS was found to be greater at ZT6 as opposed to ZT18, in another study [135]. Interestingly, it has been also shown that the rhythm in LPS susceptibility is not circadian, as survival differences are seen only upon LD injections, but not at DD [136]. Nevertheless, time variations in the inflammatory response, at the peritoneal cavity following LPS administration, were seen under DD injections with higher levels of proinflammatory cytokines/chemokines IL-6, IL-12(p40), CCL5, CXCL1, CCL2 at CT12 compared to CT0 [137]. Moreover, the route of administration seems to also be related to the rhythms in susceptibility and immune responses to LPS. For instance, upon aerosolized LPS administration in constant darkness (DD), an increased lung inflammation at CT0 and a greater neutrophil recruitment accompanied by high levels of proinflammatory cytokines IL-6 and TNFα was detected [138]. Interestingly, in this model, chemokine 5 (CXCL5) showed to be responsible for rhythmic recruitment of neutrophils. Moreover, SCN-controlled glucocorticoids showed to be important for the rhythm of CXCL5, as adrenalectomized mice showed a lack of rhythmicity in both CXCL5 levels and neutrophil migration [138]. In contrast, a recent study reported increased lung inflammation and neutrophil recruitment in response to LPS at CT12 in comparison to CT0 [139]. Moreover, splenic macrophages stimulated with LPS showed circadian rhythmicity on the secretion of TNFα and IL-6 [140].

Although rhythms in susceptibility to endotoxin were consistently reported, the reasons behind the discrepancies in respect of time of day with higher/lower immune activation are unknown. To add to this, bone marrow-derived macrophages, when stimulated with LPS at different circadian time points, resulted in rhythmic IL-6 production [141], which supports that rhythms in immune responses can be mediated by endogenous circadian clocks.

Furthermore, in a model of fulminant hepatitis induction, an effect of time of day in the production of IL-1β and IL-18 by peritoneal exudate cells was detected. Interestingly, altered rhythms were found when the experiment was performed with a transgenic mouse model lacking the clock gene *Rev-erbα* expression, with further confirmation of REV-ERBα direct binding to *Nlrp3* gene, thus controlling the NLRP3 inflammasome pathway [142].

Interactions between circadian clock proteins and immune signaling pathways have been shown by many other studies in the field [137]. Interestingly, both core clock proteins CLOCK [135] and BMAL1 [143] have been shown to directly interact with and modulate NF-κB, an important immune signaling pathway. In addition, data showing BMAL1's direct control over reactive oxygen species (ROS) generation and IL-1β production, following LPS stimulation, was recently presented [144]. Furthermore, changes in clock gene expression before (and after) an inflammatory stimulus have also been identified [134]. Altogether, over the years many studies have unrolled a complex network linking circadian clock and immune responses, with a reach far beyond the initial observations in the rhythms of host susceptibility.

1.2.3. Circadian misalignment and pathogenesis

Modern society has forced individuals to adjust to non-traditional routines with work hours at times when they are supposed to be sleeping. This is the reality of many shift workers carrying adverse health problems related to circadian misalignment, sleep deprivation, and exposure to light at night [145]. In Canada, the prevalence of individuals working a regular night shift regimen was over 300,000 (as of April 2022), representing about 1.7% workers aged 15 to 69 [146]. Moreover, according to the 2011 last edition of the Survey of Labour and Income Dynamics (SLID), the Canadian labor force had a growth of 21.7% of workers between 1996-2006 with almost half of

the growth of individuals in non-regular daytime shift work. During this period, the number of women in rotating and night shift work increased by 94.5% [147].

Night shift work has not only statistically significantly demonstrated an increased risk of work-related injuries (5.9%) as opposed to daytime work (2.9%) [147], but several studies have pointed out the long-term effects on an individual's health [148]. A cohort of 57 shift workers and 47 day workers evaluated several health parameters including blood pressure, sleep, systemic inflammation markers, and more. As a result, shift workers had a significant decrease in total sleep amount, a significantly increase in plasma cortisol and TNFα (20% higher), IL-6 (190% higher), IL-1β (96% higher), and IL-10 (100% higher) cytokines compared to daytime workers. Furthermore, mean counts of monocytes, lymphocytes, and neutrophils were significantly higher in the shift work group. No statistically significant changes in blood pressure were found [149]. Interestingly, in another study, subjection of individuals to an in-lab simulated night shift protocol has shown to induce a temporal misalignment between circadian rhythms of immune functions [150]. Phase shifts in cytokine secretion rhythms (including TNFα, IL-1β, IL-6, and IFNγ) and immune cell numbers were observed in participants subjected to this protocol compared to their baseline rhythms before intervention [150].

Similar to shift work, time-zone travels are another cause for circadian misalignment and are often referred to as jet lag. In 2001, a study with groups of flight attendants who had a "short" (less than 5 days between outward transmeridian flights across at least 7 times zones) and a "long" (more than 14 days) recovery period was conducted. Magnetic resonance imaging (MRI) analysis showed a decreased hippocampal volume in the short-recovery crew only. When cognitive performance was evaluated by a series of tasks, the long-recovery crew performed significantly better with a shorter reaction time [151].

Experimental protocols of jet lag can be held in animals, and still, nowadays they are useful tools for studying the effects of circadian misalignment (disruption). Variations of the such protocol have been extensively tested and reported [152-156]. The confirmation of circadian disruption in mammals is normally made through measurements of locomotor activity (behavioral rhythms). Repeated exposure to phase-shifted 24-h LD cycles prevents mice from entraining or displaying relative coordination once the *zeitgeber* is outside the range of entrainment. This results in a forced desynchronization which can be tested acutely or chronically. Phase shifts can consist of advances or delays, but reports showed that delays are less effective for circadian desynchronization as opposed to advances [157]. Thus, most mouse studies consist of protocols of 6-8h phase advances every week or every 2-3 days, with variable durations.

The deleterious effects of jet lag have been demonstrated by increased lethality of aged mice subjected to an 8-week jet lag protocol. More specifically, at the end of the 8 weeks, 47% survival was found in phase-advanced mice, 68% in those subjected to phase delays, and 83% in unshifted aged mice [152]. Similar findings were obtained with chronic 85-week exposure to phase advances (8 hours every 4 days) or phase delays (8 hours delay every 7 days). Interestingly, the mortality rate of phase-advanced mice was about 20 times higher than with control LD mice (not subjected to jet lag). On the other hand, there were no statistically significant differences between the survival of phase-advance and phase-delay groups [155].

The role of circadian misalignment during pre-existent diseases has been also studied. A 2004 a study aimed to investigate the effects of jet lag on tumor progression. Mice were subjected to 8-h phase advances every 2 days for 10 days before inoculation of osteosarcoma cells. Over the days, a significantly increased tumoral growth was detected in these mice compared to the control LD. Although the study did not mention whether the animals were kept in the same protocol after

tumoral injection, the authors have shown confirmation of circadian desynchrony (measured by levels of clock genes) in both tumor and liver [158].

Recently, a study was conducted to elucidate whether the deleterious effects of jet lag on cancer progression are dependent on previous exposure to circadian misalignment, or whether circadian misalignment during cancer development leads to a poor prognosis. By using a rodent lung cancer model, they saw that mice subjected to chronic circadian disruption (8-h phase advance every 2 days) 5 weeks after tumoral injection displayed reduced survival, increased tumor burden, and a shift from tumor grade 1 and 2 to 3 and 4, in comparison to LD 12:12 mice [156]. Interestingly, experiments conducted with clock gene mutant mice (full body *Per2*$^{-/-}$) also exhibited increased tumor burden and grade shift, while accelerated tumor growth was also seen in cancerous cells lacking *Bmal1*. In summary, the study showed that disruption of circadian rhythms during cancer progression had an important effect on prognosis [156].

In addition to cancer studies, the negative health effects of jet lag can be extended to further findings: For instance, reports on alteration of animals' metabolism, leptin resistance, body weight, and composition [159]. In the case of immune-mediated diseases, such as colitis, jet lag has led to an increased on histopathological score, colon length, weight loss, and more [160].

In a mouse of peritonitis induced by LPS, animals were subjected to a chronic jet lag protocol of 6-h phase-advance every week for a total of 4 weeks, resulting in 4 shifts. Mice were then put for 1 week in 12:12 LD cycle to allow re-entrainment, and then received an intraperitoneal injection of LPS [153]. In these mice, compared to an LD control group, a strong reduction in survival, increased hypothermic state and increased levels of several pro-inflammatory cytokines 24 h after injection was detected. Interestingly, such effects were not observed with acute mice exposed to jet lag (1 shift only), suggesting that chronic exposition to jet lag is needed for the

phenotype observed. Interestingly, when peritoneal exudate cells (PECs) were harvested after the 4 shifts and *ex-vivo* stimulated with LPS, PECs from jet lag mice responded with much higher levels of IL-6 cytokine [153]. Results were also confirmed with peripheral blood nuclear cells (PBMCs) [161].

Importantly, impacts on health can also be attributed to other irregular lighting protocols. For instance, mouse exposure to constant light (LL) had been reported to affect immunity. In one study, a 2-fold increase in the relative number of neutrophils and significantly fewer lymphocytes at 8 weeks after LL initiation, have been detected. Moreover, secretion of IL-1β , TNFα and IL-6 in response to LPS, was significantly higher in the LL group [162].

In summary, human and animal studies with various circadian disruptive protocols have shown an effect on host health and pathogenesis, including impacts on immunity.

1.2.4. Circadian clock in host-pathogen interactions

Aligned with rhythms in immune responses, the host's ability to fight pathogens which are greatly dependent on immunity, is known to be influenced by the time of day. The effects have been reported in a variety of pathogens including fungi, bacteria, parasitic infections, and more [163]. As one example, during an acute model of *Salmonella Typhimurium* infection, bacteria colonization in the colon was affected by the time of infection [141]. Host response was also markedly affected by increased inflammation and histopathological alterations. Interestingly, host response showed to be dependent on an intact clock, as infections with *Clock* mutant mice abolished the day vs night variations in the number of bacteria found in the colon 72 h later [141].

Furthermore, during *Trichuris muris* worm infection, the dynamics of parasite expulsion can be dictated by the time of infection, with parasite expulsion after 21 days significantly greater

when infections were performed at ZT12 [164]. As worm infections are dependent on host Th2 immune responses, humoral responses, and T cell polarization were also investigated. As a result, it has been shown that the circadian clock in dendritic cells impacts T cell polarization, specifically, BMAL1 control over IL-12 and IL-27 signaling pathways [164].

Furthermore, leishmaniasis infection of mice performed at different circadian times led to a rhythm with the lowest levels of parasite burden in the site of inoculation (footpad) and swelling during the subjective day (CT3-9). Aligned with lowest values at CT3, parasite load rhythmicity, and immune cells migration was also detected when peritoneal cavity inoculation was executed. Interestingly, the effect of time was abolished in chimeric mice reconstituted with a bone marrow from a *Bmal1*$^{-/-}$ mice, demonstrating the role of the circadian clock in hematopoietic cells in the host response to *Leishmania spp*. infection [165].

Although much has been reported on host rhythmic response to pathogens and the role of the circadian clock [166], recently, studies have shown that this interaction can be more complex than originally believed. For instance, recent reports showed an autonomous clock running in parasites such as *Plasmodium spp*. [167-169], and *Trypanosoma brucei* [170]. Recently, a daily rhythm in *Schistosoma mansoni* gene expression was identified [171]. Whether this makes parasites more tolerant to environmental changes and host rhythms is unknown, as well as if endogenous clocks are resultant of an evolutionary adaptation process. Of note, evolutionary adaptions seem to be the currently accepted explanation for many behaviors seen in parasitic infections. For example, the migratory patterns of microfilariae over 24 h are coordinated with the timing of mosquitos' bloodmeal [172, 173]. Similarly, rhythms in the activity of the *Anopheles* mosquito [174] aligned with increased infectivity of *Plasmodium spp.* gametocytes during the mosquito's blood meal [175]. Furthermore, the direct effect of parasites modulating host circadian

rhythms has been also reported, showing *Trypanossoma brucei* and its effect on the host SCN [170].

As only recently the role of host circadian clocks in parasitic infections has gained popularity, a limited number of studies are available, leaving several questions unanswered. For instance, regarding parasite manipulation of host rhythms: Can this occur during co-infections and if so, how this affects global (and pathogen-specific) host response? Also, can parasites modulate peripheral clocks?

1.2.5. Circadian rhythms during *Plasmodium spp.* infection

Plasmodium spp. dependence and/or alignment with host circadian rhythms have been reported since the 1960s. Initially, a study with monkeys infected with *Plasmodium knowlesi* demonstrated parasite schizogony adaptation to host temperature manipulations [176]. Similar results were obtained with animals infected with *Plasmodium cynomolgi*, showing that the effect was not species-specific.

Moreover, the 24 h erythrocytic cycle in *Plasmodium chabaudi* was shown to be dependent on host melatonin, whereas asynchronous infections were observed with pinealectomized mice [177]. Parasite synchronism must also rely on other host cues/rhythms as the 24-h erythrocyte cycle of *Plasmodium chabaudi* is consistently observed in infections with C57BL/6 mice, a mouse strain that naturally lacks melatonin [178].

The timing of feeding is important in *Plasmodium spp*. synchrony. More specifically, upon an altered feeding schedule (diurnal feeding in nocturnal mice), parasites have inverted almost completely their replication rhythm, in a study using *Plasmodium chabaudi adami DK* [179]. Interestingly, in another study the rhythms in *Plasmodium chabaudi* replication were dependent

on rhythms in host plasma glucose, where schizogony was aligned with the peak of food/glucose intake. Moreover, systemic TNFα production is required for this synchronized event as it contributes to host hypoglycemia acting as an "entrainment" signal for parasites [180]. Similarly, a recent study showed the influence of host feeding schedules on *Plasmodium chabaudi* replication rhythms. However, parasites were able to "catch up" with the 12-h mismatch within approximately 5-6 days, showing relatively fast parasite adaption to changes in host behavioral timing [181].

The effects of host-parasites misalignment have been shown in more studies using the *Plasmodium chabaudi* model. One interesting study showed parasite adaptation when infections were carried out using parasites originated from a host kept in an inversed LD cycle (donor) in respect to the recipient host. The protocol induced a temporal misalignment as parasites transferred to hosts with a different rhythm from their donor, disturbed parasite replication rhythms [182]. Moreover, the production of total parasites and gametocytes was markedly affected by the protocol, with a temporal phase shift observed. Nevertheless, and similarly to what was observed in O'Donnell's 2022 study, after a few cycles, parasites matched host rhythms [182].

Importantly, rhythmic events during *Plasmodium spp.* infection can be indirectly mediated. For instance, in mice infected with *Plasmodium berghei ANKA* a 24-h rhythm in sequestration was detected in the vascular endothelium. This could be resulting from a rhythmic expression of parasite adhesion molecules and/or endothelial proteins (e.g. CD36), but up-to-date no study has attempted to investigate this further. This observation suggests that although PbA is considered a partially asynchronous parasite [183], circadian control events (such as sequestration) can still occur and therefore, result in rhythms during the course of the disease, which should not be ignored [184].

Unfortunately, for studies with *Plasmodium berghei*, so far there is only one study that has looked at whether host circadian rhythms play a role in the infection, by which the focus was to measure the effects on the parasite's intraerythrocytic cycle [185], which is already known to be partially asynchronous. By applying an experimental temporal misalignment (previously used by O'Donnell 2011 study) with "mismatched" PbA parasites, the frequency of each parasite stage form (i.e. rings, trophozoites and schizonts) over the course of the infection was not affected by the treatment. Similarly, the density of ring stage infected red blood cells was not affected by time-restricted feeding [185]. That being said, literature on host rhythms and PbA infection is limited, while most of the studies focus on *Plasmodium chabaudi* for animal research, or *Plasmodium falciparum* for human studies.

On the other hand, advanced studies with both *Plasmodium chabaudi* and *Plasmodium falciparum* [168] have identified the presence of an intrinsic parasitic clock. In this study, over 5,000 *Plasmodium chabaudi* cycling transcripts were detected in the blood of infected mice sampled on day 4 post-infection. Moreover, RNA-seq data obtained from synchronized cultures of *Plasmodium falciparum* identified 361 transcripts (equivalent to approximately 6% of the total genes) with 24 h rhythms [168]. In another study, *Plasmodium chabaudi* infected mice kept in LD or DD and sampled ever 3 h, showed over 4,000 cycling genes irrespective of lighting regimen. This demonstrated that light is not an essential cue for parasite rhythmicity. Furthermore, the 24 h rhythms in the erythrocytic cycle persisted for 5-7 days when infections were performed using arrhythmic clock mutant mice (double-knockout *Cry1*$^{-/-}$*Cry2*$^{-/-}$) and were independent of host food intake [169], bringing contrasting results and suggesting the presence of an independent parasite clock machinery. Interestingly, an intrinsic oscillator has been recently proposed controlling rhythms in the malaria intra-erythrocytic cycle. In the study, transcriptomic experiments were

carried out with 4 *Plasmodium falciparum* strains and a substantial amount of cycling transcripts with characteristics of cell cycle oscillators were revealed [167]. In summary, although the role of host circadian rhythms in malaria has been reported along with the recent discovery of a clock within *Plasmodium spp.* parasites, much more yet remains to be investigated: (I) Whether other *Plasmodium spp.* species also harbor an intrinsic clock. (II) The advantages and function of a clock within parasites, considering that misalignment between host-parasite circadian rhythms often resulted in disturbed parasite rhythmicity. (III) How host circadian rhythms, the clock within immune cells, and *Plasmodium spp.* intrinsic clock, interconnect, and communicate in this disease? Lastly, further studies are still needed to confirm whether rhythms in the parasite intraerythrocytic cycle are exclusively dependent on host rhythms, including metabolism and food intake, given the contrasting results recently published. That being said, in this thesis we have aimed to elucidate the role of host circadian rhythms during *Plasmodium berghei ANKA* infection, focusing on the intra-erythrocytic stage of the disease, while exploring parasite dependency on host rhythms, including feeding behavior.

1.3. Rationale and objectives of the thesis

Considering the rhythms in malaria intra-erythrocytic cycle and host response (i.e. paroxysms), we hypothesized that the magnitude of host response and disease progression is controlled by the synchronized encounter of *Plasmodium spp.*-infected red blood cells with the host, and this is effect is circadian regulated. Therefore, a general objective in this thesis was to study the circadian regulation of *Plasmodium spp.* infection. The specific objectives proposed and executed over the course of this thesis, were:

1. To evaluate the circadian control of host response to *Plasmodium spp.*, at the cellular level (immune response) and systemically (through *in vivo* infections).

This was investigated in chapters 1 and 2, respectively.

2. To evaluate the consequences of host circadian rhythms misalignment during *Plasmodium spp*. infection.

This was investigated in chapter 2 (chronic jet lag experiments).

Chapter 2: Circadian Control of Macrophage Response to *Plasmodium spp*-infected erythrocytes

Chapter 2: Circadian Control of Macrophage Response to *Plasmodium spp.*-Infected Erythrocytes

Priscilla Carvalho Cabral[1], Vincent Richard[2], Martin Olivier[3] and Nicolas Cermakian[1].

priscilla.cabral@mail.mcgill.ca

vincent.richard@ladydavis.ca

martin.olivier@mcgill.ca

nicolas.cermakian@mcgill.ca

[1]Douglas Research Centre, McGill University, Montreal, Quebec, Canada.

[2]Lady Davis Institute for Medical Research, McGill University, Montréal, Quebec, Canada.

[3]Research Institute of the McGill University Health Centre, McGill University, Montréal, Quebec, Canada.

Corresponding author: Dr. Nicolas Cermakian, Department of Psychiatry, McGill University. Office E-2108, Perry Pavillion, 6875 Boulevard Lasalle, Montreal, Quebec, H4H 1R3, Canada. Phone: +1 514-761-6131 ext 4936.

E-mail address: nicolas.cermakian@mcgill.ca

Keywords: Macrophages, circadian rhythms, infected red blood cells, *Plasmodium spp.*, immune responses

2.1. Abstract

Malaria is a serious vector-borne disease characterized by periodic episodes of high fever and strong immune responses which are coordinated with the daily synchronized parasite replication cycle inside red blood cells. As immune cells harbor an autonomous circadian clock which controls several aspects of the immune response, we sought to determine whether the intensity of the immune response to *Plasmodium spp.*, the parasite causing malaria, depends on time of infection. Using red blood cells infected with *Plasmodium berghei ANKA* (iRBCs) we stimulated *ex vivo* bone marrow-derived macrophages (BMDMs) innate immune responses. Lysed iRBCs triggered an immune response in BMDMs. By stimulating at 4 different circadian time points (16 h, 22 h, 28 h or 34 h post-synchronization of the cells clock), rhythms in reactive oxygen species and cytokines/chemokines were found. Furthermore, the analysis of the macrophage proteome and phosphoproteome revealed global changes according to treatment (iRBC or RBC) and to the circadian time point. Interestingly, many of the proteins identified were components of various immune signaling pathways. In summary, our findings showed that the circadian clock within macrophages determines the magnitude of immune response upon stimulation with iRBCs, along with changes of the cell proteome and phosphoproteome.

2.2. Introduction

Malaria is a life-threatening infectious disease responsible over 200 million cases and nearly half a million deaths in the world [1]. It is caused by the protozoan *Plasmodium spp.* and transmitted by *Anopheles spp.* mosquito bite. Within the mammalian host, the parasite differentiates into mature forms able to infect red blood cells during the later stages of the disease. This process culminates with malaria's paroxysms, which are characterized by fever, shaking chills, muscle aches and other features [10] which are the result of the activation of innate immune cells of the monocyte lineage, mainly macrophages. Strong activation of macrophages leads to secretion of pro-inflammatory cytokines which are key factors for the disease severity outcomes, including enhancement of adhesion molecules expression, sequestration of infected red-blood cells in lungs and brain, renal impairment, disruption of the blood brain barrier. Notably, rhythms in symptomatology (malaria paroxysms) occur every 24 h (or a multiple of 24 h). The peak in paroxysms is also coincident with the period of rupture (or lysis) of infected erythrocytes and the high levels of pro-inflammatory cytokines such as TNFα in the bloodstream [38, 186].

Circadian (~24 h) rhythms have been reported in all aspects of physiology and are controlled by circadian clocks found in all tissues [117, 127, 131]. These clocks rely on clock genes, acting via transcription/ translational feedback loops. In the main loop, transcriptional factors BMAL1/CLOCK regulate *Per 1/2* (period) and *Cry 1/2* (cryptochrome) gene expression. Then PER and CRY proteins regulate their own expression by repressing BMAL1/CLOCK activity. This system assures that gene expression and protein production stay rhythmically following a 24-hour cycle as a result of coordinated post-translation modifications events

involving core clock protein phosphorylation and ubiquitin-mediated proteasomal degradation [118].

All immune cell types harbor an intrinsic clock controlling various immune functions [187] [111, 125, 188, 189]. In macrophages, approximately 8% of macrophage's transcriptome is under circadian regulation [140]. Consequently, a number of functions in these cells present circadian rhythms such as phagocytosis [129], ROS generation [144], immune cells trafficking [126, 128, 132], cytokine response to *ex vivo* LPS stimulation [137, 140], cytolytic factor's secretion (i.e. granzyme B, perforin) [190] and more.

In context of *Leishmania spp.* parasitic infection, circadian rhythms in immune cells, impact cell recruitment to the site of infection, parasite load, and cytokine and chemokine production [165]. Interestingly, circadian rhythms were found at the cellular level, upon infection of bone marrow-derived macrophages by *Leishmania spp.,* and those rhythms were lost in cells lacking a functional circadian clock (*bmal1*$^{-/-}$*)* [165].

Whether such a circadian regulation exists for macrophage infection with *Plasmodium spp.* is unknown. Given the strong contribution of the innate immune system to malaria severity [66] it is important to investigate whether host's circadian clocks, in particular macrophage's, influence the magnitude of the immune response to the parasite. In this study we aimed to study circadian rhythms in macrophages upon presentation of lysed *Plasmodium spp.*-infected red blood cells as occurs upon the daily rupture of these cells in infected individuals. We detected circadian rhythms in levels of cytokines and chemokines, and in the generation of reactive oxygen species. This was paralleled by major time-dependent changes in the response of the cellular proteome and phosphoproteome to stimulation.

2.3. Materials and Methods

Mice

Animal use was in accordance with the guidelines of the Canadian Council of Animal Care and was approved by the Douglas Institute Facility Animal Care Committee. Six-week-old male C57BL/6NCrl mice (strain code 027) were purchased from Charles River Laboratories (Saint-Constant, QC). Per2::LUC mice (strain number 006852) were purchased from The Jackson Laboratory. The latter strain was maintained as a breeding colony and placed in ventilated cages housed at the animal facility of the Douglas Mental Health University Institute, in a pathogen-free environment. Mice were under a standard laboratory lighting condition of 12 h of light: 12 h of dark for 2 weeks to acclimate to their surroundings.

BMDM generation and rhythms synchronization

Bone marrow-derived macrophages (BMDMs) were generated by culturing bone marrow from C57BL/6NCrl mice or PER2::LUC mice for 7 days in macrophage medium, composed of Roswell Park Memorial Institute (RPMI) 1640 1x medium (MultiCell, catalog # 350-000-CL) with 10% Corning Nu-Serum IV Growth Medium Supplement (catalog #355104), 1% Gibco Penicillin-Streptomycin (catalog #15070063), and 30% L-cell conditioned medium (LCCM), following published protocol (Trouplin V et al., 2013). Briefly, following euthanasia, legs were placed in 20 mL of macrophage medium. Bone marrow was aspirated from bone, centrifuged, resuspended with 1 mL erythrocyte lysis buffer (BioLegend, catalog #420301) and incubated for 3 minutes. Cells were centrifuged and 0.7×10^6 cells/well were plated in a 6-well plate containing 2 mL of macrophage medium (day 0). Cells were incubated at 37 °C, and on day 4, media was replaced

with fresh macrophage medium. On day 6, the cell rhythms were synchronized by "serum shock method", where 2 mL/well of a mixture containing 50% Gibco horse serum (cartalog #16050122) and 50% macrophages medium was added, after which the cells were incubated at 37 °C for 2 hours, washed with DPBS (Milipore-Sigma, catalog #D8537), and placed in macrophage medium for future experiments.

Bioluminescence recordings

For bioluminescence rhythms recordings, BMDMs from PER2::LUC mice after rhythms synchronization, received 1 mL/well of recording medium containing RPMI without phenol red (Gibco, catalog #11835) with 10% Corning Nu-Serum IV Growth Medium Supplement, 1% Gibco Penicillin-Streptomycin and 0.1 mM D-Luciferin. Plates were sealed with a sterile glass coverslip and bioluminescence was recorded using Lumicycle equipment (Actimetrics).

Generation of iRBCs

C57BL/6NCrl mice were injected intraperitoneally at ZT6 with 10^6 *Plasmodium berghei, strain ANKA* 676m1cl1 (MRA-868 Bei Resources) (PbA)-infected red blood cells (iRBCs) 5 days after receiving daily intraperitoneal injections of 4 mg iron dextran (Milipore-Sigma, catalog #D8517). After infection, mice received additional daily injections of 4 mg iron dextran up to day 5 post-infection. Infected blood was collected at ZT6 by cardiac puncture (terminal) when parasitemia reached 37% (day 18 post-infection). Blood was also collected from a non-infected mouse (control) at ZT6. Cells were separated by centrifugation and pellet resuspended in sterile DPBS. Cells were counted and lysed with an ultrasonic sonicator for 15 seconds. Lysates were kept at -80 °C for future stimulation assays.

BMDM stimulation and cytokine/chemokine measurement

After BMDM synchronization, recombinant murine Interferon-gamma (IFNγ) (PeproTech, catalog #315-05) was directly added to the wells to induce cell maturation and M1 polarization (final concentration of 10U/mL) 16 h, 22 h, 28 h or 34 h after synchronization. After 30 minutes, cells received either macrophage medium (negative control), lipopolysaccharides (LPS) from *Escherichia coli* O111:B4 (Milipore-Sigma, catalog #L2630) at a final concentration of 100 ng/mL (positive control), or 10^6 intact or lysed iRBCs. Wells were washed after 3 h and cells collected and either placed in TRIzol (Invitrogen™, catalog #15596026) (for mRNA assays) or supernatant was collected after 24 h for protein quantification (Mouse Cytokine Proinflammatory Focused 10-Plex Discovery Assay® Array) by Eve Technologies (Calgary, AB).

RT-qPCR

RNA was extracted using the phenol/chloroform method from samples frozen in TRIzol. Reverse transcription was performed using the "High-Capacity cDNA Reverse Transcription" kit (Applied Biosystems, catalog # 4368814) according to manufacturer's instructions. Real time quantitative PCR reaction was done using "iTaq Universal SYBR Green Supermix" (BioRad, catalog # 1725120). The reaction (final volume 10 μL) was ran using 0.4 ng of cDNA (6 μL), 10 μM Forward Primer (0.5 μL), 10 μM Reverse Primer (0.5 μL) and 5 μL SYBR Green. Samples were run at the QuantiStudio™ 6 Flex System (Applied Biosystems). Actin and GAPDH were used as housekeeping genes. Gene expression was determined using the comparative quantification method ($\Delta\Delta C_t$ method). Primers sequences are available at the supplementary materials section (Table 1).

Immunoblotting

BMDMs were stimulated as in previous section. Protein lysis cocktail (100 μL/well) was added in frozen 6-wells plated cells. The cocktail contained Protease Inhibitor (Sigma-Aldrich, catalog #P2714-1BTL), RIPA buffer (150 mM NaCl, 1% Nonidet P-40, 0.5% sodium deoxycholate, 0.1% SDS and 50 mM Tris pH 7.4), Phenylmethylsulfonyl fluoride (PMS-F), and Phosphatase Inhibitor (Sigma-Aldrich, catalog #P5726). Cells were scraped from wells and homogenized on ice, after which they were centrifuged at 13.000 g for 3 minutes, at 4 °C. Samples were added 1:1 into a solution containing 80% 2x Laemmli sample buffer + 20% DTT 1M, and placed at 95 °C for 10 minutes. Samples were stored at -20 °C. Protein concentrations were quantified using DC Protein Assay Kit (Bio-Rad, product #5000111), according to manufacturer's instructions and read using a SpectraMax® 190 Absorbance Plate Reader (Molecular Devices).

Immunoblotting was performed according to standard protocols, by SDS-PAGE (10 μg of protein/well) followed by transfer to a nitrocellulose membrane (Amersham™ Protran™ 0.45 μm) Ponceau red was used to verify transfer efficiency. Rabbit anti-phospho-ERK1/2 1:2000 (Cell signaling, catalog #9101S), and after stripping (with NaOH 0.1 M) rabbit anti-total ERK1/2 1:2000 (Cell Signaling, catalog #9102S) were used as primary antibodies. Goat horseradish peroxidase (HRP) anti-rabbit IgG 1:2000 (ThermoFisher Scientific, catalog #31460) was used as secondary antibody. Bands were visualized using Clarity™ Western ECL Substrate chemiluminescence reagent kit (BioRad, catalog #1705060). The ChemiDoc™ XRS+ Imager (BioRad) with the Image Lab™ Software (BioRad) was used. Protein relative quantification was performed using ImageJ version 2.1.0/1.53c software. For that, immunoblot images were converted to "grayscale" and the "mean grey value" within each "region of interest" (band) was measured. Background signal was

measured and subtracted from each sample. Sample protein ratio was calculated by dividing the protein value by their respective reference protein (GAPDH) value.

Reactive Oxygen Species assay

BMDMs were plated (0.2 x10^6/well) in MiliCell EZ slide 4-well glass (Milipore-Sigma, catalog # PEZGS0416) on day 5 post-extraction and had their rhythms synchronized the following day. After IFNγ pre-boost and stimulation with medium, LPS 100 ng/mL, 10^6 lysed iRBCs or RBCs for 30 minutes, CellROX Deep Red (ThermoFisher, catalog # C10422) was added to a final concentration of 5 μM along with MytoSpy Orange CMTMROs (BioLegend, catalog #424803) at the final concentration of 500 nM. After 30 minutes cells were washed with DPBS and fixed in 4% PFA for 10 minutes, then washed, and incubated with DAPI solution (1:10,000 in DPBS, Milipore-Sigma, catalog #D9542) for 2 minutes and washed. A coverslip was placed on the slides and cells were imaged at 40X using an Olympus FV1200 Confocal Microscope. Analysis was performed using ImageJ version 2.1.0/1.53c.

Sample preparation for proteomics and phosphoproteomics

BMDMs were generated as previously described. Cells were synchronized and pre-boosted with IFNγ (30 minutes) followed by the addition of 10^6 lysed iRBCs or RBCs for 2 hours, at 22 or 34 h post-synchronization. Cells were washed, detached, pooled (20 x 10^6 cells/sample) and centrifuged. Samples' pellet was flash-frozen in liquid nitrogen, followed by lysis in protein extraction buffer containing 5% SDS in 100 mM TRIS pH 8.5 supplemented with PhosStop phosphatase and cOmplete protease inhibitors (both from Roche). Samples were heated at 95 °C for 10 minutes and subjected to probe-based ultrasonication (Thermo Sonic Dismembrator).

Samples were clarified by centrifugation at 21,000 g for 5 minutes. Protein disulfides were reduced in 20 mM tris(2-carboxyethyl)phosphine for 30 minutes at 60 °C, and alkylated in 25 mM iodoacetamide for 30 minutes at room temperature. Proteins (200 µg) were proteolytically digested with trypsin (Sigma) at a 1:20 enzyme to substrate ratio overnight at 37 °C using S-TRAP mini cartridges (Protifi). Peptides were eluted from S-TRAP micro cartridges sequentially with 50 mM ammonium bicarbonate, 0.1% formic acid, and 50% acetonitrile respectively. Approximately 5% of the sample was reserved for total proteome profiling, whereas the remainder was vacuum concentrated to dryness, and reconstituted in 80% acetonitrile with 0.1% TFA prior to automated phosphopeptide enrichment using an Agilent Bravo liquid handling system equipped with an AssayMap head, and AssayMap Fe-(III)-NTA immobilized metal affinity chromatography (IMAC) enrichment cartridges. Peptide-containing eluates were frozen at -80 °C and lyophilized. An equivalent of 750 ng of peptide or the complete phosphopeptide-enriched sample were loaded onto Evotips (Evosep) according to the manufacturer's instruction prior to LC-MS/MS.

LC-MS/MS data acquisition and analysis

Samples were analyzed by data dependent acquisition (DDA) based label free quantitation using an Evosep One LC system coupled to a Thermo Q Exactive Plus mass spectrometer. Peptides were separated using the 15 samples per day extended method, with an EV1137 analytical column (Evosep). MS acquisition was conducted DDA-mode, based on the top 15 most intense precursor ions (+2 to +4 charge state). Full MS scans were acquired at 70K resolution from 350 – 1500 m/z (AGC 1E6, 50ms max injection time), and MS2 spectra were collected at 17.5K resolution (AGC 2E4, 64ms max injection time) using a normalized collision energy (NCE) of 28. Dynamic exclusion was set to 40. MS/MS data were analyzed using Proteome Discoverer version 2.5

(Thermo) and database searching was performed with the Sequest HT node, against a mouse reference proteome FASTA file containing only reviewed canonical sequences downloaded from Uniprot (v2022-06-14). Proteins were quantified based on unique peptides, scaled based on total peptide abundance, and missing values were imputed using the low abundance resampling method.

Statistical analysis

Protein expression ratios were calculated based on protein abundance, and p-values were calculated using ANOVA (individual proteins) within PD 2.5. Statistical analyses were performed using GraphPad Prism version 9.3.1. For BMDM stimulations (RT-qPCR), peritoneal cells recruitment, ROS generation and immunoblotting quantification, one-way ANOVA with Tukey's multiple comparison analysis were used. Rhythm analysis was performed using Non-linear regression (curve-fit) cosinor analysis where a cosine wave equation $y = B + (A*cos(2*\pi*((x-Ps)/24)))$, where A = amplitude, B = baseline, Ps = phase shift, with a fixed period of 24h was fit. Significance was calculated based on F-value (observed R^2, sample size and number of predictors). All p values <0.05 were considered significant. The data are expressed as the mean ± SEM.

2.4. Results

Response of macrophages to lysed *Plasmodium berghei ANKA*-infected red blood cells

To investigate the response of macrophages upon stimulation with *Plasmodium berghei ANKA*-infected red blood cells (iRBCs), bone-marrow derived macrophages (BMDMs) from C57BL/6N mice were generated and presented with 10^6 intact of lysed iRBCs, which were collected (on day 18 post-infection) from an iron dextran-treated mice infected with *P. berghei ANKA.* Iron dextran treatment has been shown to prevent mouse lethality from cerebral malaria and to generate a sustained infection with high levels of parasitemia (infected erythrocytes) when administered 5 days prior and 5 days after infection with *P. berghei ANKA* [92]. Infected blood was collected when parasitemia reached 37% (*Fig. 1A*) and was either lysed or used intact to be presented to BMDMs pre-boosted with Interferon-gamma (IFNγ). In the absence of IFNγ, BMDMs were unable to induce a pro-inflammatory response upon presentation of lysed iRBCs (data not shown). Macrophages proinflammatory response was evaluated by RT-qPCR for the pro-inflammatory cytokine interleukin-6 (IL-6). *Il-6* gene induction was not detected upon stimulation of cells with non-infected RBCs or with intact iRBCs (*Fig. 1B*). Interestingly, *Il-6* induction was achieved upon stimulation with lysed iRBCs but not with lysed non-infected RBCs (control) (*Fig. 1B*), similarly to stimulation with the positive control lypopolysaccharide (LPS).

Rhythms in macrophage proinflammatory response following stimulation with *Plasmodium berghei ANKA*-infected red blood cells

To investigate if BMDMs stimulation with lysed iRBCs leads to an inflammatory response in a time-dependent manner, cells had their circadian rhythms synchronized using a serum shock

[191] and synchronization was verified by bioluminescence recordings of BMDM from PER2::Luciferase knockin mice (*Fig. 2A*). BMDMs were synchronized 6 hours apart from each other over 24 h, and then, stimulated with IFNγ followed by addition of lysed iRBCs (or RBC) at 16 h, 22 h, 28 h or 34 h after synchronization. This allowed cells to be stimulated at the same "clock time" while they were at different phases of their circadian clock, with the same batch of iRBCs. Thus, the magnitude of the immune response generated afterwards (measured by RNA or protein) will indicate dependency of the macrophages circadian clock.

Initially, in cells collected 3 h after iRBC stimulation, the induction of genes encoding interleukin-6 (IL-6), interleukin-1 beta (IL-1β) and tumor necrosis factor alpha (TNFα) (*Fig. 2B)* showed time dependency. This was also true for IL-1β and interleukin-12p70 (IL-12p70) in cell supernatant collected 24 h after stimulation. Trends were found for monocyte chemoattractant protein-1 (MCP-1) ($p=0.088$) and IFNγ ($p=0.077$), and a lack of rhythmicity for TNFα, IL-6, granulocyte-macrophage colony-stimulating factor (GM-CSF) and interleukin-10 (IL-10) (*Fig. 2C).* As expected, in both RNA and protein measurements, immune activation was undetected when cells were stimulated with non-infected RBCs.

Next, as a first step to investigate intracellular events involved in the response of macrophage to *Plasmodium spp.*, we assessed the generation of reactive oxygen species (ROS). A pilot time-course of ROS indicated higher levels after 30 minutes of incubation of BMDMs with lysed iRBCs (data not shown), but not in cells treated with lysed RBCs (*Fig. 3A*). BMDM clock were synchronized and stimulated with lysed iRBC at 4 different time points, for 30 minutes, and ROS were measured (*Fig. 3B*). Even though a not significant rhythm in ROS generation was detected (cosinor, $p = 0.20550$), specific time-point differences were still found - stimulation of

cells at 22h after synchronization lead to significant higher levels of ROS when compared to 16 h and 28 h stimulation time-points (*Fig. 3B*).

Changes in macrophage proteome and phosphoproteome following stimulation with *Plasmodium berghei ANKA*-infected red blood cells

For an in-depth investigation of the intracellular networks and key players affected by iRBC in macrophages in a circadian time-dependent manner, we have used the same experimental approach and have analyzed the whole proteome of BMDMs stimulated at 22 h or 34 h time-points post-synchronization. From each sample, 5% was used for cell proteome analysis and the remaining material was enriched using immobilized metal affinity chromatography (IMAC) to obtain cell phosphopeptides. Analysis was performed using liquid chromatography and high-resolution mass spectrometry (LC/MS) (*Fig. 4A*). Approximately 3500 proteins were quantified, among which 425 were found to be differentially expressed in at least one of the 4 comparisons (iRBC vs CTRL 22 h, iRBC vs CTRL 34 h, iRBC 22 h vs 34 h, CTRL 22 h vs 34 h). Furthermore, 4600 phosphopeptides were detected among which 825 were differentially expressed in at least one of the 4 comparisons (*Fig. 4B*). Also, 747 phosphosites showed more than a half of the phosphorylation events happening at the serine residues, followed by threonine, and in lesser extent, tyrosine (*Fig. S2*). We next analyzed the pool of proteins differentially expressed in iRBC treated samples 22 h vs 34 h, and we detected 100 downregulated and 57 upregulated proteins. In addition to that, 234 upregulated and 162 downregulated phosphopeptides were detected (*Fig. 4C*) within the pool of samples treated with iRBC and compared between time points (i.e. iRBC 22 h vs 34 h).

Interestingly, when we analyzed the list of 157 proteins affected by time point and treatment (iRBC), we found that the majority of proteins were involved in stress response,

metabolism, cell adhesion and cell cycle. By using this list, we were able to identify 3 main signaling pathways: PI3K-Akt-mTOR, Type II Interferon and MAPK signaling pathway (*Fig. 4D)*. Proteins such as, Itgb5, Col1a1, Rap1a, KRAS (PI3K-Akt-mTOR pathway), IL-1β, CXCL9 (Type II Interferon pathway), Mapk3k20 (MAPK pathway) and more, were significantly affected by time point and iRBC stimulation. Additionally, we have identified a list of 16 phosphopeptides upregulated at 22 h time point, and 24 at 34 h time point (*Table 1)*. These were exclusively upregulated in samples treated with iRBC. In other words, they were not upregulated in any other comparison (i.e. control samples). To complement this, Ingenuity Pathway Analysis (IPA) revealed enrichment in both proteome and phosphoproteome datasets, showing over 30 signaling pathways, either positively or negatively enriched in the iRBC treated samples when compared between time points (*Fig. 5A*).

Furthermore, the interconnection of both cellular proteome and phosphoproteome revealed a repertoire of upregulated proteins and phosphopeptides at 22 h and 34 h time points following stimulation with iRBCs. Their relationship within intracellular networks, such as JNK and p38 signaling pathway and chemokine signaling pathway, was illustrated in a simplified diagram (*Fig. 6*).

Investigation of ERK MAPK signaling pathway following stimulation of macrophages with *Plasmodium berghei ANKA*-infected red blood cells

We next sought to investigate if activation of the ERK MAPK pathway, which is known to be involved in the response of macrophages to *Plasmodium spp*. [69] exhibit circadian rhythms in our model. Stimulation of BMDMs with lysed iRBCs (but not with uninfected RBCs led to activation of phosphorylated ERK1/2 with a peak after 2-4 h (*Fig. S3*). BMDM clocks were then

synchronized and stimulated at different time points post serum shock with lysed iRBCs for 2 h. Despite MAPK signaling pathway was predicted to be affected by time and iRBC treatment in our proteomics analysis, phosphorylation of ERK1/2 was not significantly affected by time points (*Fig. 7*).

2.5. Discussion

Here we reported that the response of macrophage to *Plasmodium spp.*-derived molecules, more specifically lysed infected red blood cells, is affected by the circadian clock in these cells. In this context, we have detected rhythms in cytokine/chemokine production, reactive oxygen species generation, and strong effects in the cell proteome and phosphoproteome. We have also observed that immune responses to *Plasmodium spp.* infected red blood cells is restricted to the nature of the material presented to cells (intact vs lysed), with a failure to induce pro-inflammatory responses upon presentation of intact cells.

During malaria pathogenesis, innate immunity, in particular macrophages/monocytes, play a crucial role at recognizing *Plasmodium spp.*-derived particles, resulting from the burst of red blood cells, and initiating a cascade of pro-inflammatory responses. Several studies have demonstrated strong immunomodulatory effects of such molecules, in special haemozoin, through the activation of a variety of signaling pathways, such as NF-kB [69, 74], MAPK [73, 74], NLRP3 inflammasome [77]. Moreover, during the burst of infected red blood cells, malarial DNA is often engulfed by macrophages/monocytes, which are induces Toll-like receptor 9 activation as well as several cytokines [71, 72].

Given that, not only one, but several molecules are known to be released from infected red blood cells during lysis, we chose to stimulate macrophages with mouse blood containing *P. berghei ANKA*-infected red blood cells, as a more realistic "proxy" to study circadian rhythms in immunity during malaria pathogenesis, considering that studies performed with isolated compounds, such as haemozoin, lack a more accurate representation of the events at the erythrocyte stage of the disease [192]. To circumvent this, our stimulation model consisted of a

mix of infected and non-infected red blood cells, collected from a mouse with parasitemia of 37% (iRBCs). Interestingly, a macrophage immune response was detected upon presentation of a lysed material, but not its non-lysed form, consistent with other studies [82, 83].

After confirming that our lysed iRBC model led to a pro-inflammatory response in both *ex vivo* and *in vivo* approaches, we found that the magnitude of this response is influenced by the phase of the macrophage's clock at the time of iRBC stimulation. In other words, stimulations at different time points (6 h apart) after macrophage circadian clock synchronization, led to variable levels of immune activation. Nevertheless, not all cytokines/chemokines showed rhythmic expression, such as TNFα and IL-6, as both demonstrated no changes in protein expression across time points. Aligned with this, when we correlate the findings obtained with the multiplex cytokine/chemokine screen with the proteomics dataset, even though TNFα was detected among the pool of proteins affected by our iRBC treatment, it did not pass the criteria of significantly being affected by time. Despite this, we found that production of IL-1β was highly rhythmic, which was further supported by our proteomic screen, where IL-1β was detected as one of the proteins affected by iRBC treatment in a time-dependent manner (upregulation at 22 h post-synchronization). Rhythms in pro-inflammatory cytokines, including IL-1β, corroborate with the paroxysms events in malaria, as a result of rhythms in the burst of infected red blood cells [36]. Moreover, a murine air pouch model to study host response to malaria detected increased levels of proinflammatory cytokines (IL-6, IL-1α, IL-1β) and chemokines (MCP-1, MIP-1α, MIP-1β) and more, following haemozoin challenge [75].

In addition, our proteomics screen showed IFNγ upregulated at 34 h in the pool of iRBC-stimulated samples, which is one of the cytokines involved in malaria rhythmic fevers [193]. In addition to that, in our data, a trend for a 24-h rhythm in IFNγ was detected. Interestingly, the

circadian clock in immune cells been extensively reported as regulating activation and production of pro-inflammatory cytokines [137, 140]

Other aspects of the immune response in a context of iRBC stimulation were affected by the circadian time-points, including ROS generation. Upon iRBC presentation, but not RBC, the ROS levels were strongly affected by the time points. Notably, ROS induction is also known to be important during haemozoin presentation and it is directly linked to the activation of NLRP3 inflammasome pathway, and IL-1β production [80]. Moreover, NF-$\kappa\beta$ translocation following haemozoin administration requires ROS, as in the presence of antioxidant enzyme SOD, this event is impaired [73]. ROS generation has also been shown to be controlled by PKC activity. In the context of haemozoin stimulation, phosphorylation of PKC dependent substrates was detected in BMDMs. Interestingly, administration of a PKC inhibitor impaired ROS production and IL-1β maturation [80].In our study, 22 h time point was the peak of both IL-1β (protein) and ROS generation. Interestingly, it has been previously shown that macrophages circadian clock directly controls ROS and IL-1β production, through direct interaction of BMAL1 with NRF2 [144]. Moreover, clock protein, REV-ERBα, was showed to bind to *Nlrp3* promoter and repress its transcription [160], demonstrating that NLRP3 is regulated by the circadian clock. Furthermore, proteins such as Ras-related protein Rap-1 (Rap1), G protein subunit γ 14 (GBγ), Proto-oncogene c-Src (Src), and Rho associated coiled-coil containing protein kinase 2 (ROCK2) were upregulated at 22 h time point in our proteomics and phosphoproteomics screen, which are all known to be involved in the chemokine signaling pathway and ROS events [194, 195]. Interestingly, haemozoin in monocytes have already been showed to induce IL-1β production via Src kinases [77].

Proteomics analysis of samples treated with iRBCs also revealed, at 22 h, upregulation of chemokines, including CXCL2 and CXCL9, as well as transcriptional factors involved in in

immune signaling pathways, such as IRF3. These downstream events are linked to an activation of NF-κB, and JNK and p38 signaling pathway at 22 h post-synchronization. Interestingly, phosphorylation of p38 and JNK1/2 was reported in monocytes stimulated with haemozoin, as well as phosphorylation of MAPK activated protein kinase 2 (MAPKAPK-2), a substrate of p38 [70]. Moreover, involvement of NF-κB pathway in haemozoin response has been already reported, with phosphorylation of IκBα and p50/p65 nuclear translocation [74]. Interestingly, clock regulation (through REV-ERBα repression) of NF-κB have been reported [160]. Recently, the role of NF-κB regulating the clock has been also demonstrated with subunit RELA repressing BMAL1/CLOCK activity [196]. Furthermore, IPA analysis additionally confirmed the enrichment of acute phase signaling pathways at the proteome of cells stimulated with iRBCs in a time-dependent manner. Moreover, at 34 h post-synchronization, MKK4, a JNK activator, was upregulated. Altogether, these results showed that JNK and p38 signaling pathway are modulated by time and treatment.

Interestingly, a comprehensive database analysis study detected 24-h rhythms in the proteome of *Plasmodium vivax* and *Plasmodium falciparum*-infected patients in the serum, plasma and tissue. In this study, analysis of rhythmic host proteins in severe *Plasmodium falciparum*-infected patients showed an enrichment of pathways related to immune response. This included interleukin signaling, acute inflammatory response, post-translational protein phosphorylation and more [197].

Following phagocytosis of *Plasmodium spp.*-derived molecules, phosphorylation of ERK1/2 was also shown to be dependent on the presence of haemozoin, with highest activation in the initial 2-4 hours [69]. Although a time-dependent effect on ERK1/2 phosphorylation was not detected in the immunoblotting assays, our proteomics screen showed that MAPK signaling

pathway is influenced by time points and iRBC treatment, with proteins such as MKK4 and MKK3, upregulated when BMDM were stimulated at 34 h post-synchronization.

Interestingly, it is well known that intracellular signaling pathways, such as p38 and JNK pathway, are intrinsically linked with the circadian clock. Rhythms in MAPK activation as a result of rhythms on phosphorylation of key components, environmental cues (i.e. light), rhythmic expression of activators (i.e. p38 activation by TNFα) have been demonstrated [198]. Downstream effects on the clock have also been reported. For instance, *Per1* is activated while *Dbp* is repressed upon p38 activation via TNFα [199]. Similarly, a recent study showed co-activation of BMAL1 via Vps15, a subunit class of 3 PI3K [200]. Moreover, when BMAL1 is knockdown, many PI3K/AKT signaling proteins such as AKT, ERK1/2 and mTOR, are inhibited [201].

Furthermore, in our list of phosphoproteins upregulated at 22 h, in comparison to 34 h, in samples treated with iRBCs, several Rho GTPases were present. Aligned with this, we have also detected "Fcγ Receptor Mediated Phagocytosis" as one of the top 3 enriched pathways in our IPA analysis of the cellular phosphoproteome. The role of Rho GTPases in phagocytosis (endocytic pathway) is well known [202]. Not surprisingly, haemozoin engulfment via phagocytosis is an important event [70], and a clock control of macrophages phagocytosis has already been demonstrated [203].

A limitation of the proteomics assay conducted in this study is that only 2 time points (22h and 34h post-synchronization) were used. In order to confirm if the proteins and phosphoproteins identified in the macrophage response to iRBC are under the control of the macrophage circadian clock, follow up experiments would need to be carried out. More specifically, assessment of protein expression level (as well as its phosphorylation status) at 4 time points or more over 24 h would allow the validation of circadian rhythmicity. Alternatively, stimulations with clock genes

knockout macrophages could be performed. Nevertheless, in our proteomics cohort we were able to identified several proteins and phosphoproteins affected by time of stimulation in a iRBC-dependent manner.

In summary, we showed that stimulation of macrophages at different circadian time points with *P. berghei ANKA*-derived molecules, results to different levels of immune response. Our study represents the first study to look at the effects of the macrophage circadian clock in the response to *Plasmodium spp.*-derived molecules. By using an iRBC stimulation model which represents a realistic approach to study immune activation during malaria erythrocytic stage.

2.6. Acknowledgments

The authors thank the members of Cermakian and Olivier laboratories for discussions, knowledge sharing, technical training and reagents. We also thank Marie-Ève Cloutier for experimental assistance. Furthermore, we thank the staff of the Immunophenotyping Platform at the McGill University Health Centre, the Molecular and Cellular Microscopy Platform and the Animal Facility at the Douglas Research Centre, plus all their respective staffs. This study was supported by grants from the Canadian Institutes of Health Research (PJT-168847, to NC and MO), and from Douglas Foundation, and doctoral fellowships from Faculty of Medicine and Health Sciences – McGill (to PCC), and from Fonds de Recherche du Québec – Santé (to PCC).

2.7. Figures

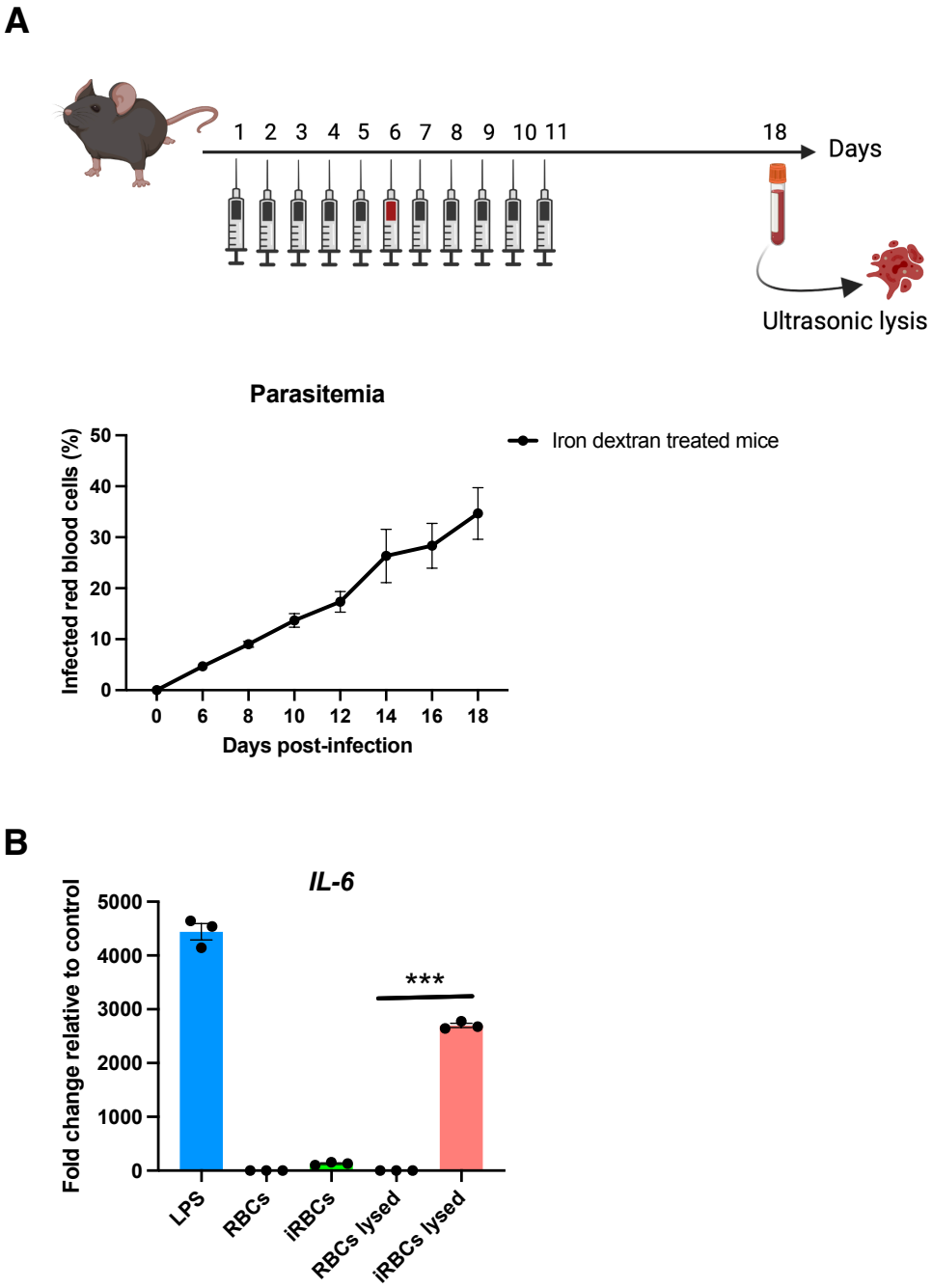
A
1 2 3 4 5 6 7 8 9 10 11
18
Days
Ultrasonic lysis
Parasitemia
Iron dextran treated mice
Infected red blood cells (%)
50
40
30
20
10
0
0 6 8 10 12 14 16 18
Days post-infection
B
IL-6
Fold change relative to control
5000
4000
3000
2000
1000
0
***
LPS
RBCs
iRBCs
RBCs lysed
iRBCs lysed

Figure 1. Lysed infected RBCs, but not intact cells, leads to macrophage proinflammatory response.

Generation of lysed infected RBCs and non-infected RBCs, followed by macrophage stimulation. **(A)** Mice were treated with 10 injections of iron dextran (5 before and 5 after infection) and infected with *Plasmodium berghei ANKA* infected red blood cells. Blood was collected on day 18 post-infection, processed, and parasitemia was measured every 2 days after day 6 post-infection. **(B)** BMDM were pre-boosted with IFNγ followed by stimulation with intact or lysed infected red-blood cells, intact or lysed non-infected red-blood cells, medium or LPS. RNA was collected 3 hours after for RT-qPCR assay. Legend for illustration: dark syringes: iron dextran administration, red syringe: *Plasmodium berghei ANKA* infected red blood cells administration on day 6, blood collection tube: collection of red blood cells on day 18 post-infection. One-way ANOVA with Tukey's multiple comparisons test for (B). Sample size of 3-4 mice per group. Data are shown as mean $\pm$ SEM. ***$p<0.001$. The left panel of (A) was created with BioRender.com.

A

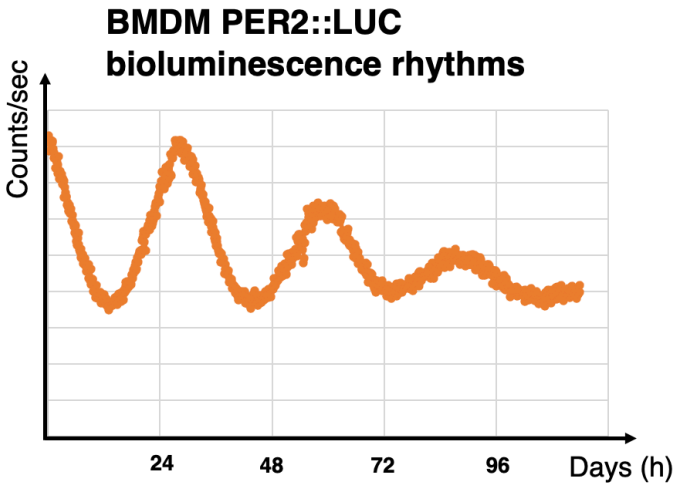
BMDM PER2::LUC
bioluminescence rhythms
Counts/sec
24
48
72
96
Days (h)

B

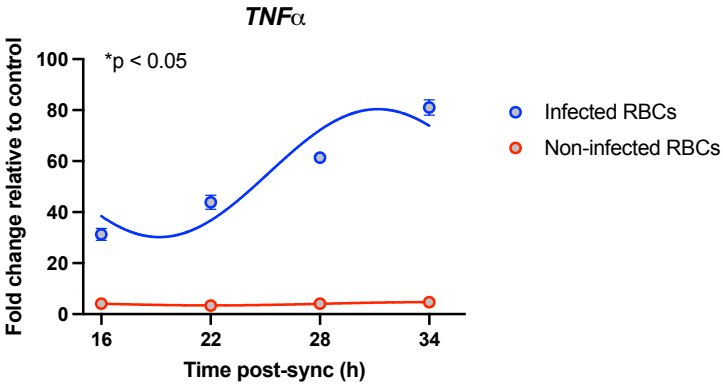
TNFα
*p < 0.05
Fold change relative to control
100
80
60
40
20
0
16
22
28
34
Time post-sync (h)
Infected RBCs
Non-infected RBCs

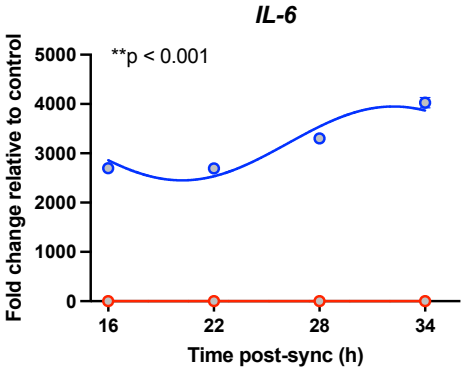
IL-6
**p < 0.001
Fold change relative to control
5000
4000
3000
2000
1000
0
16
22
28
34
Time post-sync (h)

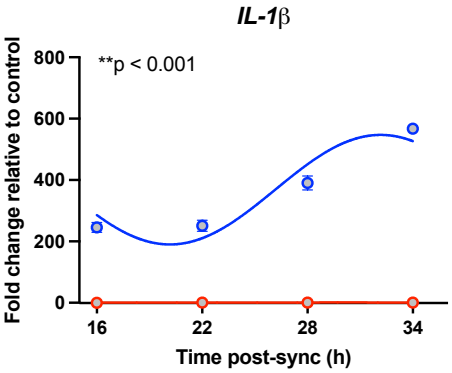
IL-1β
**p < 0.001
Fold change relative to control
800
600
400
200
0
16
22
28
34
Time post-sync (h)

C

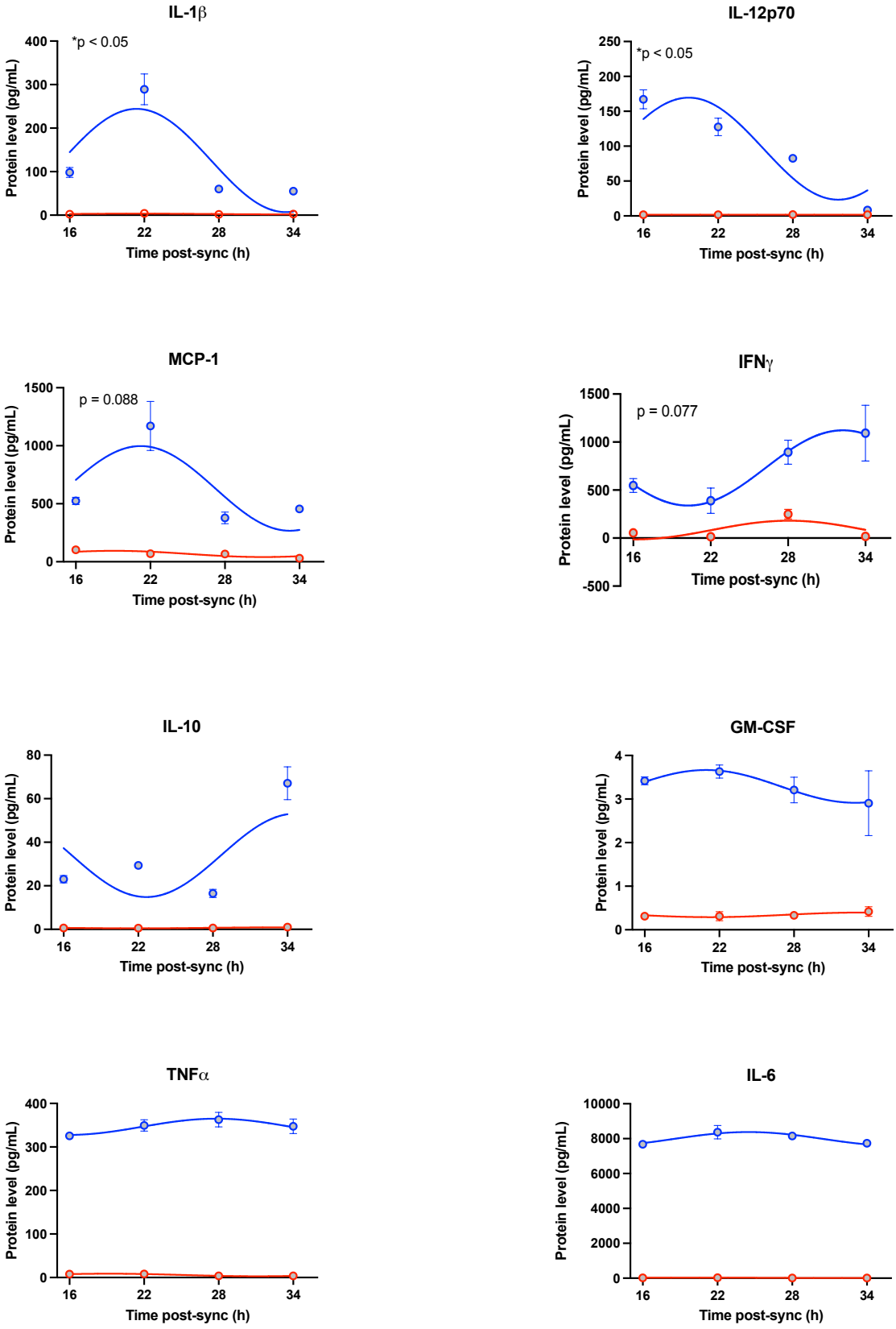
IL-1β
*p < 0.05
Protein level (pg/mL)
Time post-sync (h)
IL-12p70
*p < 0.05
MCP-1
p = 0.088
IFNγ
p = 0.077
IL-10
GM-CSF
TNFα
IL-6

Figure 2. Circadian regulation of macrophage proinflammatory response.

Rhythms in macrophage response following lysed RBC stimulation. **(A)** Real-time analysis of circadian rhythms of BMDMs from PER2::LUC mice. Bioluminescence was recorded across 5 days. **(B, C)** BMDM were synchronized with a serum shock at different time points across 24 h and pre-boosted with IFNγ followed by stimulation with lysed infected red blood cells or non-infected red blood cells at 16 h, 22 h, 2 8h or 34 h post-synchronization. RNA was collected 3 h after and subjected a RT-qPCR or supernatant collection 24 h later for multiplex cytokine/chemokine array. Control samples for RNA: BMDM stimulated with medium. Non-linear regression (curve fit): Cosinor analysis for (B) and (C). Sample size of 3-4 samples per group. Data are shown as mean $\pm$ SEM. $p < 0.05$.

A

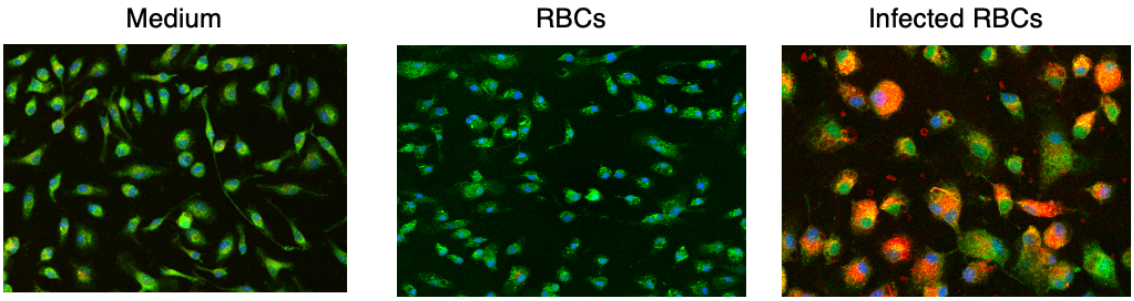
Medium
RBCs
Infected RBCs

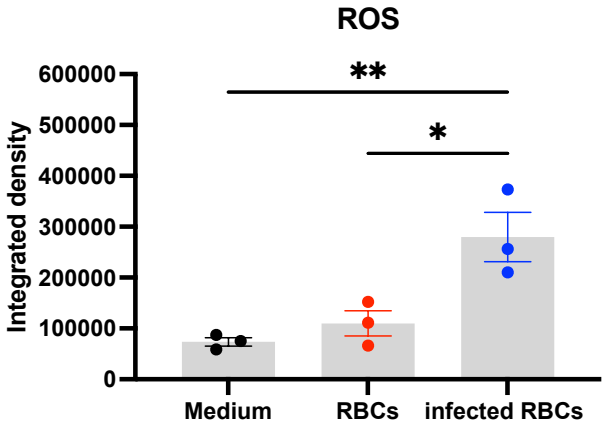
ROS
**
*
Integrated density
600000
500000
400000
300000
200000
100000
0
Medium
RBCs
infected RBCs

B

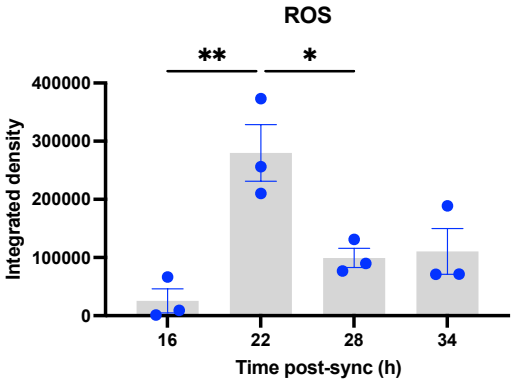
ROS
**
*
Integrated density
400000
300000
200000
100000
0
16
22
28
34
Time post-sync (h)

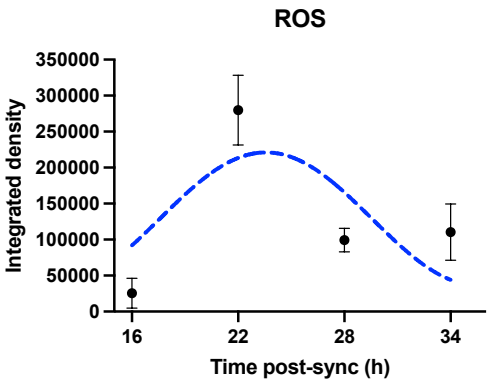
ROS
Integrated density
350000
300000
250000
200000
150000
100000
50000
0
16
22
28
34
Time post-sync (h)

Figure 3. Lysed infected RBCs leads to generation of reactive oxygen species in a time-dependent manner in macrophages.

BMDM stimulation with lysed infected RBCs and ROS measurements. **(A)** Confocal microscopy at 40 X (and its quantification) of BMDMs pre-boosted with IFNγ and stimulated with lysed RBCs or iRBCs for 30 minutes followed by the addition of CellROX Deep Red (in red), Mytospy Orange CMTMRoS (in green) and DAPI (in blue). **(B)** Quantification of the integrated density (sum of pixels values) of BMDMs stimulated with lysed iRBCs at 16 h, 22 h, 28 h or 34 h post-synchronization. One-way ANOVA with Tukey's multiple comparisons test (A, B) and non-linear regression (curve fit): Cosinor analysis for (B). Sample size of 2-3 biological replicates originated from the average of 20 cells per sample. Data are shown as mean $\pm$ SEM. *p < 0.05, **p<0.01.

A

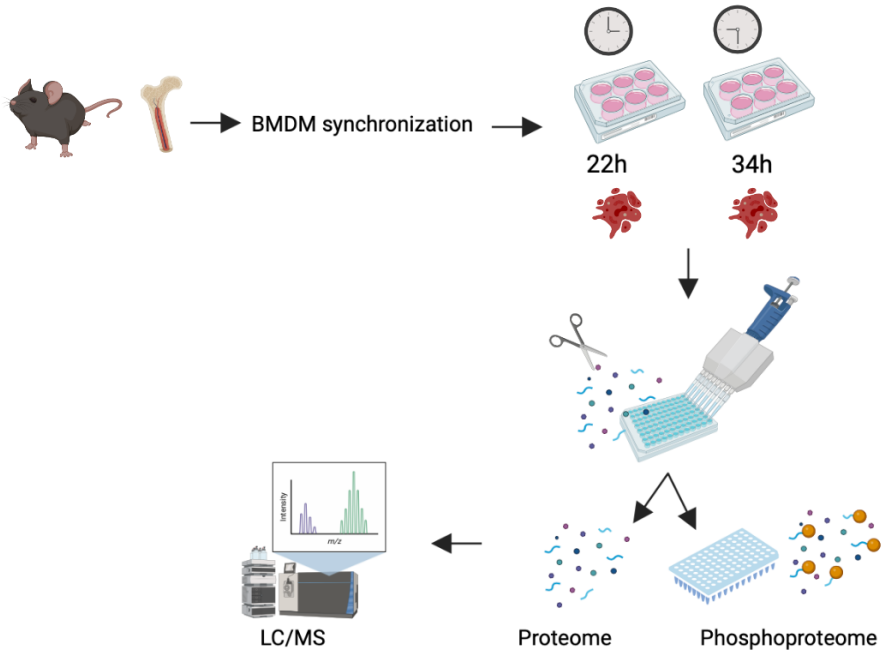
BMDM synchronization
22h
34h
LC/MS
Proteome
Phosphoproteome

B

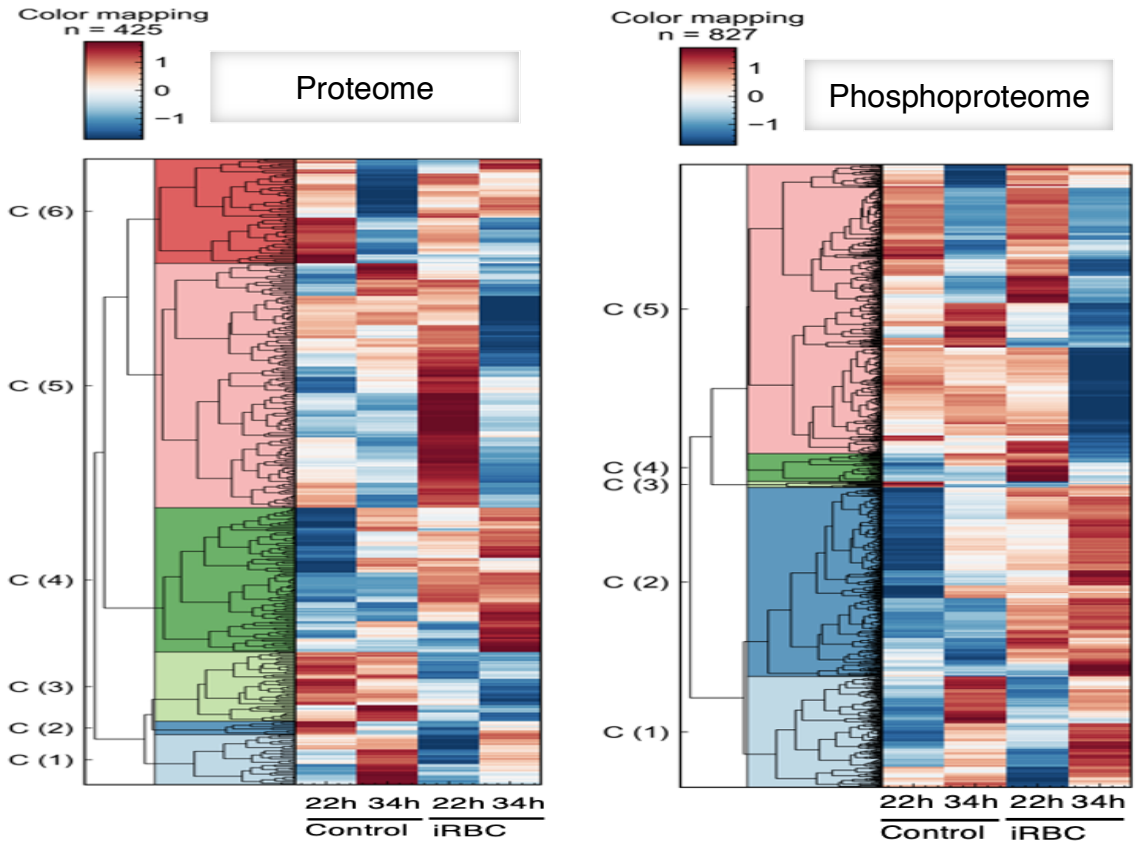
Color mapping
n = 425
1
0
−1
Proteome
C (6)
C (5)
C (4)
C (3)
C (2)
C (1)
22h 34h 22h 34h
Control iRBC
Color mapping
n = 827
1
0
−1
Phosphoproteome
C (5)
C (4)
C (3)
C (2)
C (1)
22h 34h 22h 34h
Control iRBC

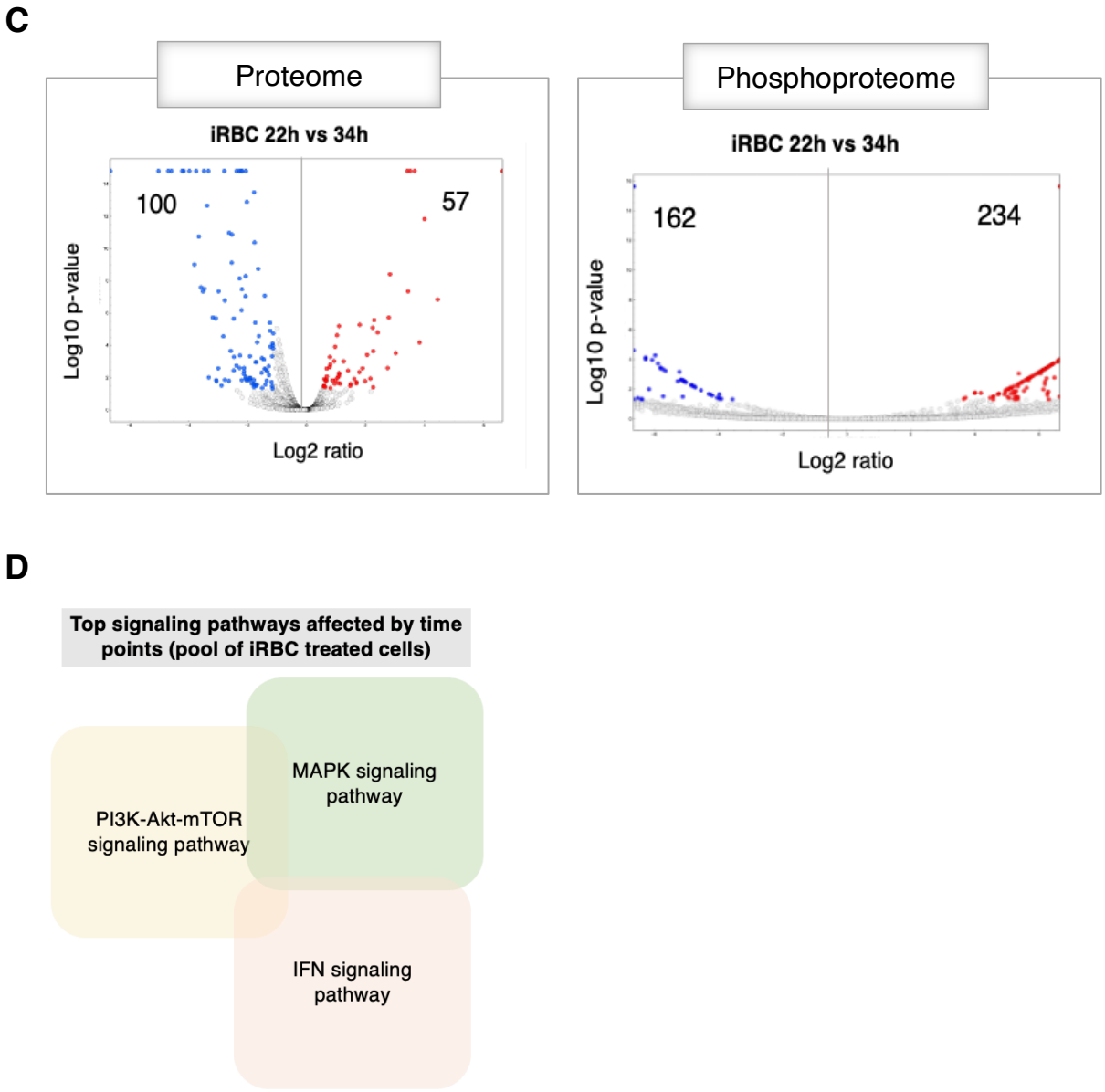

Figure 4. Changes in proteome and phosphoproteome upon stimulation with lysed infected RBCs at different circadian time-points.

Analysis of BMDM proteome and phosphoproteome following infected RBCs stimulation. **(A)** Schematics of the experimental design used to quantify BMDMs proteome and phosphoproteome following 2 h of stimulation with lysed iRBCs at 22 h or 34 h after synchronization. **(B, C)** Hierarchical clustering, and volcano plot of proteins up or downregulated in cells treated with

lysed iRBC or RBC at 2 different time-points, in the proteome and phosphoproteome. **(D)** Summary of the top signaling pathways in the proteome affected by time points (within the pool of iRBC stimulated cells). The illustration on (A) was created with BioRender.com.

Upregulated at 22 h

Gene	Protein
Sirt2	NAD-dependent protein deacetylase sirtuin-2
Prpf38a	Pre-mRNA-splicing factor 38A
Nes	Nestin
Rock2	Rho-associated protein kinase 2
Arhgap45	Rho GTPase-activating protein 45
Src	Proto-oncogene tyrosine-protein kinase Src
Ranbp3	Ran-binding protein 3
Arhgap25	Rho GTPase-activating protein 25
Ptpn12	Tyrosine-protein phosphatase non-receptor type 12
Niban1	Protein Niban 1
Plec	Plectin
Mtmr3	Myotubularin-related protein 3
Nucks1	Nuclear ubiquitous casein and cyclin-dependent kinase substrate 1
Ccnl1	Cyclin-L1
Cbx3	Chromobox protein homolog 3
Hp1bp3	Heterochromatin protein 1-binding protein 3

Upregulated at 34 h

Gene	Protein
Brix1	Ribosome biogenesis protein BRX1 homolog
Manf	Mesencephalic astrocyte-derived neurotrophic factor
Dync1li2	Cytoplasmic dynein 1 light intermediate chain 2
Vps13c	Intermembrane lipid transfer protein VPS13C
Cfl2	Cofilin-2
Hpgd	15-hydroxyprostaglandin dehydrogenase [NAD(+)]
Igf2bp3	Insulin-like growth factor 2 mRNA-binding protein 3
Cdk1	Cyclin-dependent kinase 1
Ctsg	Cathepsin G
Baz1a	Bromodomain adjacent to zinc finger domain protein 1A
Arfip1	Arfaptin-1
Lamc1	Laminin subunit gamma-1
Kpna2	Importin subunit alpha-1
Ldhb	L-lactate dehydrogenase B chain
Fscn1	Fascin
Smc4	Structural maintenance of chromosomes protein 4
Xrcc6	X-ray repair cross-complementing protein 6
Rnps1	RNA-binding protein with serine-rich domain 1
Uhrf1	E3 ubiquitin-protein ligase UHRF1
Ythdf3	YTH domain-containing family protein 3
Zcchc10	Zinc finger CCHC domain-containing protein 10
Naa50	N-alpha-acetyltransferase 50
Ilkap	Integrin-linked kinase-associated serine/threonine phosphatase 2C
Ddx27	Probable ATP-dependent RNA helicase DDX27

Table 1. Analysis of BMDM phosphoproteome following infected RBCs stimulation.

Summary of phosphopeptides upregulated at 22 h or 34 h (exclusively within the pool of iRBC stimulated cells).

Proteome

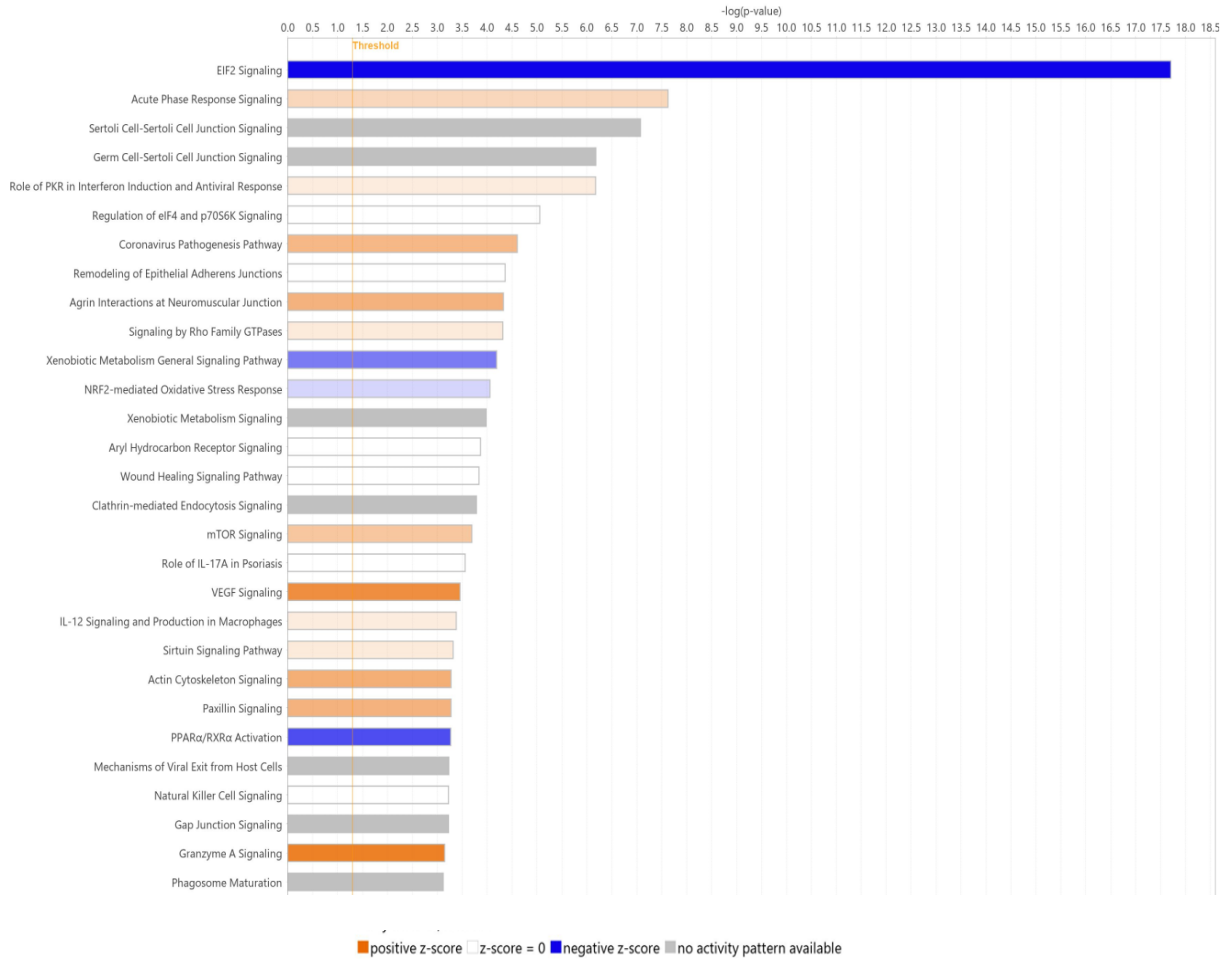
-log(p-value)
0.0 0.5 1.0 1.5 2.0 2.5 3.0 3.5 4.0 4.5 5.0 5.5 6.0 6.5 7.0 7.5 8.0 8.5 9.0 9.5 10.0 10.5 11.0 11.5 12.0 12.5 13.0 13.5 14.0 14.5 15.0 15.5 16.0 16.5 17.0 17.5 18.0 18.5
Threshold
EIF2 Signaling
Acute Phase Response Signaling
Sertoli Cell-Sertoli Cell Junction Signaling
Germ Cell-Sertoli Cell Junction Signaling
Role of PKR in Interferon Induction and Antiviral Response
Regulation of eIF4 and p70S6K Signaling
Coronavirus Pathogenesis Pathway
Remodeling of Epithelial Adherens Junctions
Agrin Interactions at Neuromuscular Junction
Signaling by Rho Family GTPases
Xenobiotic Metabolism General Signaling Pathway
NRF2-mediated Oxidative Stress Response
Xenobiotic Metabolism Signaling
Aryl Hydrocarbon Receptor Signaling
Wound Healing Signaling Pathway
Clathrin-mediated Endocytosis Signaling
mTOR Signaling
Role of IL-17A in Psoriasis
VEGF Signaling
IL-12 Signaling and Production in Macrophages
Sirtuin Signaling Pathway
Actin Cytoskeleton Signaling
Paxillin Signaling
PPARα/RXRα Activation
Mechanisms of Viral Exit from Host Cells
Natural Killer Cell Signaling
Gap Junction Signaling
Granzyme A Signaling
Phagosome Maturation
positive z-score
z-score = 0
negative z-score
no activity pattern available

Phosphoproteome

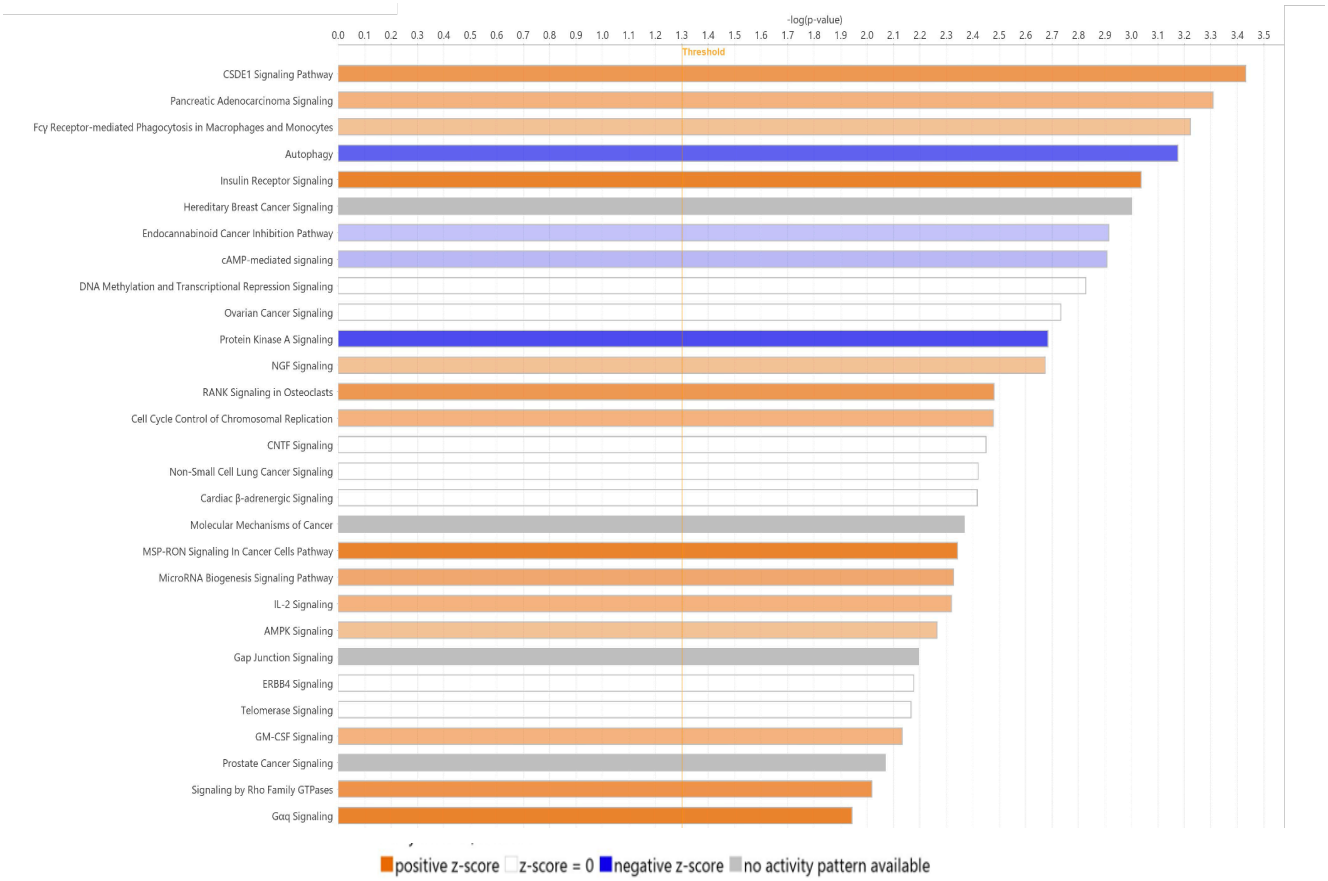

Figure 5. Enriched pathways on the proteome and phosphoproteome upon stimulation with lysed infected RBCs at different circadian time-points.

Pathway analysis of the proteome and phosphoproteome dataset, showing the top 29 positively or negatively enriched canonical pathways in iRBC treated samples, in a time-dependent manner. List of pathways are ordered by statistical significance (p-value) Pathways analysis was performed using Qiagen Ingenuity Pathway Analysis (IPA).

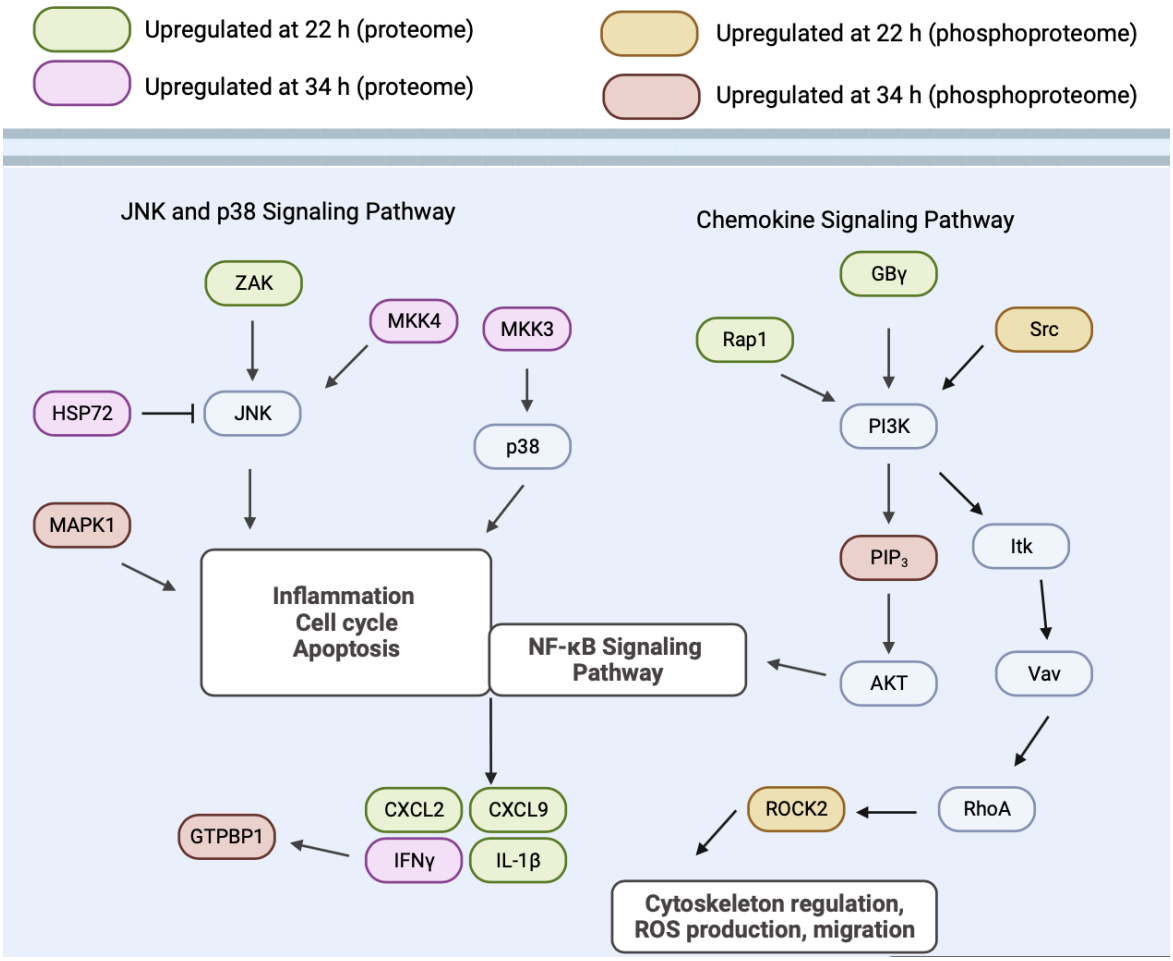

Figure 6. Graphical summary of key pathways and their players detected at the proteome and phosphoproteome of macrophages stimulated with lysed infected RBCs in a time-dependent manner.

Schematics of intracellular signaling pathways and key players upregulated upon stimulation with iRBCs at 22 h or 34 h post-synchronization. Network created based on the KEGG Pathway database. The illustration was created with BioRender.com.

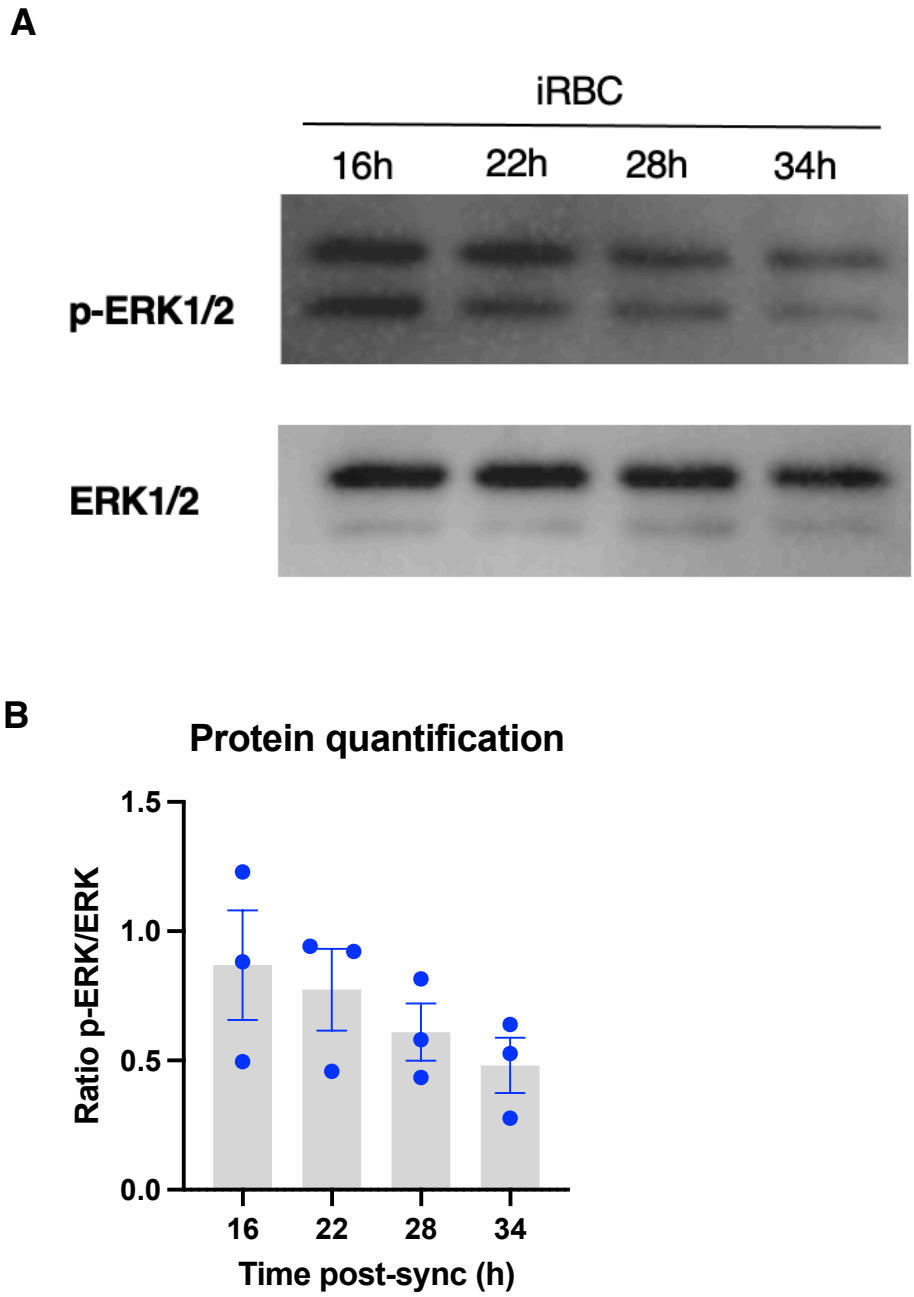

Figure 7. Phosphorylation of ERK is not affected, in a time-dependent way, by lysed infected RBCs stimulation in macrophages.

ERK MAPK signaling pathway in macrophages stimulated with lysed infected RBCs. **(A, B)** BMDMs were stimulated with lysed iRBCs at 16 h, 22 h, 28 h or 34 h post-synchronization and

levels of phosphorylated ERK1/2 (p-ERK1/2) and total ERK1/2 proteins measured by immunoblotting. Relative protein quantification was plotted and analyzed by One-way ANOVA with Tukey's multiple comparisons test. Data are representative of one of the three independent experiments performed. Data are shown as mean ± SEM.

2.8. Supplementary Materials

Primer	Forward Sequence	Reverse Sequence
IL-6	ACGGCCTTCCCTACTTCACA	TGCCATTGCACAACTCTTTTCTC
IL-1β	TGCCACCTTTTGACAGTGATG	GTGCTGCTGCGAGATTTGAA
TNFα	CGGACTCCGCAAAGTCTAAG	CGTCAGCCGATTTGCTATCT
GAPDH	GGGTCGGTGTGGAACGATTTG	TGCCGTGAGTGGAGTCATACTG
ACTIN	GAACCCTAAGGCCAACCGTG	GGTACGACCAGAGGCATACAGG

Table S1. List of primers used on the RT-qPCR run of BMDM stimulated samples.

Forward and reverse sequence of primers used to quantify immune response in stimulated BMDMs.

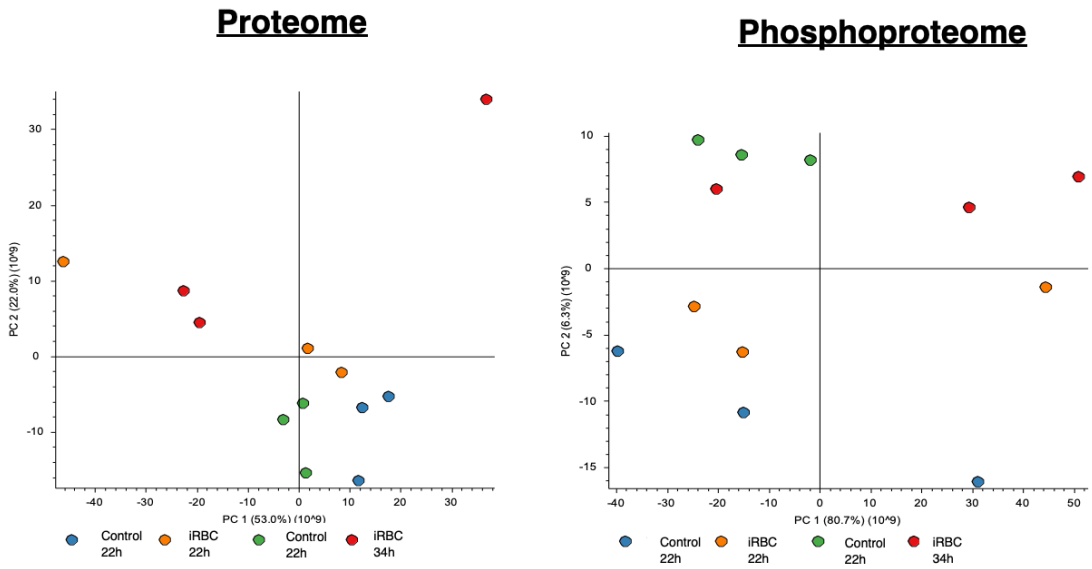

Figure S1. Proteome and phosphoproteome sample analysis.

Principal component analysis of each sample from all the 4 groups (control 22 h, control 34 h, iRBC 22 h and iRBC 34 h) in both proteome and phosphoproteome datasets.

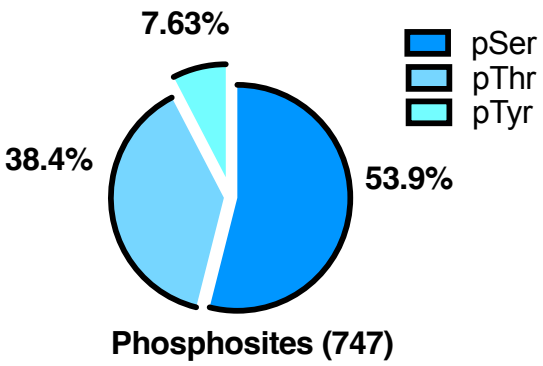

Figure S2. Phosphorylation status on BMDMs stimulated with lysed infected RBCs at 22 h or 34 h post-synchronization.

Phosphorylation distribution of the phosphosites identified in the dataset, based on serine (pSer), threonine (pThr) and tyrosine (pTyr) aminoacids residues.

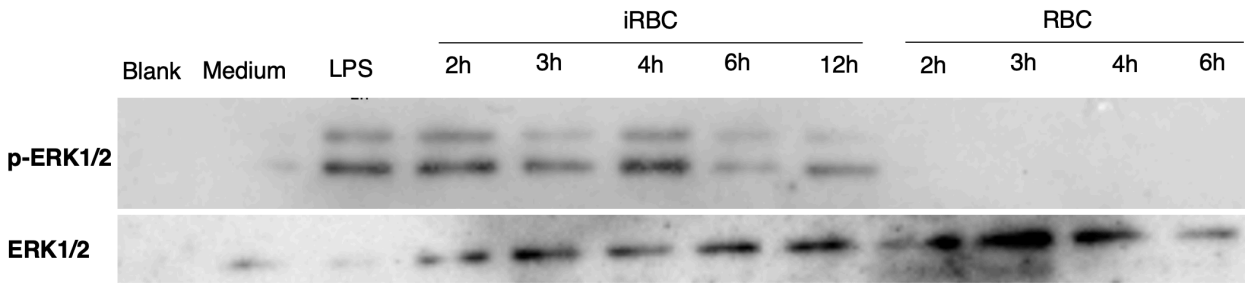

Figure S3. Phosphorylation of ERK measured after a time course stimulation of BMDMs with lysed infected RBCs.

BMDMs were pre-boosted with IFNγ and stimulated with LPS, lysed RBCs or iRBCs and levels of phosphorylated ERK1/2 (p-ERK1/2) and total ERK1/2 proteins measured by immunoblotting.

Preface to Chapter 3

In Chapter 2 we developed a model to study macrophages circadian rhythms in response to *Plasmodium spp.*-infected red blood cells. This was fundamentally based on malaria paroxysms as a rhythmic host response due to the synchronized encounter of innate immune cells with *Plasmodium spp.*-infected red blood cells. Upon stimulation assays, rhythms in macrophages proinflammatory response were detected, accompanied by time and treatment-dependent changes on intracellular networks and proteins. Therefore, we confirmed that host circadian rhythms determine the magnitude of immune responses in a context of *Plasmodium spp.*-infected red blood cells stimulation.

As we have established this *ex-vivo*, we then wanted to check whether this could be true *in vivo*. This way, on Chapter 3, by infecting mice with *Plasmodium spp.*-infected red blood cells at different times across 24 h, we aimed to determine if host response, as well as disease progression, could be affected in a time-dependent way. After confirming that time of infection impacted these parameters, we moved to investigate the consequences of circadian misalignment, once again, on host response and disease progression, by using the same infection model. Lastly, we have ended this chapter by addressing parasite dependency on host circadian rhythms, more specifically, through manipulation of glucose rhythms and feeding behavior.

The data presented in this chapter consist of the first time ever study demonstrating that time of infection and circadian disruption influence the magnitude of infection in the PbA model. We have detected rhythms in parasite load, during PbA infection, which are new to the field. We have also showed the influence of host metabolism in parasite rhythmicity.

Altogether, the findings bring another evidence that circadian rhythms modulate the course of parasitic infections, and that parasites are aligned with host rhythms in order to grow and sustain infection. Interestingly, our study demonstrates that this is true even for asynchronous malaria parasites.

Chapter 3: Time of Day and Circadian Disruption Influence Host Response and Parasite Growth in a Mouse Model of Cerebral Malaria

Chapter 3: Time of Day and Circadian Disruption Influence Host Response and Parasite Growth in a Mouse Model of Cerebral Malaria

Priscilla Carvalho Cabral[1], Joelle Weinerman[1], Martin Olivier[2] and Nicolas Cermakian[1].

priscilla.cabral@mail.mcgill.ca

martin.olivier@mcgill.ca

nicolas.cermakian@mcgill.ca

[1]Douglas Research Centre, McGill University, Montreal, Quebec, Canada.

[2]Research Institute of the McGill University Health Centre, McGill University, Montréal, Quebec, Canada.

Corresponding author: Dr. Nicolas Cermakian, Douglas Research Centre, McGill University. 6875 Boulevard Lasalle, Montreal, Quebec, H4H 1R3, Canada. Phone: +1 514-761-6131 ext 4936. E-mail address: nicolas.cermakian@mcgill.ca

Keywords: Circadian rhythms, malaria, jet lag, time of infection, glucose

3.1. Abstract

Malaria is a parasitic disease caused by *Plasmodium spp.* which leads to intense immune responses. As immune cells harbor a circadian clock which regulates immune functions, including the response to pathogens, our aim was to study the circadian regulation of host responses to *Plasmodium spp.* by using a mouse model of malaria. First, to investigate whether the time of infection influences disease progression, mice were infected with *Plasmodium berghei ANKA* at different time points across 24 h. As a result, the rate of infection was markedly affected by the time of infection with decreased parasitemia in mice infected in the middle of the night (ZT19). Interestingly, we also identified a time-dependent variation in the abundance of reticulocytes, a subset of red blood cells which are the target cells of *Plasmodium berghei ANKA.* In this experiment, we detected a lower frequency of these cells at ZT19, suggesting that reduced availability of this population could promote the parasite growth impairments observed in these mice. We next investigated the effects of a systemic desynchronization of host circadian clocks on the outcome of the infection. After 10 weeks of recurrent shift of the light-dark cycle, mice had decreased parasite growth and lack of parasite load rhythmicity. This was paralleled by a loss of the plasma glucose rhythm, suggesting that host metabolism is required to sustain rhythmicity in parasite growth. Accordingly, disrupting host metabolism through time-restricted feeding or sucrose administration impacted parasite load rhythmicity. In summary, our findings demonstrate a modulation by time of day and long-term circadian disruption of the ability of malaria parasites to establish and sustain infection.

3.2. Introduction

Circadian rhythms are defined as physiological and behavioural oscillations with a period length of approximately 24 hours, matching the earth rotation, that persist in the absence of environmental timing cues. These rhythms are regulated by a master pacemaker located in the suprachiasmatic nucleus in the brain, which receives light information captured by the retina. Many organism's body functions, such as temperature regulation, levels of activity, and hormonal secretion are known to be under circadian control [118]. Interestingly, circadian rhythms in immunity (including cytokine/chemokine activation, cells expansion, humoral responses and more) have been widely reported [127, 132, 188, 204]. This has important consequences for host susceptibility to infections depending on the time of the day host encounters pathogens [163, 166].

In infectious diseases, rhythms in host response have also been widely reported [138, 141, 205], and in many cases, as direct consequence of rhythmic immune responses [165]. This is the case for parasitic infections such as leishmaniasis, showed by a recent study where mice infected with *Leishmania major* promastigotes at the beginning of the subjective day resulted in reduced swelling at the site of inoculation (footpad) and lower parasite load, when compared to mice infected at the end of the subjective day. Interestingly, when the time variations were furthered investigated *in vivo,* the authors identified that the clock within immune cells was controlling the magnitude of *Leishmania major* infection, more specifically, impacting innate cell recruitment through a mechanism dependent on chemoattractant release [165].

In a model of parasitic worm infection, it has been showed that infection in the early night resulted in a higher parasite burden at day 21 post-infection and decreased Th2 response, in comparison to early day infected mice [164].

Despite these few reports, much is still unknown about mechanisms driving the rhythms in susceptibility to infections, especially in parasitic diseases. One parasitic disease with a daily component is malaria, a vector-transmitted disease caused by *Plasmodium spp.* parasite, affecting hundreds of millions of people around the globe [1]. In some cases, mostly children, this infection can lead to severe immune responses resulting in multi-organ damage and death. Fevers often occur in rhythms of 24 h or multiples, and the replication cycle of the parasite inside the host target cells (red blood cells) follows a daily rhythm [32, 206, 207]. It is known, in malaria, that the time of day by which *Anopheles* mosquito bites the host and transmits the sporozoite form of the parasite matters for the transmission success [174, 175, 208]. However, it remained to be investigated, during malaria intraerythrocytic stage of the disease, if the time of day at which hosts encounter malaria parasite blood stages can also have an impact on the progression of the disease.

Interestingly, host metabolism and timing of host feeding have been shown to be important in regulating *Plasmodium chabaudi* rhythmic replication cycle [179, 180], although contrasting results have been reported [169]. More specifically, inversion of the parasite replication cycle was found when mice fed in the daytime, despite the 24 h synchronization of the cycle remaining unaffected [179]. Parasite proliferation has been shown to occur during host food intake when levels of plasma glucose are highest [180]. Furthermore, leukocytes energy metabolism regulated by IFNγ culminating in TNFα production demonstrated to be responsible for parasite replication synchronism. Nighttime diet restriction has also been shown to influence the rhythms in the parasite cycle, confirming that schizogony was dependent on food and glucose intake period [180].

Up to date, most biological rhythm studies on malaria have been using *Plasmodium chabaudi* parasite strain. Interestingly, circadian misalignment between the mouse host and the parasite, has impacted on parasite growth and virulence [182, 209]. As previously shown that host

rhythms can impact malaria parasite proliferation and the establishment of infection [179, 210], it is logical to expect that the time by which hosts encounter parasites (time of infection) should also matter in this context.

Furthermore, the immune activation component of this disease can result in fatal cases attributed to cerebral malaria [3]. To understand the mechanisms underlying this serious outcome, a mouse model of experimental cerebral malaria (ECM) is widely used [101, 107], characterized by infections using *Plasmodium berghei ANKA* strain, closely recapitulating the symptoms and the pathogenesis [4].

Here we aimed to study the circadian regulation of host response to *Plasmodium berghei ANKA* infected mice. As a result, we have observed that time of infection influences host response and disease progression, where infected in the middle of the night mice showed parasite growth impairments. Moreover, similar parasite growth impairments we observed in mice subjected to chronic circadian disruption and clock mutant mice, and under experimental protocols of host metabolism disruption (time-restricted feeding and sucrose administration).

3.3. Materials and Methods

Mice

Animal use was in accordance with the guidelines of the Canadian Council of Animal Care and was approved by the Douglas Institute Facility Animal Care Committee. Six-week-old male C57BL/6N mice were purchased from Charles River Laboratories (St-Constant, QC). *Rev-erbα* knockout mice, B6.Cg-Nr1d1^{tm1Ven}/LazJ strain # 018447, were purchased from The Jackson Laboratory (Maine, USA), and were bred in house at the Douglas Research Centre. Mice were under a standard laboratory lighting condition of 12 h of light: 12 h of dark unless otherwise noted.

Lighting conditions

For time point experiments, mice were placed in ventilated cages under a standard laboratory lighting condition of 12 h of light: 12 h of dark for 3 weeks (entrainment period) followed by *Plasmodium berghei ANKA* infection at specified time points. For circadian disruption experiments, mice were subjected to either a "shorter" circadian disruption protocol (6-h phase advance every week for a total of 4 weeks prior to infection), an "acute" circadian disruption protocol (8-h phase advance every 2 days for a week after infection) or a "chronic circadian disruption" protocol (8-h phase advance every 2 days for a total of 10 weeks prior to infection). Another group (control group) remained on a normal LD 12 h:12 h schedule for the entire duration of the protocol and was infected at ZT7 or ZT19. Circadian disrupted mice were infected at ZT7.

Plasmodium spp. infections

Two mice were used as pass mice and injected intraperitoneally with 10^6 *Plasmodium berghei, strain ANKA* 676m1cl1 (MRA-868 Bei Resources) (PbA)-infected erythrocytes (PbA iRBCs) or 10^6 *Plasmodium chabaudi adami DK*-infected erythrocytes (Pc iRBCs). On day 6 post-infection, blood was collected from the pass mouse and used to infect experimental mice (10^6 iRBCs, intraperitoneal injection) at the time point indicated for each experiment.

Time-restricted feeding protocol

Mice were housed for 3 weeks under LD 12 h:12 h with food and water *ad libitum*, followed by infection with 10^6 iRBCs at ZT7. Twenty-four hours after infection, mice were randomly assigned to the "control" group or "food restriction" group. In the "control" group, food *ad libitum* (Tekland Global 18% protein) was given. In the "food restriction" group, food was accessible only between ZT19 and ZT7 every day until day 4 post-infection inclusively.

Sucrose administration protocol

Mice were housed for 3 weeks under LD 12 h:12 h with food and water *ad libitum,* followed by infection with 10^6 iRBCs at ZT7. Twenty-four hours after infection, mice were randomly assigned to the "control" group or "sucrose" group. In the "control" group, regular drinking water was given *ad libitum*. In the "sucrose" group, mice received regular water supplemented with 50% sucrose w/v daily, from ZT13 to ZT1, until day 4 post-infection inclusively. The water bottles were replaced with regular water after the 12 hours of protocol, every day until day 4 post-infection inclusively. This rotation of water bottles regimen occurred in both groups, for consistency purposes.

Mouse survival and clinical scores

Mice survival and clinical scores were checked 3 times per day starting on day 4 post-infection. Clinical scores were assessed using The Rapid Murine Coma and Behavior Scale (RMCBS) [211]. Scores were given based on 5 categories: Coordination (gait, balance), exploratory behavior (motor performance), strength and tone (body position, limb strength), reflexes (touch scape, pinna reflex, toe pinch and aggression) and hygiene (grooming). Mice with a sum of the scores equal of below 15 (out of a maximum total of 20) were considered as under experimental cerebral malaria (ECM).

Blood-brain barrier integrity

The integrity of the blood-brain barrier was assessed by Evans blue dye incorporation in the brain tissue. Mice received a single intraperitoneal injection of 0.3 mL of 2% Evans blue (Sigma-Aldrich) in PBS 1x. Mice were euthanized 2 hours later, and brains were collected to verify the presence of the dye (colorimetric based).

T cell analysis

On day 7 post-infection, mice were euthanized, and spleens were collected. Organs were mechanically dissociated, and erythrocytes were lysed using 1x RBCs Lysis Buffer (Biolegend, #420301) as per the manufacturer's instructions. After lysis, samples were centrifuged, and 5 x 10^6 cells per sample were resuspended in PBS 1x with 2% FBS. Cells were incubated with an antibody cocktail containing FITC anti-mouse CD4 (Biolegend, #100405), APC/Cyanine7 anti-mouse CD8a (Biolegend, #100714), PE anti-mouse/human CD44 (Biolegend, #103007) and APC anti-mouse CD62L (Biolegend, #104411) antibodies, for 30 minutes in the dark and on ice. Cells

were washed and incubated in 1% PFA for 15 minutes on ice. Cells were washed, resuspended in PBS 1x with 2% FBS and acquired the following day using a BD FACS Canto II flow cytometer. Analysis was performed using FlowJo software version 10.8.2.

Parasitemia and parasite stage forms

The frequency of infected red blood cells (parasitemia) and the proportion of ring forms, trophozoites, schizonts and gametocytes (parasite stage forms) were assessed by tail tip blood collection. A blood smear was stained with Diff Quick Stain set (RAL diagnostics) and by using an inverted microscope with 100X immersion oil objective, non-infected and infected red blood cells were counted (300 cells) and the percentage of parasite-containing cells was determined. Multi-infected (red blood cells with 2 or more parasites internalized) and single-infected RBCs (red blood cells with 1 parasite internalized) were also counted.

Parasite load (blood and organs)

One microliter of blood was collected from the tail tip once a day starting day 4 post-infection. Blood was centrifuged and red blood cells were lysed using a commercial Lysis buffer 1x (Biotium). For parasite organ sequestration, on day 7 post-infection, animals were euthanized by cervical dislocation and intracardially perfused with PBS 1x for 3 minutes. The liver, spleen, and lungs were removed and mechanically processed in Lysis buffer 1x (Biotium). Bioluminescence in the red blood cell extract and organ supernatant was measured following reaction with D-luciferin, according to manufacturer's instructions (Firefly Luciferase Assay Kit 2.0 - Biotium) on an Orion II Microplate Luminometer equipment.

Cytokine/chemokine measurements

Blood from infected mice (ZT7 or ZT19) and their respective uninfected controls were collected using cardiac puncture (terminal) on day 7 post-infection. ZT7-infected mice had their blood collected at ZT7, and ZT19-infected mice at ZT19. Blood was allowed to coagulate for 30 minutes prior to centrifugation at 500 g. Serum was collected and diluted 1:10 with sterile endotoxin-free PBS 1x. Aliquots were kept at -80 °C and shipped on dry ice to Eve Technologies (Calgary, CA) and cytokine/chemokine levels were quantified using the Mouse Cytokine Proinflammatory Focused 10-Plex Discovery Assay Array (MDF10).

Reticulocytes assessment

On day 4 post-infection, 10 µl of blood from ZT7- and ZT19-infected mice and their respective uninfected controls were collected (sampling time ZT7 or ZT19) and diluted in PBS 1x containing 20 U/mL of heparin, on ice. Animals were euthanized and spleens were also collected. Spleens were mechanically dissociated. Blood and spleen samples were passed through a 0.40 µm cell strainer, stained with trypan blue, and counted to determine cell viability. Samples were centrifuged and 5 x 10^6 cells/sample were resuspended in PBS 1x with 2% FBS and stained with eBioscience Fixable Viability Dye eFluor 780 for 15 minutes followed by a washing step and incubation with anti-mouse CD16/32 antibody (Biolgend, #101319) for 15 minutes in the dark and on ice. Cells were then washed and incubated with an antibody cocktail containing PE/Cyanine7 anti-mouse CD45 (Biolegend, #103113), BV421 rat anti-mouse TER-119/Erythroid Cells (BD Biosciences, #563998), APC rat anti-mouse CD71 (BD Biosciences, #567258) and PE anti-mouse/human CD44 (Biolegend, #103023) antibodies for 30 minutes, in the dark and on ice. Cells were washed and incubated in PFA 1% for 5 minutes on ice. Cells were washed, resuspended in

PBS 1x with 2% FBS and analyzed on the same day using BD FACS Canto II flow cytometer. Analysis was performed using FlowJo software version 10.8.2.

Glucose measurements

One microliter of blood was collected from tail tip from infected mice their respective uninfected controls, and plasma glucose was measured using Contour NEXT EZ glucometer device every 6 hours (ZT1,7,13, and 19 time points).

Statistical analysis

Statistical analyses were performed using GraphPad Prism software version 9.3.1. Circadian rhythmicity was evaluated by non-linear regression analysis (cosinor) by fitting a cosine wave equation $y = B + (A*\cos(2*\pi*((x-Ps)/24)))$, where A = amplitude, B = baseline, Ps = phase shift, with a fixed period of 24 h. Significance was calculated based on F-value (observed R^2, sample size and number of predictors). Survival analysis was performed by Log-rank (Mantel-Cox) analysis. Comparisons between 2 or more groups over time were done using mixed-effects model (REML) or two-way ANOVA with multiple comparisons test. Comparisons for 3 or more groups were performed using one-Way ANOVA with multiple comparisons test. Comparisons between 2 groups were performed using Mann-Whitney test. All comparisons with p values <0.05 were considered significant. The data was expressed as mean ± SEM.

3.4. Results

The time of day of infection impacts sickness behavior and immune response, but not survival, in a mouse model of cerebral malaria

To investigate if the time of infection dictates host susceptibility to cerebral malaria, mice were entrained to a 12h :12 h light-dark (LD) cycle and received an intraperitoneal injection of *P. berghei ANKA*-infected erythrocytes (iRBCs) at either one of the following time points: ZT1 (beginning of the day), ZT7 (middle of the day), ZT13 (beginning of the night), ZT19 (middle of the night). All mice were monitored 3 times daily starting 4 days post-infection to assess clinical scores of experimental cerebral malaria (ECM) and survival. We observed that regardless of the time of infection, all mice succumbed to the infection within days 6-9 post-infection (log-rank test, $p = 0.9700$) (*Fig. 1A*), an expected range for ECM [60]. ECM was confirmed by Evans blue dye incorporation in the brain of ECM-affected mice as a result blood-brain barrier disruption (*Fig. S1*). Up to day 6 post-infection, all mice had scored above 15 (no cerebral malaria), and as the infection progressed, most mice of all groups (except ZT19) had scores under 15 (i.e. cerebral malaria) (*Fig. 1B*). When the criteria for the behavioral evaluation was analyzed separately, ZT19 mice scored higher in all 3 parameters (reflexes, coordination & exploration, strength & tone) (*Fig. 1C*), indicating that the global sickness behavior was milder within this group. Nevertheless, ZT19 mice eventually underwent ECM and by day 9 post-infection they had succumbed to the infection.

As the *P. berghei ANKA* is known to induce strong inflammatory responses during the course of the disease [2, 60, 212, 213], we evaluated the levels of 10 cytokines and chemokines in the blood (serum) of mice infected at ZT7 or ZT19 on day 6 post-infection (*Fig. 2A)*. When we compared cytokines/chemokines induced upon infection we found that 4 proteins were

significantly induced by infection exclusively at ZT19 infected mice (IL-10, TNFα, MCP-1, and IL-6) and only 1 (IFNγ) was induced upon infection irrespective of time point of infection (*Fig. 2B)*.

Taken together, our data showed that in a mouse model of ECM the time of infection affects the host inflammatory response and the development of ECM, without affecting survival.

The time of day of infection affects parasite growth and cells invasion

Given the time-dependent differences in the appearance of clinical scores features, we looked at parasite growth. Both blood parasite load (*Fig. 3A*) and parasitemia (*Fig. 3B*) were markedly affected, with lowest levels in mice infected at ZT19. Consistently with the blood data (*Fig. 3A*), parasite load in peripheral organs such as the lung, liver and spleen (*Fig. 3C*) also showed decreased levels in mice infected at ZT19.

As a rhythmic pattern in hematopoietic stem and progenitor cells (HSPCs) have been observed [214], we then hypothesized that rhythms in erythrocytes abundance could underlie parasite invasion efficacy and the establishment of the infection. Blood and spleen were collected at ZT7 or ZT19 and cells were stained for different populations of erythrocytes (Gating strategy in *Fig. S2*). Although the total population of erythrocytes ($CD45^-$, $Ter119^+$ cells) was not different between time points in the blood (*Fig. 4A)*, both early and late reticulocyte subsets were lower in ZT19-infected mice and, early reticulocytes were also reduced in uninfected control sampled at ZT19 (*Fig.4B*). In the spleen, there was a decrease in total erythrocytes at sampling time ZT19, counterbalanced by an increased frequency of immune cells, and reduced frequency of early reticulocytes in the controls (*Fig. 4B*).

To determine if the time-dependent variation in erythrocyte subsets lead to differences in the efficacy of parasite invasion, we looked at the proportion of cells with internalized parasites (GFP^+) (*Fig. 5, S2*). Interestingly, and in accordance with our parasitemia and parasite load data, ZT19-infected mice showed a lower frequency of infected erythrocytes in both blood and spleen (*Fig. 5A*). However, among the erythrocyte subsets, only infected normocytes in the blood were decreased on ZT19-infected mice, whereas infected late reticulocytes were increased in the spleen (*Fig. 5B)*. As the spleen has been shown to be a more parasitized target [97], we compared the frequency of infected erythrocytes in both compartments and detected an increased accumulation of infected cells in the spleen on day 4 post-infection (*Fig. 6A*). We have also confirmed the preference for parasite invasion of immature erythrocytes as opposed to mature cells (normocytes) (*Fig. 6B*).

In summary, we showed that the time of infection affects parasite growth with impairments in ZT19-infected mice. Furthermore, our data suggest that time-of-day variation in erythrocytes and their subsets contributes to parasite invasion efficacy.

Long-term circadian disruption affects parasite growth

We next investigated the effects of a chronic systemic desynchronization of host circadian clocks on ECM. Mice were subjected to a "weekly jet lag protocol" (6-h phase advance of the LD cycle every week for a total of 4 weeks) right before being infected with PbA iRBCs and kept under this protocol throughout the infection. As a result, this "less" disruptive protocol was first tested, and did not lead to statistically significant changes in host response or parasite progression, in comparison to a control LD group (*Fig. S3*).

We then used a "more disruptive" approach with an 8-h phase advance every 2 days for a total of 10 weeks. Using this long-term circadian disruption protocol, mouse survival or development of ECM were not affected (*Fig. S6*). Accordingly, the host immune response was not affected (measured by the frequency of activated T CD8+ lymphocytes in the spleen) (*Fig. S7*). On the other hand, large effects were seen with respect to parasite growth: Jet lag mice showed reduced levels in parasite load in the blood, lung and liver (*Fig. 7A, B*).

As a reduced parasite load was also an outcome observed when mice were infected at ZT19 vs ZT7 (*Fig. 3A, C*), we ran another cohort with 3 experimental groups (a ZT7, a ZT19, and a "jet lag" group infected at ZT7). As expected, both ZT19-infected mice and jet lag mice had a reduced parasite load compared to ZT7-infected mice (*Fig. 7C*).

To verify if a chronic disruptive approach is truly needed in our phenotype, we have also tested an acute circadian disruption protocol, where mice were subjected to a disruptive lighting schedule (8-h phase advance every 2 days) only after they were infected (day 1 post-infection) and remained on the disruptive schedule throughout the infection (until days 7-8 post-infection). This protocol did not induce the phenotype observed with the long-term approach (*Fig. S4*), confirming that a chronic exposure to circadian disruption impacts parasite growth, most likely by creating an unfavorable environment for parasite proliferation.

Interestingly, the "long-term" disruptive protocol also seemed to impact parasite growth when mice were infected with *Plasmodium chabaudi adami DK*. The known 24-h time variations in the frequency of *P. chabaudi* blood stages were markedly affected by our chronic jet lag protocol. Late-stage forms (including trophozoites) were reported to reach higher frequencies in the blood at the end of the day/early night time points, whereas early-stage forms are more abundant during daytime [182]. In accordance with this, we observed that trophozoites were at

higher levels (trend p = 0.0868 on day 7, and p = 0.0019 on day 8 post-infection) at ZT14 compared to ZT2, in the control LD group. In contrast, time-dependent variations in trophozoites were absent in "jet lag" mice (*Fig. S5A)*. In addition to that, when the levels were compared between groups, we detected significantly fewer trophozoites in the blood of "jet lag" mice when compared to control LD, on day 8 post-infection (p = 0.0014) (*Fig. S5B*). These results show that chronic circadian disruption can impair parasite growth in both mouse *P. chabaudi adami DK* and *P. berghei ANKA*.

Interestingly, infection of mice knockout for the clock gene *Rev-erbα* also led to a reduced parasite load compared to wild-type mice, with unchanged values for parasitemia and host response, including survival (*Fig. S8*). These results suggest that undisturbed host circadian rhythms are necessary for parasite growth during infection.

Long-term circadian disruption affects the frequency of multi-infected red blood cells

Interestingly, the reduction of parasite load was not associated with changes in parasitemia levels and parasite stage forms (*Fig. 7D, E)*. Therefore, given the known ability of *Plasmodium spp.* to poly parasitize erythrocytes [215], we re-analyzed the blood smears according to the number of parasite per red blood cell. Consistently with the blood load data, jet lag mice had fewer multi-infected cells and more single infected cells on days 4 and 5 post-infection (*Fig. 7F*). Among these cells, there were significantly fewer red blood cells infected with 2 parasites per cell in the jet lag group compared to controls (for both cells infected with either trophozoites or ring stage forms) (*Fig. 7G)*. Altogether, these data show that the reduced parasite load induced by circadian disruption is associated with a reduced parasite/RBC ratio.

Rhythms in blood parasite load are absent in jet lag mice

We next investigated whether blood parasite load follows a 24-h rhythm during the infection. For this purpose, mice were infected as previously described (at ZT7 or ZT19 under LD or ZT7 under jet lag) and blood was collected every 6 hours on day 5 post-infection, generating 4 sampling time points (ZT1, 7, 13, and 19). For each mouse, there was a significant rhythm for ZT7- ($p < 0.0001$) and for ZT19-infected mouse ($p < 0.001$). Interestingly, rhythmicity was lost in jet lag mice, with an acrophase between ZT7 and ZT13, with similar and low levels at all sampling time points (*Fig. 8A*).

Plasma glucose is altered in jet lag mice

Since glucose was shown to induce parasite growth (schizogony) in *P. chabaudi* [180] we quantified glucose in plasma from mice sampled every 6 hours on days 4 and 5 post-infection. As expected for *P. berghei ANKA* infection, mice of all groups (ZT7, ZT19, and jet lag) developed hypoglycemia throughout the infection [216] (*Fig. 8B*). Interestingly, a robust rhythm of glucose was observed for control mice whereas jet lag mice had a rhythm with a sharp decreased amplitude and a phase-advance (*Fig. 8C*). Taken together, the loss of rhythm in blood parasite load upon circadian disruption is paralleled by a greatly reduced rhythmicity of plasma glucose during PbA infection.

Parasite load rhythmicity is affected by time-restricted feeding and high sucrose administration

The concurrent effects of the jet lag protocol on parasite load and glucose rhythms, suggested that host metabolism, and particularly glucose levels, might be mediating the effect of

jet lag on PbA infection. To address this, we first subjected mice to time-restricted feeding, starting after 24 h of infection. Mice were given access to food from ZT19 until ZT7 every day until day 4 post-infection inclusively (control mice were fed *ad libitum*). Plasma glucose and parasite load were measured every 6 hours of day 4 post-infection *(Fig. 9A*). While control mice showed a rhythm of both plasma glucose and parasite load, those rhythms were abolished in mice under time-restricted feeding (*Fig. 9B, C*).

As feeding restriction protocol limits the parasite's access to a range of food-derived nutrients, we interrogated more specifically the effect of glucose via sucrose administration: 24 h after infection, mice were given water containing 50% w/v sucrose from ZT13 to ZT1 (control mice remained on regular water *ad libitum*) (*Fig. 10A*). Again, control mice had rhythms of glucose and parasite load, which were abolished in sucrose-treated mice (*Fig. 10 B, C*).

Altogether, these results indicate that host metabolism, and in particular blood glucose levels, impact parasite load rhythmicity.

3.5. Discussion

Here we reported that the growth of malaria parasite and, the host response to this infection are influenced by the time of day of infection. We have also detected daily variations in the abundance of parasite's target cells (red blood cells), a factor that might account for the phenotype. Moreover, parasite growth is also influenced by disruptive light-dark cycles. Interestingly, we showed that parasite load rhythmicity was dependent on host glucose levels. Notably, in the context of cerebral malaria, our study is the first one to look at host response and parasite growth in a time of day-dependent manner.

Initially, we showed that time of infection with *P. berghei ANKA* influences host response and the parasite's ability to establish and sustain infection in mice. Rhythms in host response are known to follow a 24 h cycle and could therefore be responsible for the phenotype observed. It has been shown that the number of circulating immune cells varies across the day, with a peak during daytime (ZT4-8) in the blood of mice [217], whereas recruitment of leukocytes to peripheral tissues peaks during nighttime as a result of circadian rhythms in promigratory factors [127]. Furthermore, we have also observed that during daytime (ZT7) $CD45^{+}$, $Ter119^{-}$ immune cells are increased in the blood as compared to nighttime (ZT19). Although our study has not looked into the frequency of leukocytes in the peritoneal cavity (site of infection), it is possible that if investigated, an increased number of resident cells during nighttime could have been found - based on studies by others which showed a rhythm in the number of some peritoneal macrophages over 24 h, with highest values during nighttime (ZT15) [165]. This rhythm in local immunity at the peritoneal cavity level could potentially impact the rate of infection. In other words, an increased frequency of phagocytes at ZT19 at the peritoneal cavity could be implicated on why we detected

low levels of parasite load observed on days 4 and 5 post-infection in ZT19-infected mice. Furthermore, in a context of parasitic infection, a rhythm in host response to *Leishmania spp*. inoculation in the mouse peritoneal cavity has been reported [165]. Moreover, route of inoculation is an important factor when looking at parasite density at later days post-infection, according to a study using the *Plasmodium chabaudi* malaria model. In their study, an intraperitoneal injection resulted in lower parasite levels when compared to intravenous injection [209]. Furthermore, although not investigated in this study, a potential contribution of splenic macrophages eliminating infected erythrocytes through erythrophagocytosis should be considered [218]. Aligned with this, time variations in *Tlr9* in the spleen have been reported, with a peak at ZT19 [219]. Importantly, toll-like receptor 9 is known to be activated in response to malarial DNA [71].

Along with circadian rhythms in immune cells migration, 24-h oscillations in erythrocytes were reported as a result of rhythms in progenitors' egress from bone marrow and differentiation into mature erythrocytes [214]. Given this rhythmicity and *P. berghei ANKA* preference for immature erythrocytes (reticulocytes) invasion [97], we hypothesized that rhythms in the abundance of these cells affect the efficiency of the infection in a time-dependent manner. In line with this hypothesis, we observed a reduced frequency of both early and late reticulocytes cells in the blood at ZT19 compared to ZT7. Moreover, in the both blood and spleen, ZT19-infected mice had a significantly lower frequency of erythrocytes with internalized GFP^+ parasites. The phenotype observed corroborates with the existence of migratory systemic factors which control rhythms in cells frequency, as shown by others in the field [127, 128, 217]. Furthermore, our results are aligned with other studies reporting *Plasmodium berghei ANKA* preference for reticulocytes as opposed to normocytes [220]. In addition to that, the frequency of early reticulocytes is known to

be very low, contributing little to overall parasite biomass, whereas the greater abundance of late erythrocytes contributes to parasite tropism [220].

Interestingly, despite the infection, the time variations in reticulocytes (lower at ZT19) were also observed in uninfected mice. This suggests that erythropoiesis at the level of extra-medullary sites (a phenomenon that is known to occur during malaria) [221] might not be responsible for the phenotype observed, although further confirmation is needed. Furthermore, the role of erythropoietin (Epo) mediating the time variations detected is unlikely, despite a circadian control of Epo has been reported [222], given that malaria infection suppresses Epo activity [223].

We have sought to determine the effects of host circadian disruption. For that, after the 10-week protocol, jet lag mice were infected at ZT7, and non-jet lag at ZT7 or ZT19 time points. Importantly, for the jet lag group, ZT7 time point reflected the light-dark schedule mice were currently subjected to. Importantly, at the time of infection, the internal time of the mice might be different - a known phenomenon already reported by others in the field [157].

In inflammatory models, chronic circadian disruption was shown to increase the production of proinflammatory cytokines, such as IL-1β, GM-CSF, IL-12 and, more, in response to LPS challenge [153] whereas desynchronization of immune responses has also been detected in humans subjected to simulated night shift work [150]. Interestingly, studies with other *Plasmodium spp*. species have shown parasite dependency on environmental cues (e.g. light-dark schedules) or host circadian rhythms for parasite replication and growth [182, 209]. Thus, given the inflammatory nature of our ECM model, we originally hypothesized that circadian disruption would affect host response and parasite growth, leading to increased and faster ECM development. Surprisingly, we have not seen effects on these parameters indicating that circadian disruption does not affect disease progression, development or survival, in this mouse model of cerebral malaria. Despite

this, interestingly, circadian disruption impaired parasite growth. As reported in other *Plasmodium spp.* strains, host-parasite circadian misalignment can lead to impairments in parasite replication and generation of transmission forms (gametocytes) [182]. In our experiments, circadian-disrupted mice consistently showed impairments in parasite load throughout the days of infection in both blood and organs (lung and liver). The reduced levels of parasite load in "jet lag" mice could be due to a reduction in the efficiency of erythrocyte invasion. In line with this, even though the frequency of infected cells (parasitemia) did not differ between the groups, the frequency of multi-infected cells on days 4 and 5 post-infection was significantly reduced in the "jet lag" mice. Multi-infected cells with either rings or trophozoites were similarly increased in "jet lag" mice, indicating that this is not restricted to a developmental stage of the parasite. Similarly, a recent study with *P. berghei ANKA* showed that the proportion of each parasite stage form (ring, early and mid and late-trophozoite, and schizont) do not display a 24-h rhythm [185].

Given the impairments on parasite growth in "jet lag" mice, we investigated if rhythms in parasite load are present, given the partially synchronized nature of *P. berghei ANKA* (length of developmental cycle 22-24 hours) [224, 225], and if such rhythms are present, whether "jet lag" mice display altered rhythms. Surprisingly, a rhythm in blood parasite load was detected in ZT7- and ZT19-infected mice but not in "jet lag" mice. This was paralleled by a dampening of the rhythm in plasma glucose. This would be consistent with a dependency of the parasite on host metabolism as studies using *Plasmodium spp.* have shown that parasite proliferation requires host metabolites [226, 227], and disruption of circadian rhythms results in altered glucose rhythms [228]. Moreover, host metabolism and feeding behavior regulate rhythms of *P. chabaudi* developmental cycle [179-181]. To investigate this further, we assessed rhythms of plasma glucose and parasite load under time-restricted feeding. The removal of food for 12 h from ZT7 to ZT19

aimed at preventing mice to access food at a time when food consumption is expected to be maximal [229]. Consistent with the literature, plasma glucose followed a 24-h rhythm with an acrophase at the first hours of the night [230]. We found that animals with 24-h *ad libitum* food displayed a robust rhythm of plasma glucose and parasite load, which was not observed in the food-restricted mice.

When we investigated if parasite rhythms were directly modulated by host glucose, we found a similar lack of rhythm of parasite load in sucrose-administered mice, and elevated levels of plasma glucose during daytime, when compared to control mice. Therefore, manipulating plasma glucose affects blood parasite rhythmicity. Nevertheless, it remains to be elucidated if other nutrients and host metabolites contribute to the parasite rhythm as well as other host circadian rhythms and clocks potentially affected by feeding and sucrose administration. Moreover, the presence of additional mechanisms promoting the arrythmic parasite load phenotype must be considered. The assessment of host processes (e.g. splenic erythrophagocytosis), known to be important over course of this disease as per controlling iRBC and parasite levels, and whether they are affected by timed-restricted feeding/sucrose administration, would help to build a link between the phenotype observed and host intrisinc mechanisms. Furthermore, it is important to mention that the observed effects on plasma glucose were less prominent than the effects seen in parasite load rhythmicity upon both metabolic disruptive approaches. This could be due to the existence of compensatory mechanisms modulating glucose levels (i.e. hormones, hepatic gluconeogenesis) that take place during fasting [230]. Although further investigation is needed, these factors could potentially affect (direct or indirectly) parasite load rhythmicity, contributing as an “additional” disruptive factor for parasite dependency on host rhythms.

In conclusion, our study represents the first one to demonstrate that time of infection affects host response and parasite growth *in vivo* in a mouse model of cerebral malaria and that *P. berghei ANKA* parasite load harbors a 24-h rhythm that is affected by irregular lighting conditions (chronic jet lag), time-restricted feeding and sucrose administration.

3.6. Acknowledgements

The authors thank the members of Cermakian and Olivier laboratories for discussions, knowledge sharing, technical training, and reagents; the Douglas Mental Health University Institute Animal Facility staff for the training and animal procedure assistance; the Immunophenotyping Platform at the McGill University Health Care for flow cytometry assistance. This study was supported by a grant from the Canadian Institutes of Health Research (PJT-168847, to NC and MO), and Douglas Foundation, and doctoral fellowships from Faculty of Medicine and Health Sciences - McGill (to PCC), and from Fonds de Recherche du Québec – Santé (to PCC).

3.7. Figures

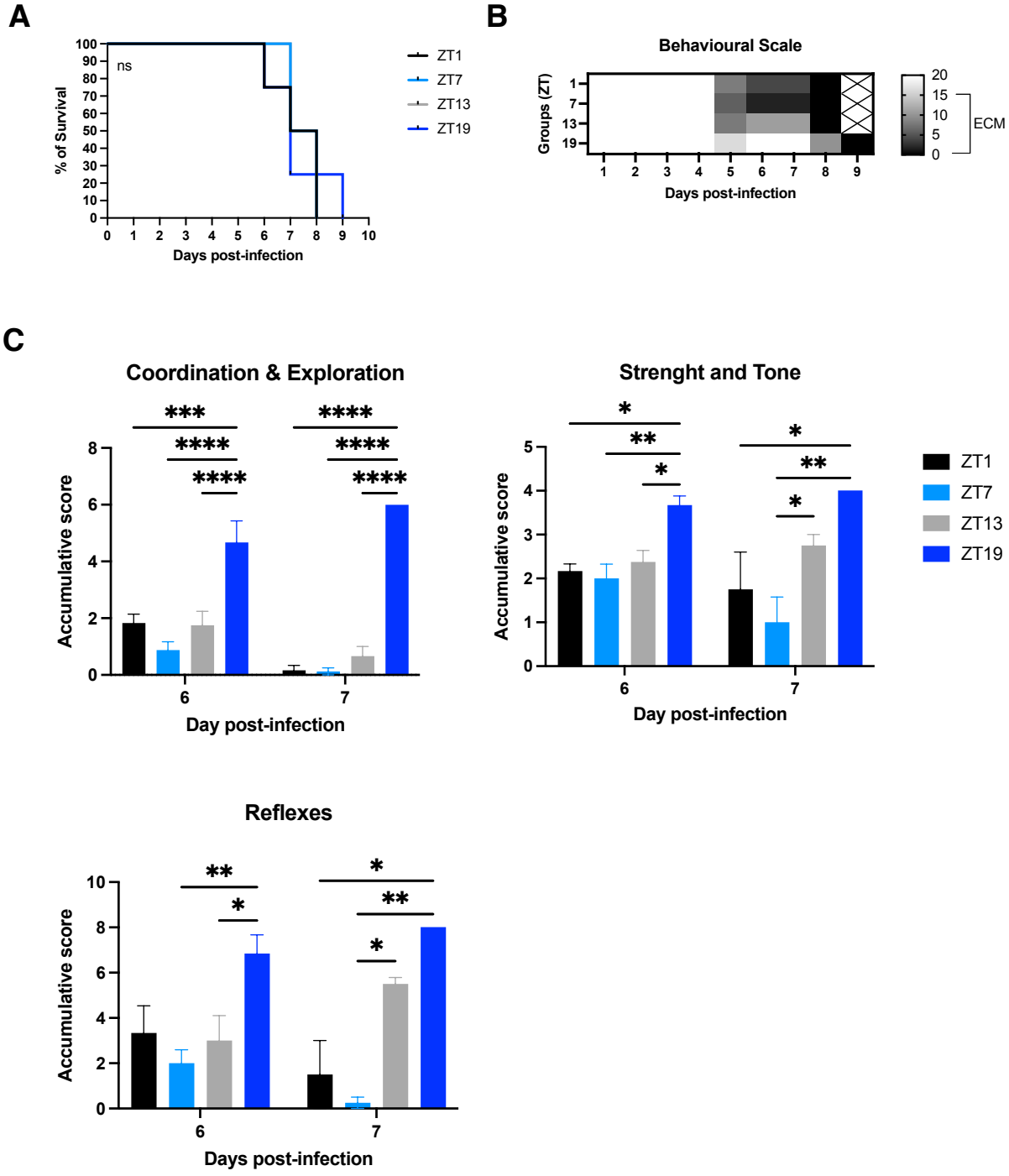
A
ns
% of Survival
Days post-infection
ZT1
ZT7
ZT13
ZT19
B
Behavioural Scale
Groups (ZT)
Days post-infection
ECM
C
Coordination & Exploration
Accumulative score
Day post-infection
Strenght and Tone
Reflexes
Days post-infection

Figure 1. Host survival and sickness behavior in response to *Plasmodium berghei ANKA* infection.

Mice were injected with *Plasmodium berghei ANKA*-infected erythrocytes ZT1, ZT7, ZT13 or ZT19 time points. **(A)** Survival curve with Log-rank (Mantel-Cox) test analysis. **(B)** Heat-map illustration of the ECM behavioral scale. ECM as a score equal to or below 15 is interpreted as ECM. The "X" mark in indicates an absence of the dataset (no more mice alive). **(C)** Individual criteria assessment of infected mice. Mixed-effects model (REML) with Tukey's multiple comparisons test. Data are representative of one of the three independent experiments performed, containing 8 mice per group. Data are shown as mean ± SEM. *p<0.05, **p<0.01, **** p<0.0001.

A

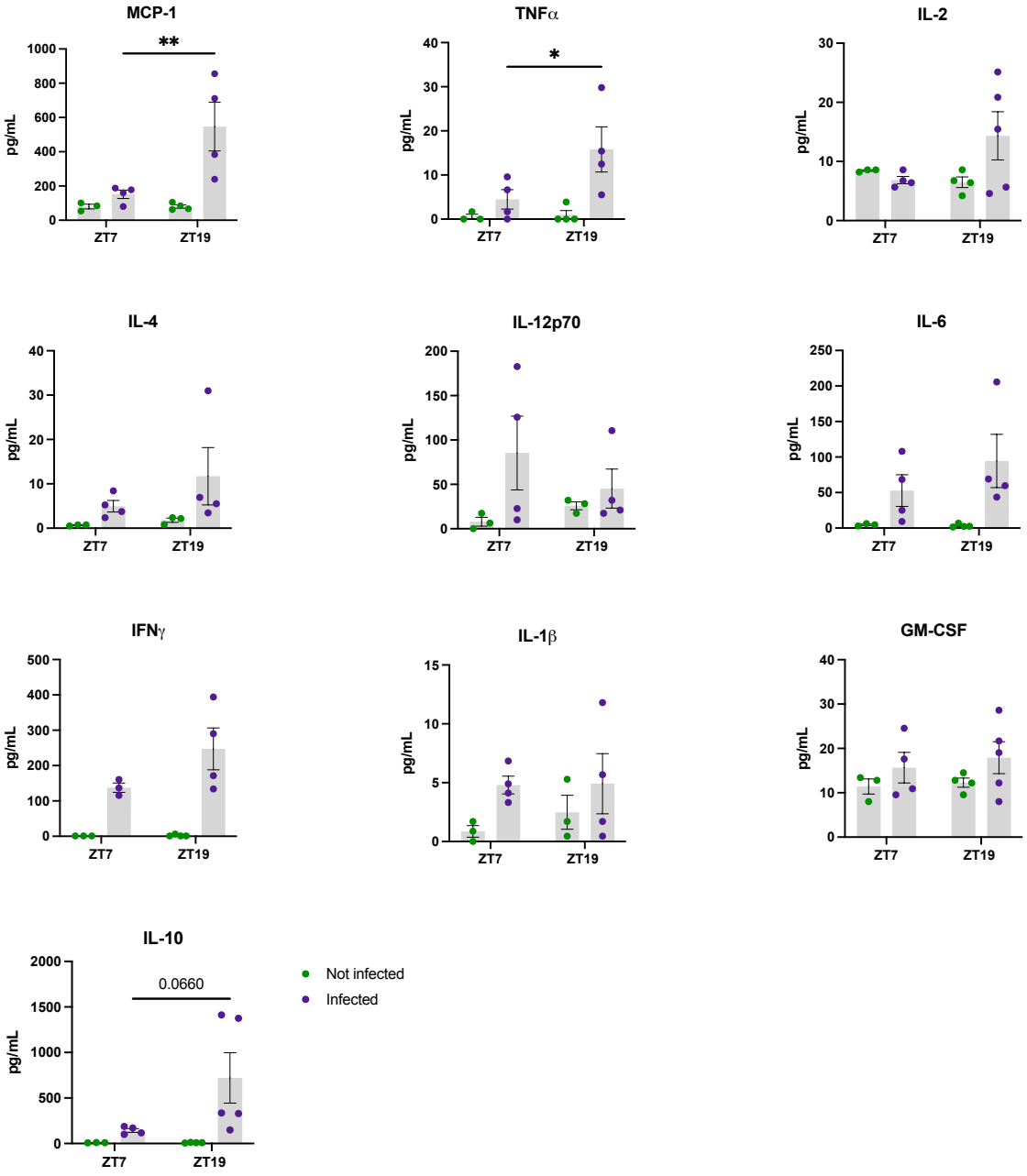
MCP-1
**
TNFα
*
IL-2
IL-4
IL-12p70
IL-6
IFNγ
IL-1β
GM-CSF
IL-10
0.0660
pg/mL
ZT7
ZT19
Not infected
Infected

B

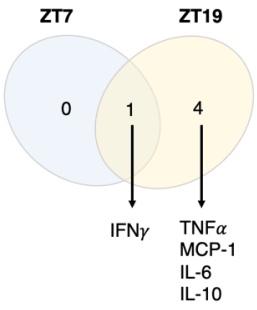
ZT7
ZT19
0
1
4
IFNγ
TNFα
MCP-1
IL-6
IL-10

Figure 2. Host immune response to *Plasmodium berghei ANKA* is affected by the time of infection.

Mice were injected with *Plasmodium berghei ANKA*-infected erythrocytes (infected) or saline (not infected) at ZT7 or ZT19 time points. **(A)** Blood was collected on day 6 post-infection and the levels of cytokine/chemokines were quantified in the serum, by multiplex array. **(B)** Venn diagram to illustrate, from among proteins that were significantly induced upon infection, which ones were induced exclusively at ZT19 (n=4), ZT7 (n=0), or in both time points (n=1). Two-way ANOVA with Sidak multiple comparisons test for (A) and (B). 3-4 mice per group. Data are shown as mean ± SEM. *$p<0.05$, **$p<0.01$.

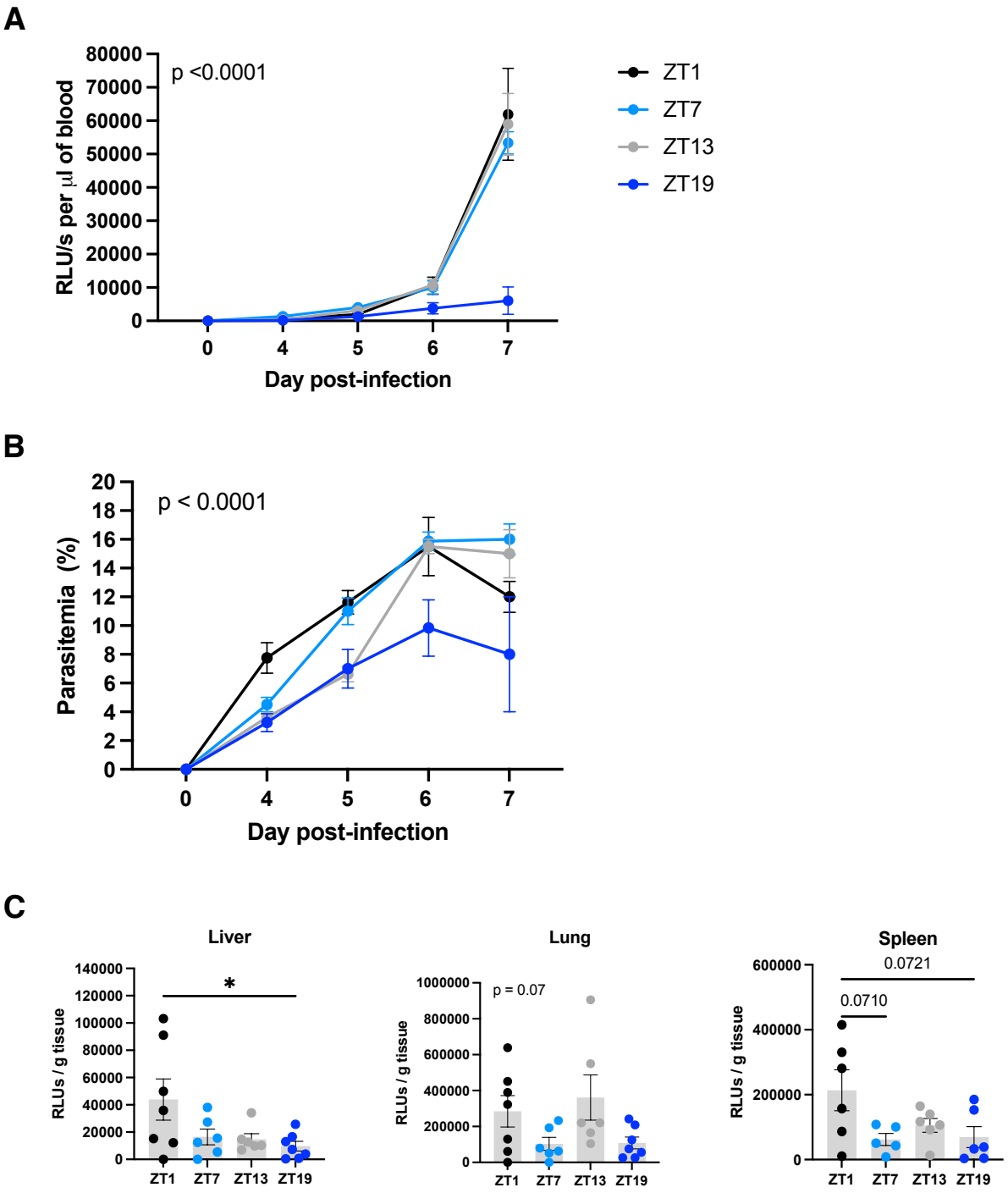

Figure 3. Parasite growth is affected by the time of infection.

Mice were injected with *Plasmodium berghei ANKA*-infected erythrocytes at ZT1, ZT7, ZT13, or ZT19. **(A,C)** Parasite load in the blood and peripheral organs of infected mice, measured by bioluminescence across the days of infection. Organ parasite load was measured upon sacrifice

(day 7 post-infection). **(B)** Percentage of infected erythrocytes (parasitemia) across the days of infection. Measurements for blood parasite load and parasitemia were taken daily starting from day 4 post-infection until sacrifice (day 7 post-infection). Two-way ANOVA with Sidak multiple comparisons test for (A) and (B), and ordinary One-way ANOVA with Tukey's multiple comparisons test for (C). Data are representative of one of the three independent experiments performed, containing 8 mice per group. Data are shown as mean ± SEM. *$p<0.05$.

A

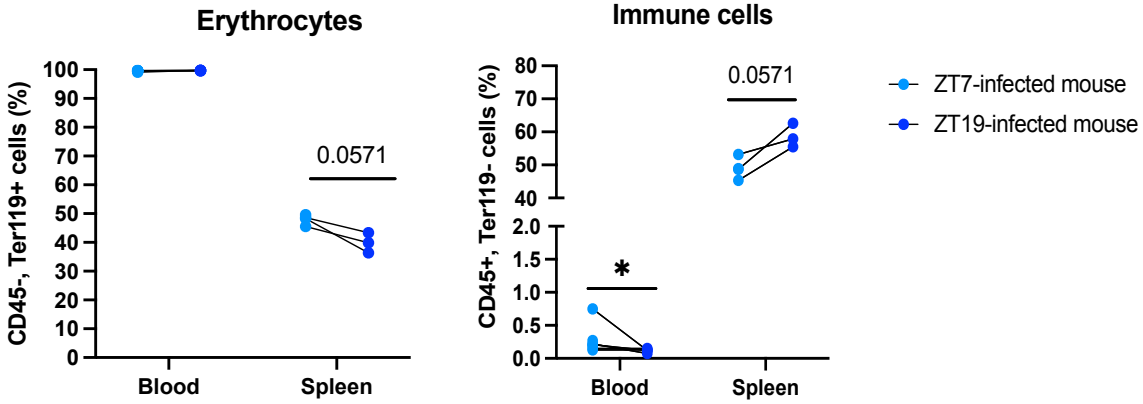

B

Early Reticulocytes

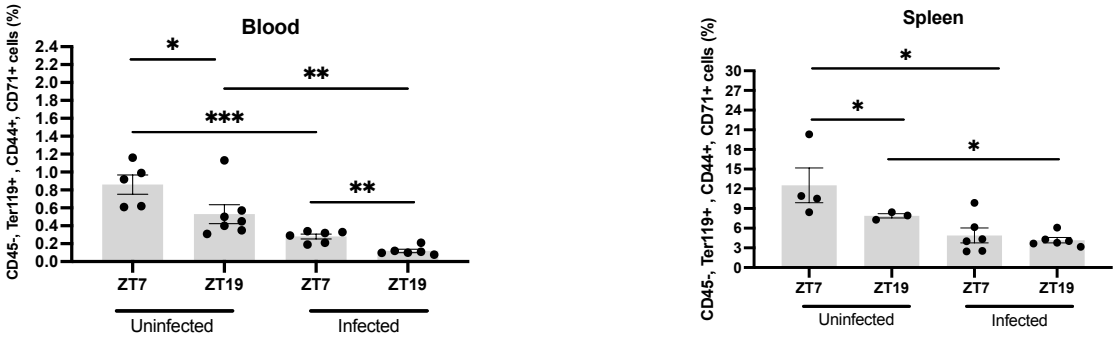

Late Reticulocytes

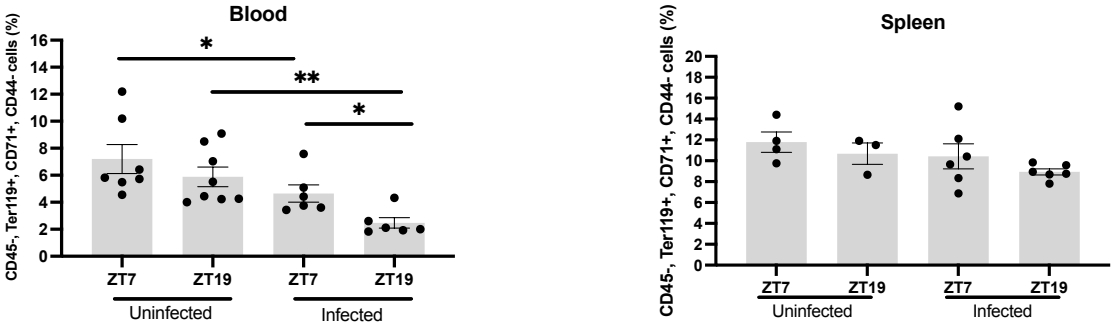

Figure 4. Time-of-day variation in immune cells and erythrocyte subsets.

Blood and spleen harvested on day 4th post-infection from control uninfected sampled at ZT7, control uninfected sampled at ZT19, ZT7-infected and sampled at ZT7, and ZT19-infected mice and sampled at ZT19. Cells were stained with CD45, Ter-119, CD44, and CD71 conjugated fluorochromes, and their frequencies were accessed by flow cytometry. **(A)** Frequency of $CD45^{+}$, $Ter119^{-}$ (immune cells) and $CD45^{-}$, $Ter119^{+}$ (erythrocytes) cells collected at ZT7 and ZT19 time-points in the blood and spleen of ZT7- and ZT19-infected mice **(B)** Frequency of $CD45^{-}$, $Ter119^{+}$, $CD44^{+}$, $CD71^{+}$ cells (early reticulocytes) and $CD45^{-}$, $Ter119^{+}$, $CD44^{-}$, $CD71^{+}$ cells (late reticulocytes) in control uninfected sampled at ZT7, control uninfected sampled at ZT19, ZT7-infected and sampled at ZT7, and ZT19-infected mice and sampled at ZT19, in the blood and spleen. Two-way ANOVA with Sidak multiple comparisons test for (A), and Ordinary One-way ANOVA with Tukey's multiple comparisons test for (B). Data are representative of one of the two independent experiments performed, containing 3-8 mice per group. Data are shown as mean ± SEM. *p<0.05, **p<0.01, ***p<0.001.

A

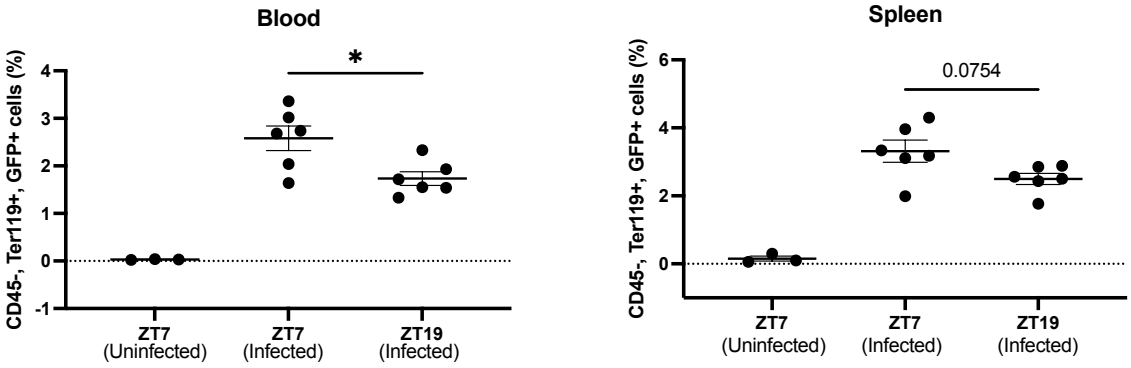

B

Normocytes

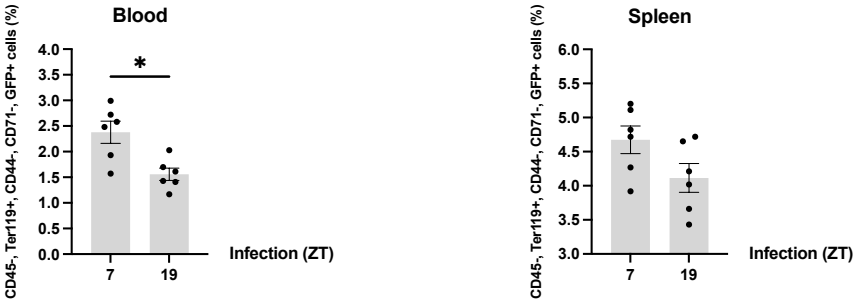

Early Reticulocytes

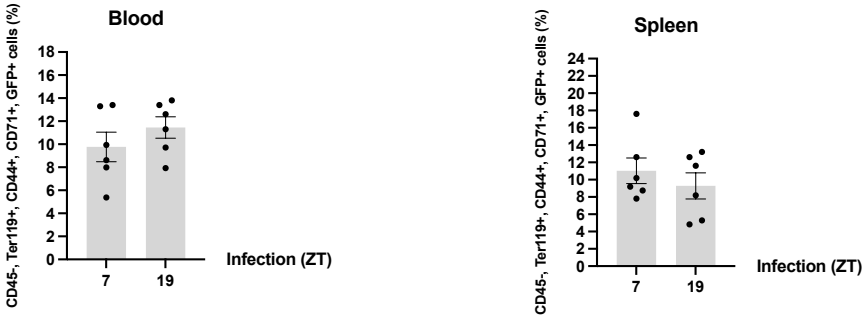

Late Reticulocytes

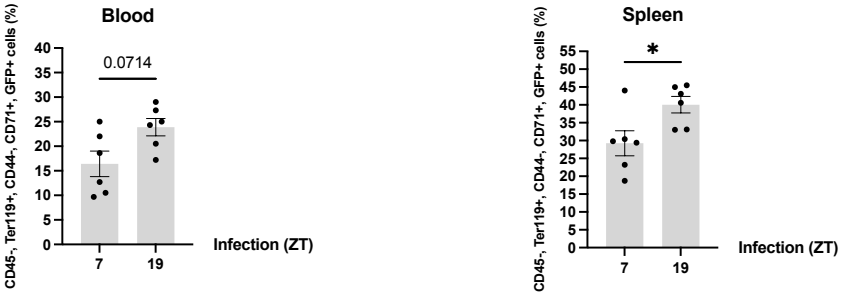

Figure 5. ZT19-infected mice have fewer infected cells.

Blood and spleen from control uninfected sampled at ZT7, ZT7-infected and sampled at ZT7, and ZT19-infected mice and sampled at ZT19. Cells were stained with CD45, Ter-119, CD44, and CD71 conjugated fluorochromes, and their frequencies were accessed by flow cytometry. **(A)** Frequency of $CD45^-$, $Ter119^+$, GFP^+ cells (erythrocytes infected cells) in the blood and spleen of ZT7 and ZT19 infected mice. **(B)** Frequency of $CD45^-$, $Ter119^+$, $CD44^-$, $CD71^-$, GFP^+ cells (infected normocytes), $CD45^-$, $Ter119^+$, $CD44^+$, $CD71^+$, GFP^+ cells (infected early reticulocytes) and $CD45^-$, $Ter119^+$, $CD44^-$, $CD71^+$, GFP^+ cells (infected late reticulocytes). One-way ANOVA with Tukey's multiple comparisons test for (A) and Mann-Whitney test for (B). Data are representative of one of the two independent experiments performed, containing 3-8 mice per group. Data are shown as mean ± SEM. *$p<0.05$.

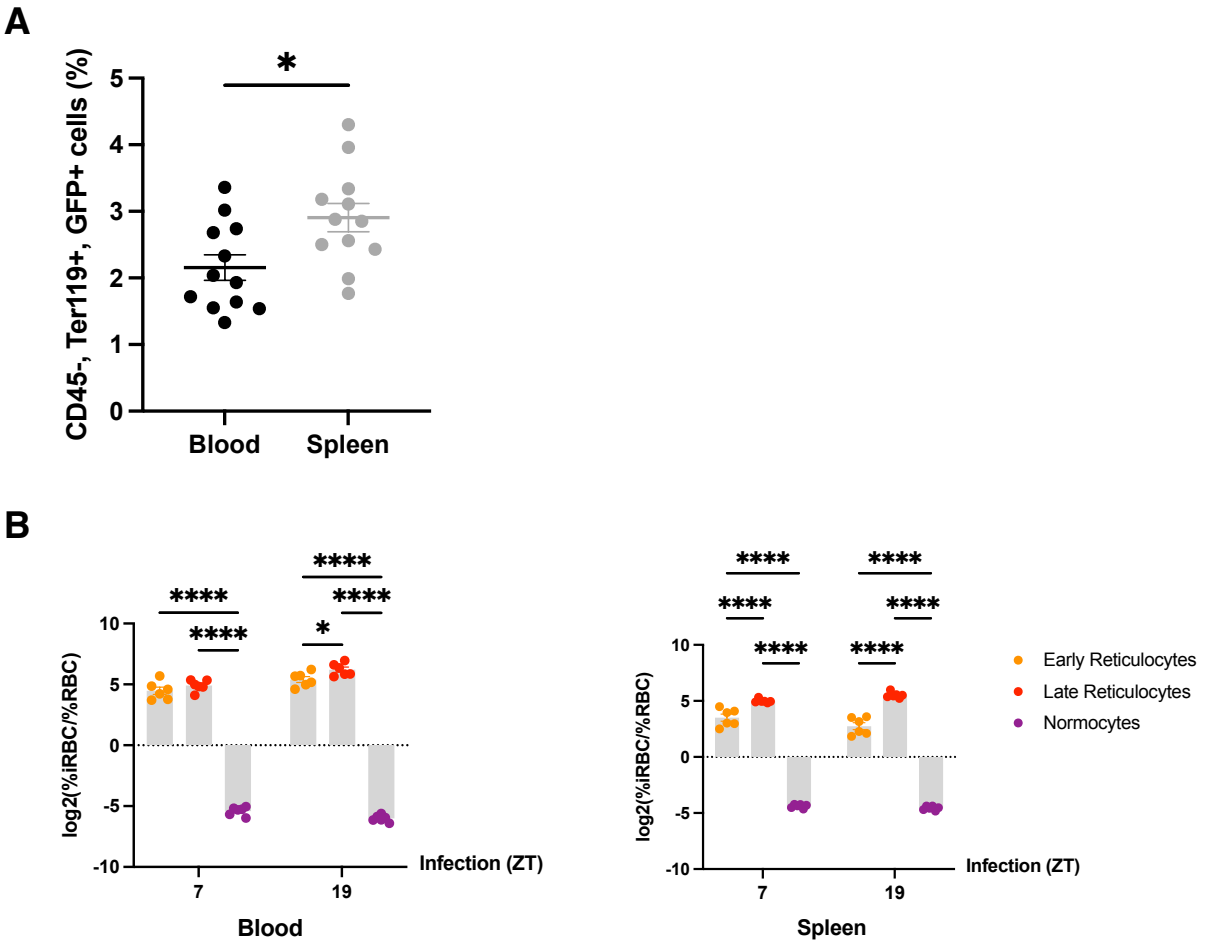

Figure 6. The spleen is a more parasitized target with a preference for reticulocyte invasion similar in both ZT7 and ZT19 groups.

Blood and spleen ZT7-infected and sampled at ZT7, and ZT19-infected mice and sampled at ZT19. **(A)** Frequency of $CD45^-$, $Ter119^+$, GFP^+ infected cells in the blood and spleen. **(B)** Relative enrichment of the subpopulations of erythrocytes in infected cells versus the erythrocytes pool. Values > 0 correspond to an enhanced parasite tropism for this subpopulation, whereas values < 0 correspond to a decreased parasite tropism. Mann-Whitney test for (A) and Two-way ANOVA with Sidak multiple comparison test for (B). 6-8 mice per group and data are shown as mean ± SEM. *p<0.05, **** p<0.0001.

A

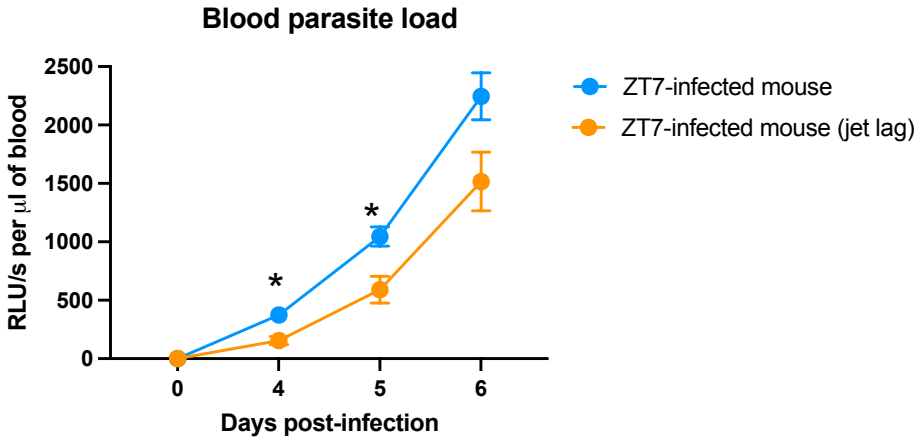
Blood parasite load
RLU/s per μl of blood
2500
2000
1500
1000
500
0
0
4
5
6
Days post-infection
*
*
ZT7-infected mouse
ZT7-infected mouse (jet lag)

B

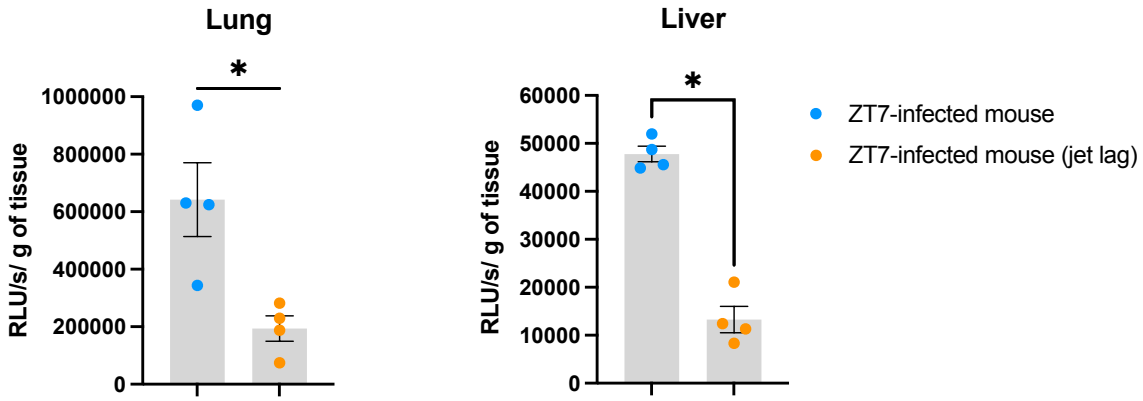
Lung
RLU/s/ g of tissue
1000000
800000
600000
400000
200000
0
*
Liver
RLU/s/ g of tissue
60000
50000
40000
30000
20000
10000
0
*
ZT7-infected mouse
ZT7-infected mouse (jet lag)

C

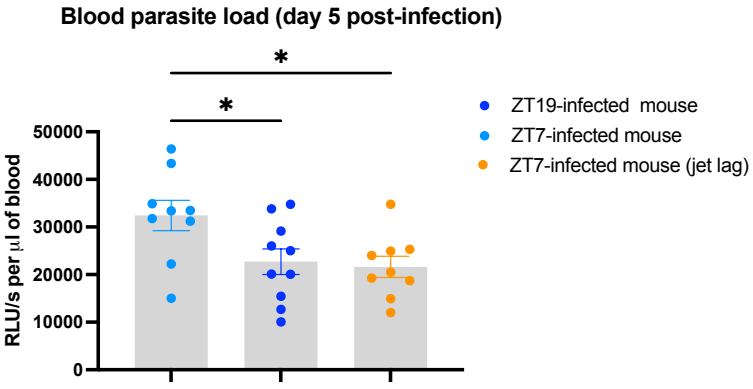
Blood parasite load (day 5 post-infection)
RLU/s per μl of blood
50000
40000
30000
20000
10000
0
*
*
ZT19-infected mouse
ZT7-infected mouse
ZT7-infected mouse (jet lag)

D

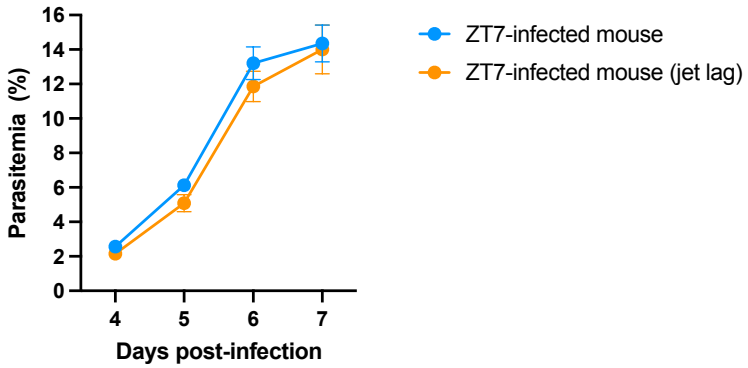
Parasitemia (%)
16
14
12
10
8
6
4
2
0
4
5
6
7
Days post-infection
ZT7-infected mouse
ZT7-infected mouse (jet lag)

E

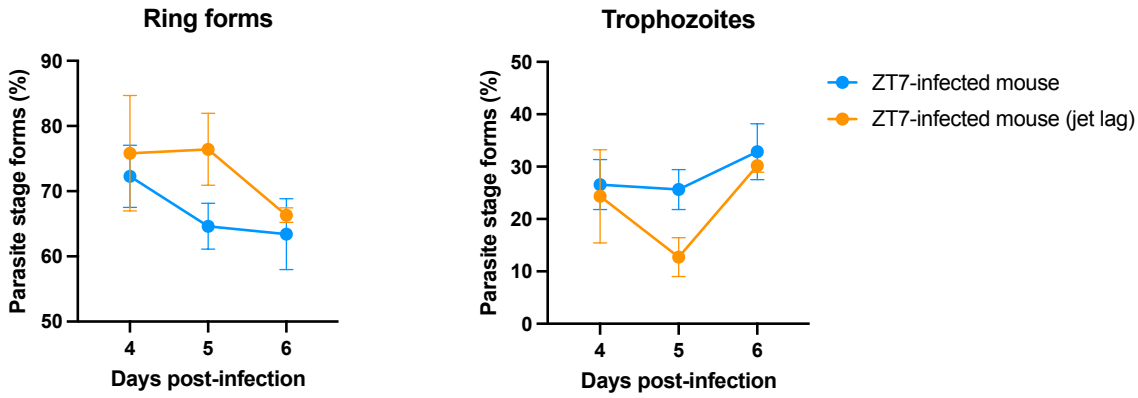
Ring forms
Parasite stage forms (%)
90
80
70
60
50
4
5
6
Days post-infection
Trophozoites
Parasite stage forms (%)
50
40
30
20
10
0
4
5
6
Days post-infection
ZT7-infected mouse
ZT7-infected mouse (jet lag)

F

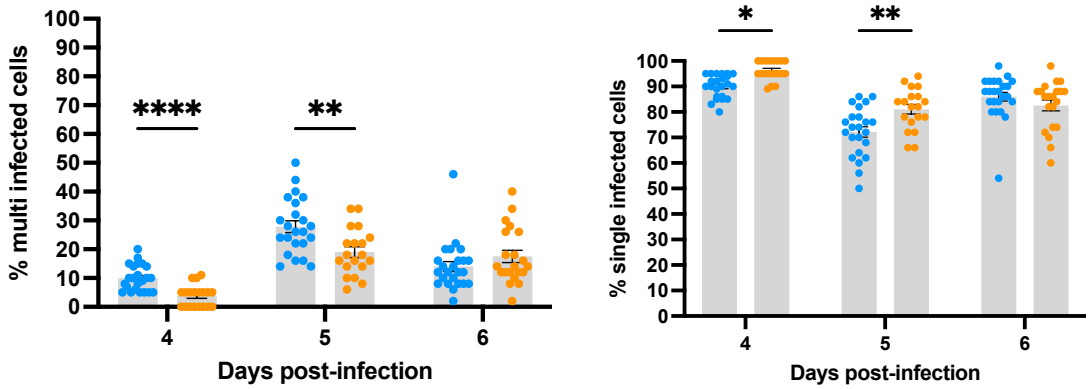
% multi infected cells
100
90
80
70
60
50
40
30
20
10
0
****
**
4
5
6
Days post-infection
% single infected cells
*
**
100
90
80
70
60
50
40
30
20
10
0
4
5
6
Days post-infection

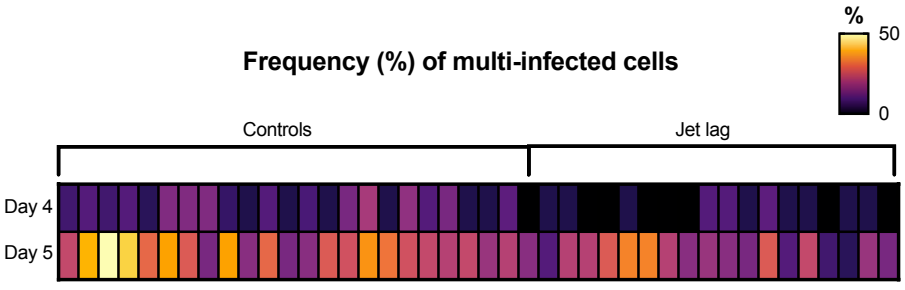
Frequency (%) of multi-infected cells
%
50
0
Controls
Jet lag
Day 4
Day 5

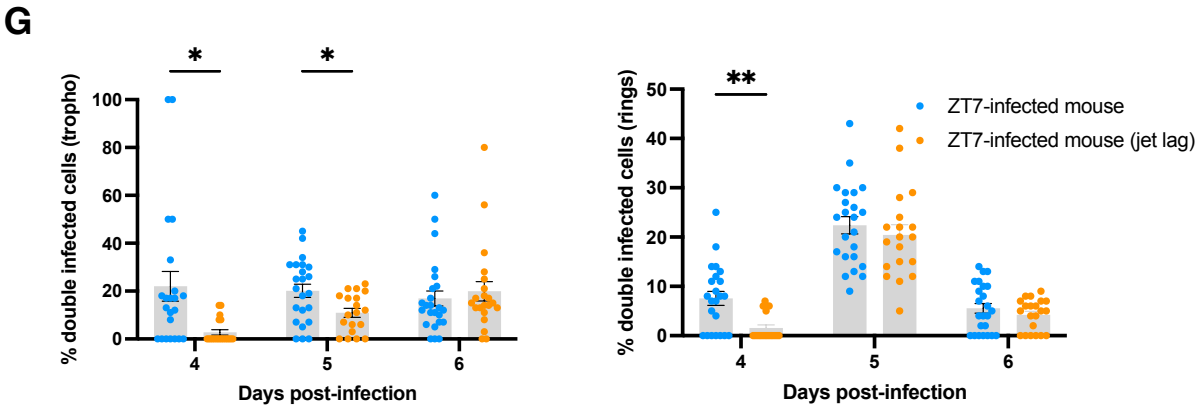

Figure 7. Circadian disruption affects parasite growth and number of parasites per cell.

Mice were injected with *Plasmodium berghei ANKA*-infected erythrocytes after the 10-week chronic jet lag protocol at ZT7 or, at ZT7 or ZT19. **(A,B, C)** Parasite load in the blood and peripheral organs of infected mice, measured by bioluminescence across the days of infection, or at day 5 post-infection. **(D)** Percentage of infected erythrocytes (parasitemia) across the days of infection. **(E)** Percentage of infected erythrocytes containing ring stage forms or trophozoites, across the days of infection. **(F)** Frequency of single-infected and multi-infected erythrocytes across the infection, and heatmap illustrating cell frequency at days 4 and 5 post-infection. **(G)** Frequency of double-infected cells with trophozoites or ring stage forms. Mixed-effects model (REML) with Sidak multiple comparisons test for (A), (E), (D), (F) and (G), and One-way ANOVA with Tukey's multiple comparisons test for (C), and Mann-Whitney test for (B). Data are representative of one of the three independent experiments performed for (A), (B), (C), (D) and (E), and a sum of three independent experiments for (F) and (G), containing 8-10 mice per group. Data are shown as mean ± SEM. *p<0.05, **p<0.01, **** p<0.0001.

A

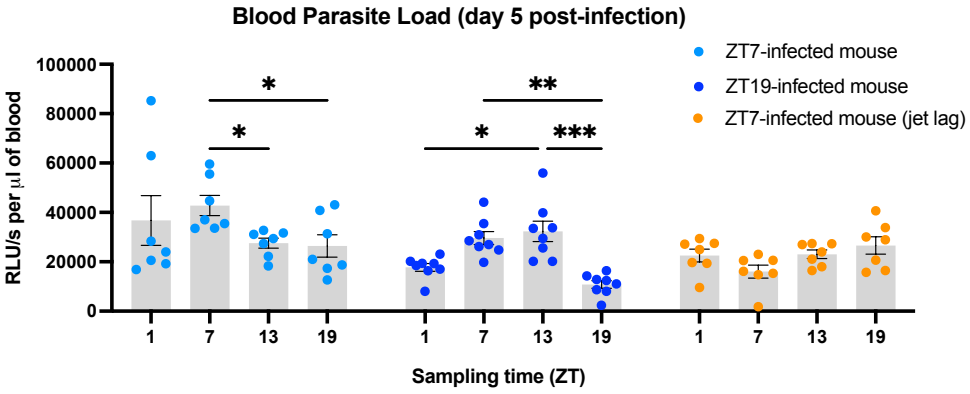
Blood Parasite Load (day 5 post-infection)
ZT7-infected mouse
ZT19-infected mouse
ZT7-infected mouse (jet lag)
RLU/s per µl of blood
Sampling time (ZT)

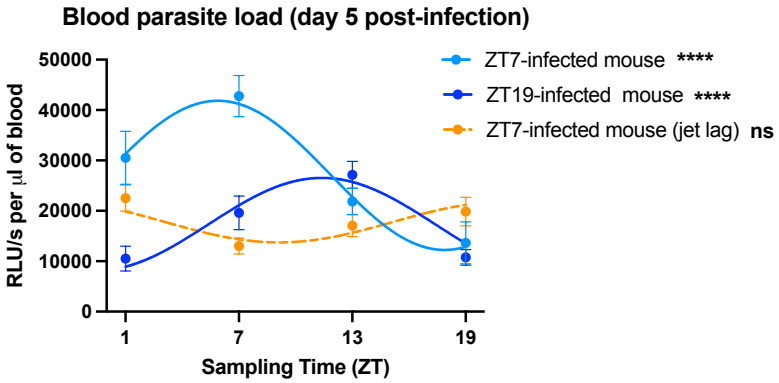
Blood parasite load (day 5 post-infection)
ZT7-infected mouse ****
ZT19-infected mouse ****
ZT7-infected mouse (jet lag) ns
RLU/s per µl of blood
Sampling Time (ZT)

B

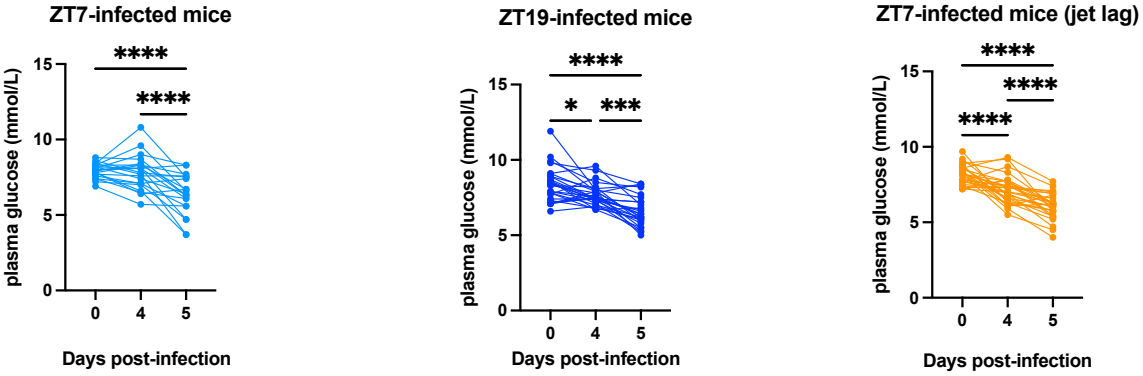
ZT7-infected mice
ZT19-infected mice
ZT7-infected mice (jet lag)
plasma glucose (mmol/L)
Days post-infection

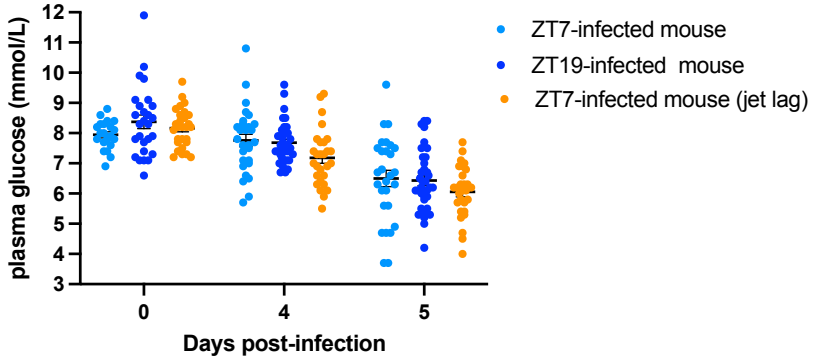
ZT7-infected mouse
ZT19-infected mouse
ZT7-infected mouse (jet lag)
plasma glucose (mmol/L)
Days post-infection

C

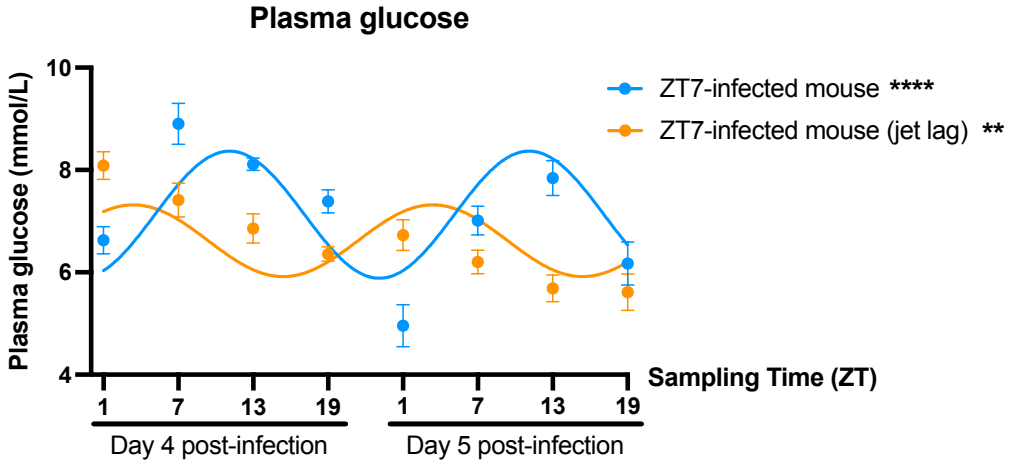

Figure 8. Rhythms in blood parasite load and plasma glucose are disrupted in jet lag mice. Mice were injected with *Plasmodium berghei ANKA*-infected erythrocytes after the 10-week chronic jet lag protocol at ZT7 or, at ZT7 or ZT19 time points. **(A)** Rhythms in blood parasite load of infected mice, measured by bioluminescence, every 6 hours on day 5 post-infection. **(B)** Levels of plasma glucose were compared between groups on day 4 and 5 post-infection and baseline (day 0). **(C)** Rhythms in plasma glucose on days 4 and 5 post-infection. Rhythmicity was evaluated by Non-linear regression (curve-fit): Cosinor analysis for (A) and (C). Dashed lines represent a lack of statistical significance. Two-way ANOVA with Tukey's multiple comparisons test for (A). One-way ANOVA with Tukey's multiple comparisons test for (B) right panel and Two-way ANOVA with Tukey's multiple comparisons test for (B) left panel. Data are representative of one of the three independent experiments performed, containing 8-10 mice per group. Data are shown as mean ± SEM. *p<0.05, **p<0.01, ***p<0.001, **** p<0.0001. ns = not significant.

A

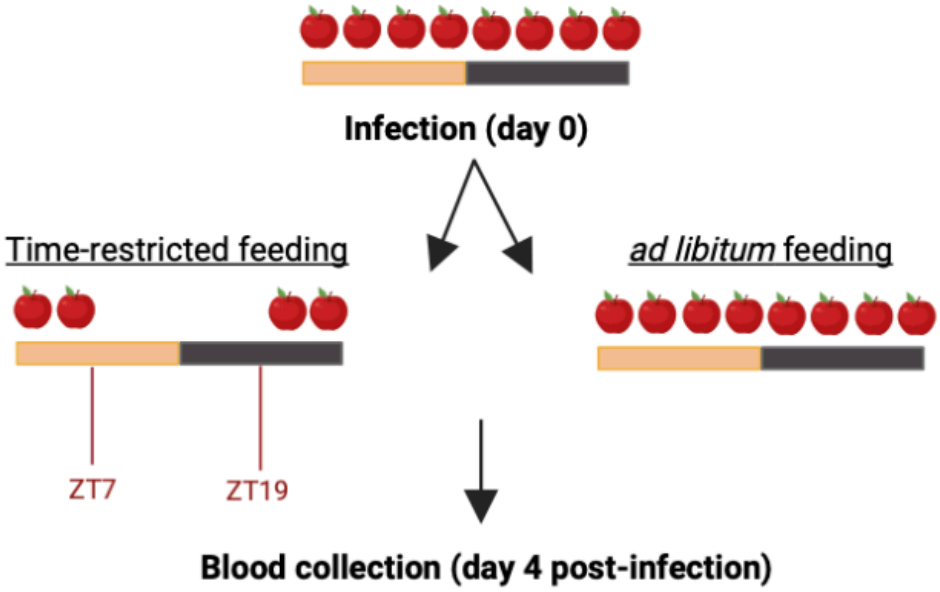
Infection (day 0)
Time-restricted feeding
ad libitum feeding
ZT7
ZT19
Blood collection (day 4 post-infection)

B

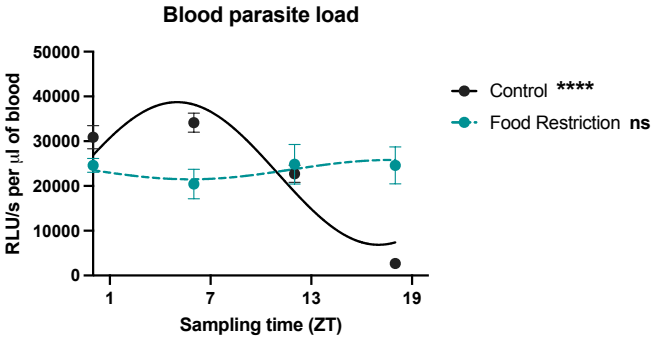
Blood parasite load
RLU/s per µl of blood
50000
40000
30000
20000
10000
0
1
7
13
19
Sampling time (ZT)
Control ****
Food Restriction ns

C

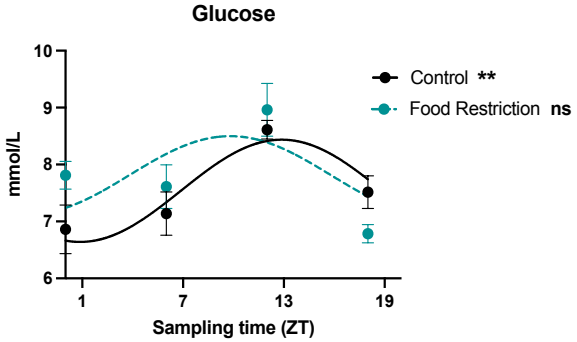
Glucose
mmol/L
10
9
8
7
6
1
7
13
19
Sampling time (ZT)
Control **
Food Restriction ns

Figure 9. Rhythms in glucose and blood parasite load are disrupted following time-restricted feeding in infected mice.

Mice were injected with *Plasmodium berghei ANKA*-infected erythrocytes and assigned to either time-restricted feeding or control group. **(A)** Schematics of time-restricted feeding protocol in infected mice. 24 h after infection, mice were allocated to either a food restriction protocol (food restriction group) with access to food only from ZT19 until ZT7 or, to a non-restriction protocol (control group) with food available 24/7. Mice were subjected to the protocol daily until day 4 post-infection where blood was collected every 6 hours. **(B, C)** Levels of blood parasite load and plasma glucose in the control and food restriction group. Rhythmicity was evaluated by Non-linear regression (curve-fit): Cosinor analysis for (B) and (C) right panels. Dashed lines represent a lack of statistical significance. Data are representative of two independent experiments containing 8 mice per group. Data are shown as mean ± SEM. **p<0.01, **** p<0.0001. ns = not significant. Illustrations created with BioRender.com.

A

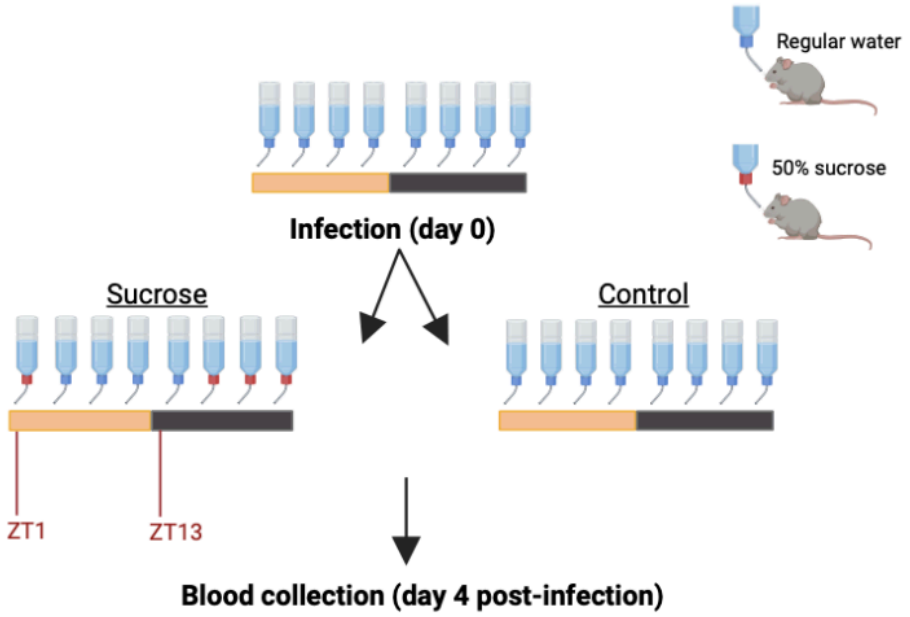
Regular water
50% sucrose
Infection (day 0)
Sucrose
Control
ZT1
ZT13
Blood collection (day 4 post-infection)

B

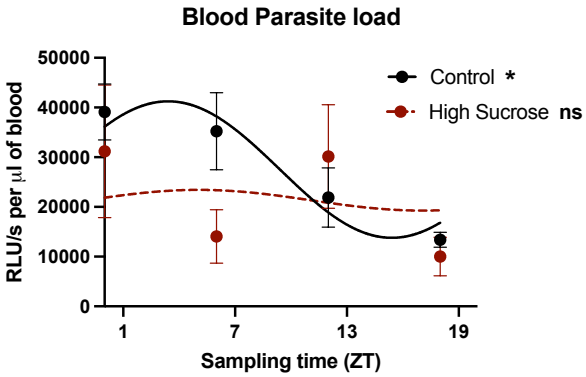
Blood Parasite load
RLU/s per µl of blood
50000
40000
30000
20000
10000
0
1
7
13
19
Sampling time (ZT)
Control *
High Sucrose ns

C

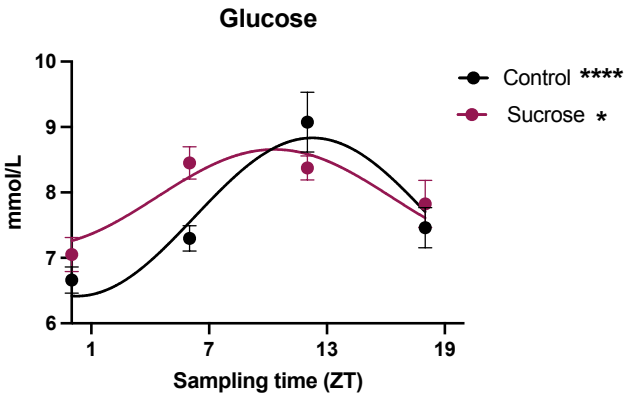
Glucose
mmol/L
10
9
8
7
6
1
7
13
19
Sampling time (ZT)
Control ****
Sucrose *

Figure 10. Rhythms in glucose and blood parasite load are affected by sucrose administration in infected mice.

Mice were injected with *Plasmodium berghei ANKA*-infected erythrocytes and assigned to either sucrose or control group. **(A)** Schematics of sucrose administration protocol in infected mice. 24 h after infection mice were allocated to a water rotation schedule (sucrose group), whereas 50% sucrose water was given from ZT13 until ZT1 followed by replacement with regular water, or to a non-water rotation schedule (control group) with regular water available 24/7. Mice were subjected to the protocol daily until day 4 post-infection where blood was collected every 6 hours. **(B, C)** Levels of blood parasite load and plasma glucose in the control and sucrose group. Rhythmicity was evaluated by Non-linear regression (curve-fit): Cosinor analysis for (B) and (C) right panels. Dashed lines represent a lack of statistical significance. Data are representative of two independent experiments containing 8 mice per group. Data are shown as mean ± SEM. *$p<0.05$, **** $p<0.0001$. ns = not significant. Illustrations created with BioRender.com.

3.8. Supplementary Materials

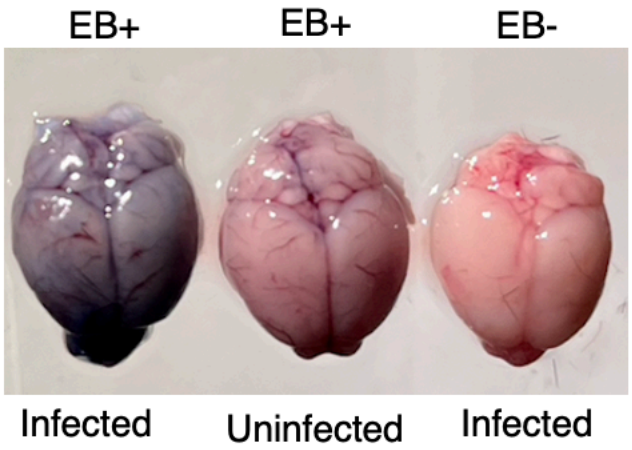

Figure S1. Blood-brain barrier integrity assessment.

Mice were injected with Evans blue dye (EB) and euthanized 2 hours after to assess the presence of the dye in the tissue. From left to right: Infected mouse on day 7 post-infection injected with Evans blue, uninfected mouse injected with Evans blue, and infected mouse on day 7 post-infection injected with saline.

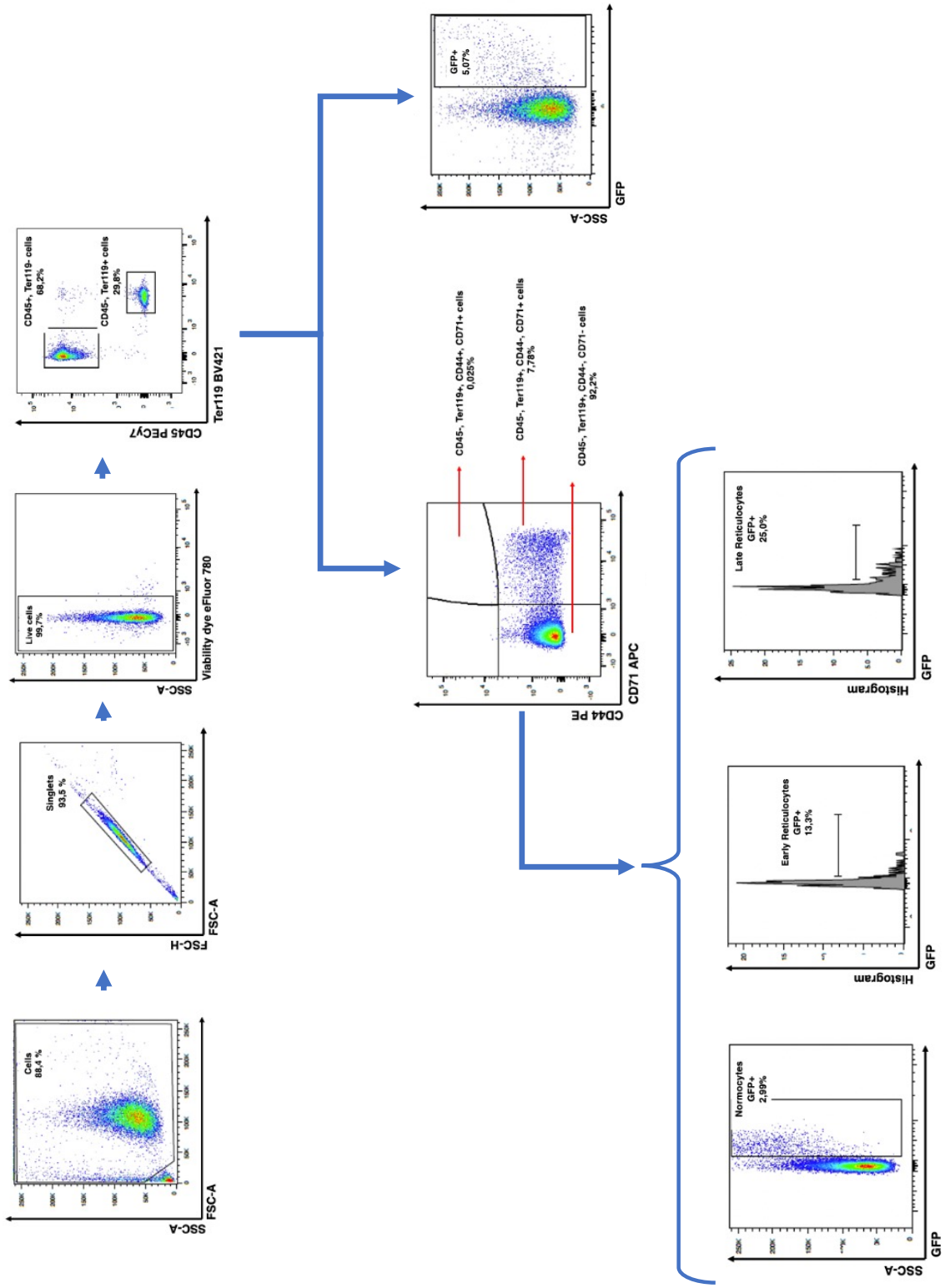
Cells
88,4 %
SSC-A
FSC-A
Singlets
93,5 %
FSC-H
FSC-A
Live cells
99,7%
SSC-A
Viability dye eFluor 780
CD45+, Ter119- cells
68,2%
CD45-, Ter119+ cells
29,8%
CD45 PECy7
Ter119 BV421
CD45-, Ter119+, CD44+, CD71+ cells
0,025%
CD45-, Ter119+, CD44+, CD71+ cells
7,78%
CD45-, Ter119+, CD44-, CD71- cells
92,2%
CD44 PE
CD71 APC
GFP+
5,07%
SSC-A
GFP
Normocytes
GFP+
2,99%
SSC-A
GFP
Early Reticulocytes
GFP+
13,3%
Histogram
GFP
Late Reticulocytes
GFP+
25,0%
Histogram
GFP

Figure S2. Flow cytometry gating strategy for erythrocyte subsets, and infected cells.

Spleen and blood cells were gated based on FSC-A x SSC-A for debris exclusion, followed by singlet gating (FSC-A x FSC-H) for doublets exclusion, followed by viability gating (negative fluorescence) for non-viable cells exclusion, followed by immune cells gating ($CD45^+$, $Ter119^-$) and erythrocytes gating ($CD45^-$, $Ter119^+$). From the erythrocytes gating, infected erythrocytes were gated ($CD45^-$, $Ter119^+$, GFP^+). In parallel, still from within the erythrocyte gate, early reticulocytes ($CD45^-$, $Ter119^+$, $CD44^+$, $CD71^+$), late reticulocytes ($CD45^-$, $Ter119^+$, $CD44^-$, $CD71^+$) and normocytes ($CD45^-$, $Ter119^+$, $CD44^-$, $CD71^-$) were gated, followed by a histogram plot gating GFP^+ cells, for each of the subsets generated (normocyte, late and early reticulocyte subsets) to determine parasite internalized cells.

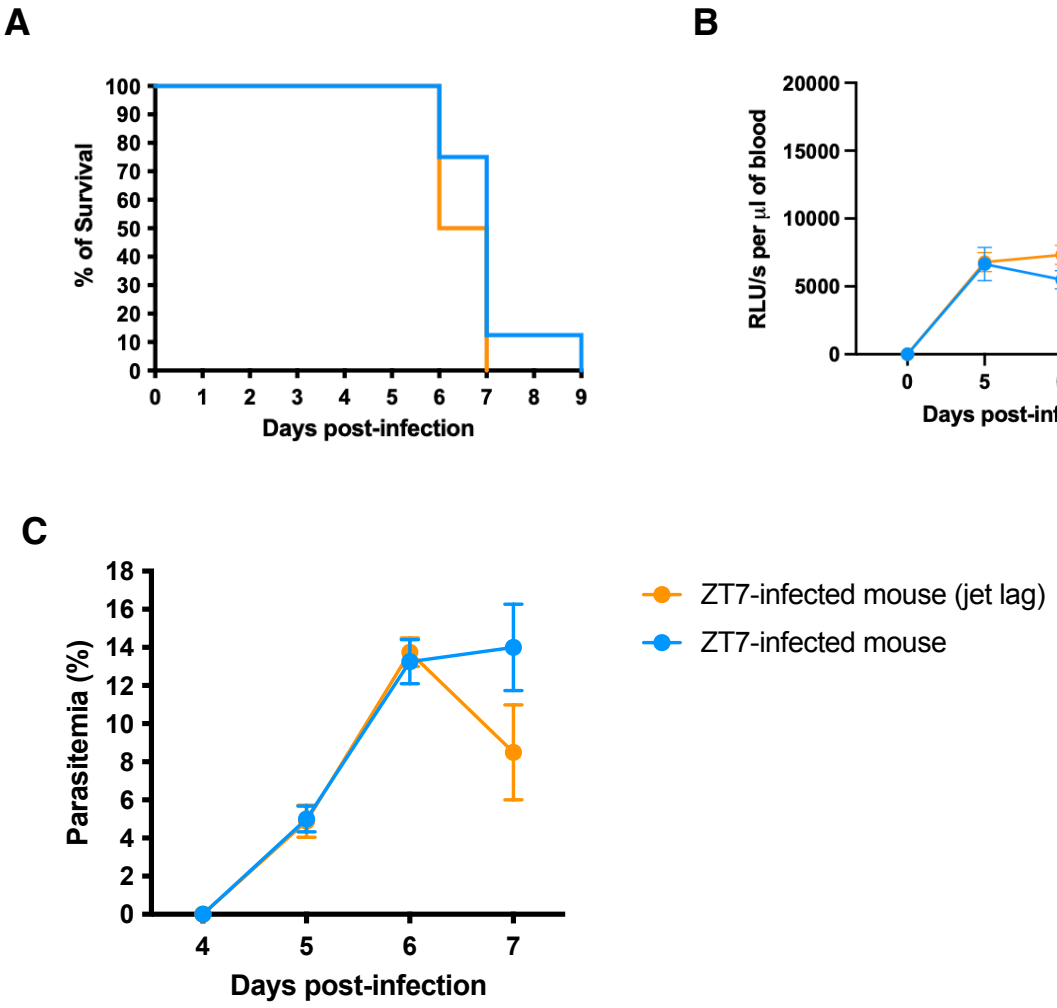

Figure S3. "Short" circadian disruption protocol does not affect host survival or parasite growth.

Mice were injected with *Plasmodium berghei ANKA*-infected erythrocytes after the 4-week short jet lag protocol at ZT7, or at ZT7 (control). **(A)** Survival curve with Log-rank (Mantel-Cox) test analysis. **(B)** Parasite load in the blood of infected mice, measured by bioluminescence across the days of infection. **(C)** Parasitemia across the days of infection. Mixed-effects model (REML) with Sidak multiple comparisons test for (B) and (C). 8 mice per group. Data are shown as mean ± SEM.

A

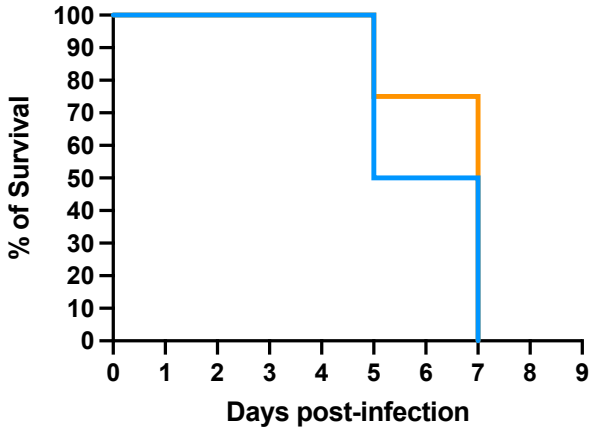
% of Survival
100
90
80
70
60
50
40
30
20
10
0
0 1 2 3 4 5 6 7 8 9
Days post-infection

B

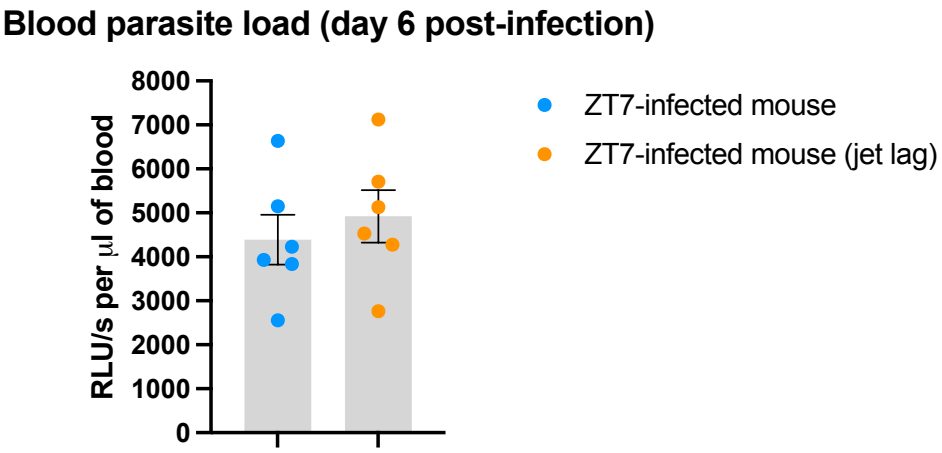
Blood parasite load (day 6 post-infection)
RLU/s per µl of blood
8000
7000
6000
5000
4000
3000
2000
1000
0
ZT7-infected mouse
ZT7-infected mouse (jet lag)

C

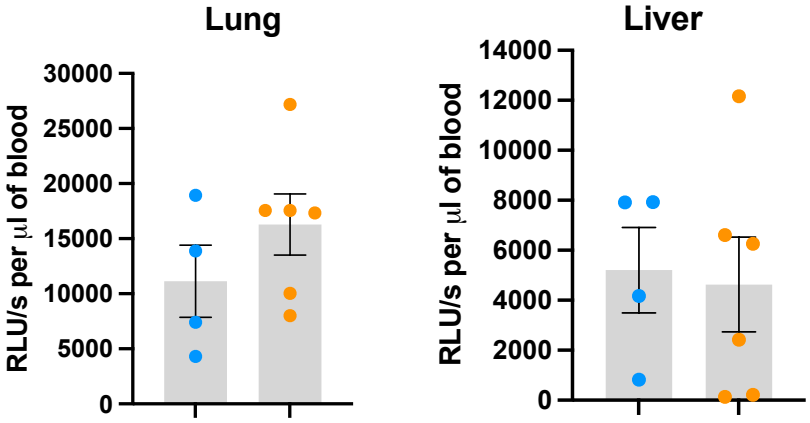
Lung
Liver
RLU/s per µl of blood
30000
25000
20000
15000
10000
5000
0
RLU/s per µl of blood
14000
12000
10000
8000
6000
4000
2000
0

Figure S4. An acute circadian disruption protocol does not affect host survival or parasite growth.

Mice were injected with *Plasmodium berghei ANKA*-infected erythrocytes after a week of acute jet lag protocol at ZT7, or at ZT7 (control). **(A)** Survival curve with Log-rank (Mantel-Cox) test analysis**. (B, C)** Parasite load in the blood and peripheral organs of infected mice, measured by bioluminescence on day 6 post-infection. Mann-Whitney test for (B) and (C). 6 mice per group. Data are shown as mean ± SEM.

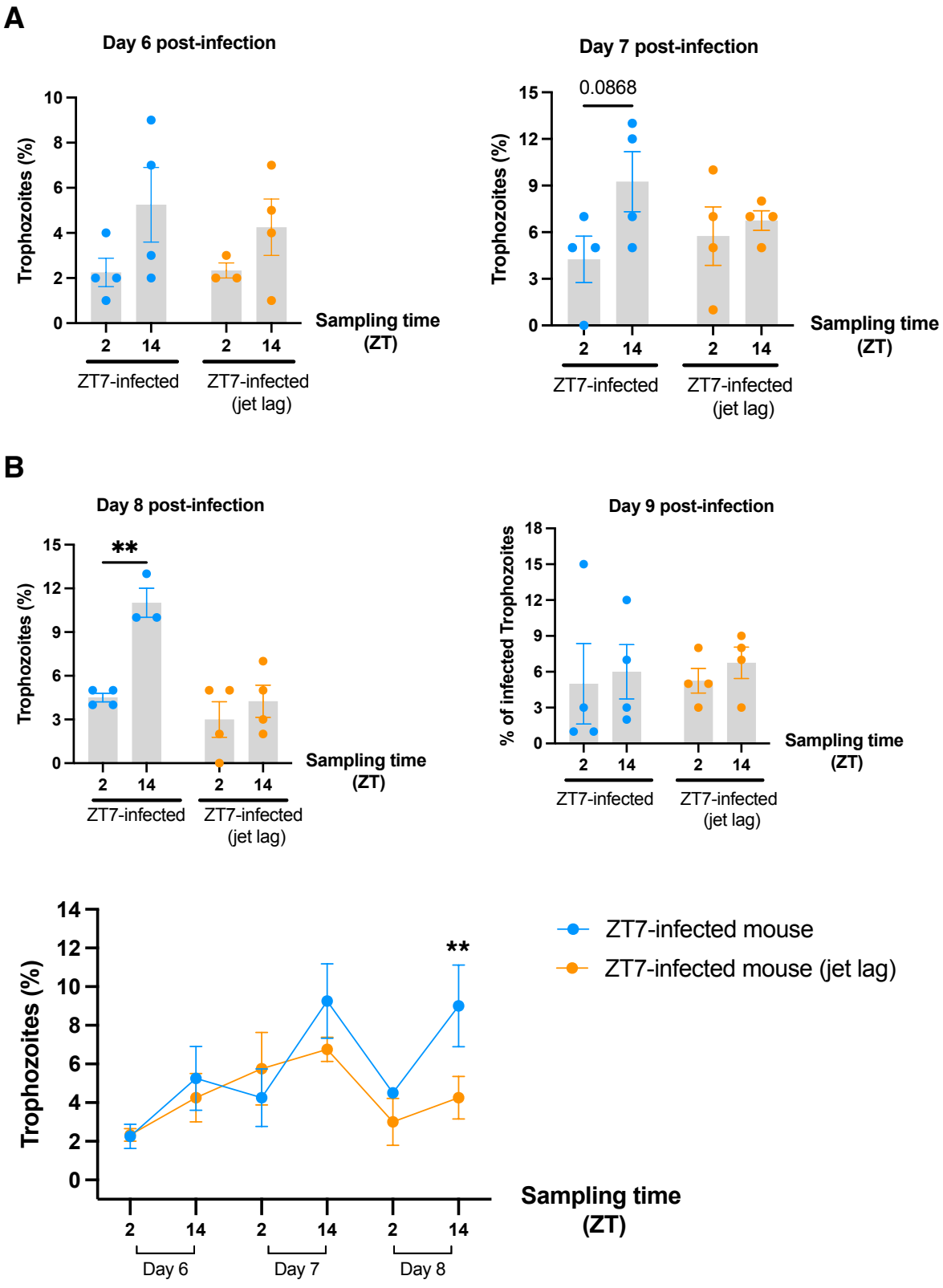
A
Day 6 post-infection
Trophozoites (%)
10
8
6
4
2
0
2
14
2
14
Sampling time (ZT)
ZT7-infected
ZT7-infected (jet lag)
Day 7 post-infection
0.0868
15
12
9
6
3
0
B
Day 8 post-infection
**
Day 9 post-infection
% of infected Trophozoites
18
15
12
9
6
3
0
ZT7-infected mouse
ZT7-infected mouse (jet lag)
Day 6
Day 7
Day 8

Figure S5. Long-term circadian disruption protocol impacts parasite growth in *Plasmodium chabaudi* infected mice.

Mice were injected with *Plasmodium chabaudi*-infected erythrocytes after a 10-week of chronic jet lag protocol (jet lag) at ZT7, or at ZT7 (control). **(A, B)** Frequency of trophozoites in the blood on days 6, 7, and 8 post-infections. Two-way ANOVA with Sidak multiple comparisons test. 3-4 mice per group. Data are shown as mean ± SEM. **p<0.01

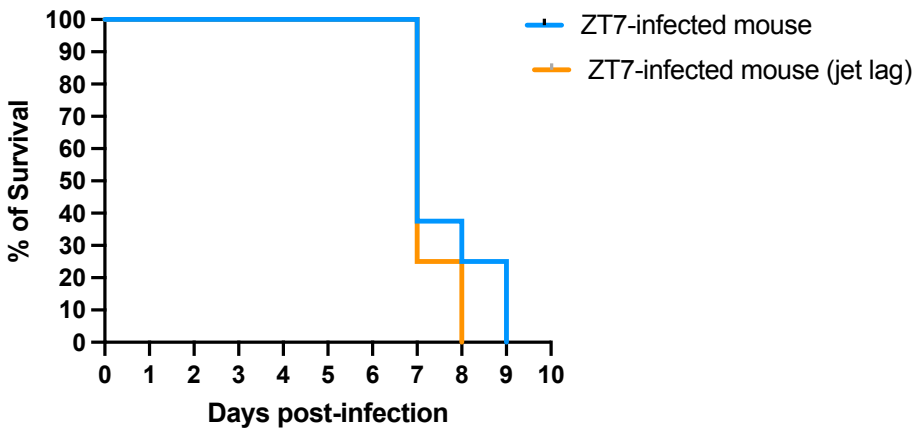

Figure S6. Long-term circadian disruption protocol does not affect host survival.

Mice were injected with *Plasmodium berghei ANKA*-infected erythrocytes after a 10-week of chronic jet lag protocol at ZT7 or, at the ZT7 (control). 8-10 mice per group. Survival curve with Log-rank (Mantel-Cox) test analysis.

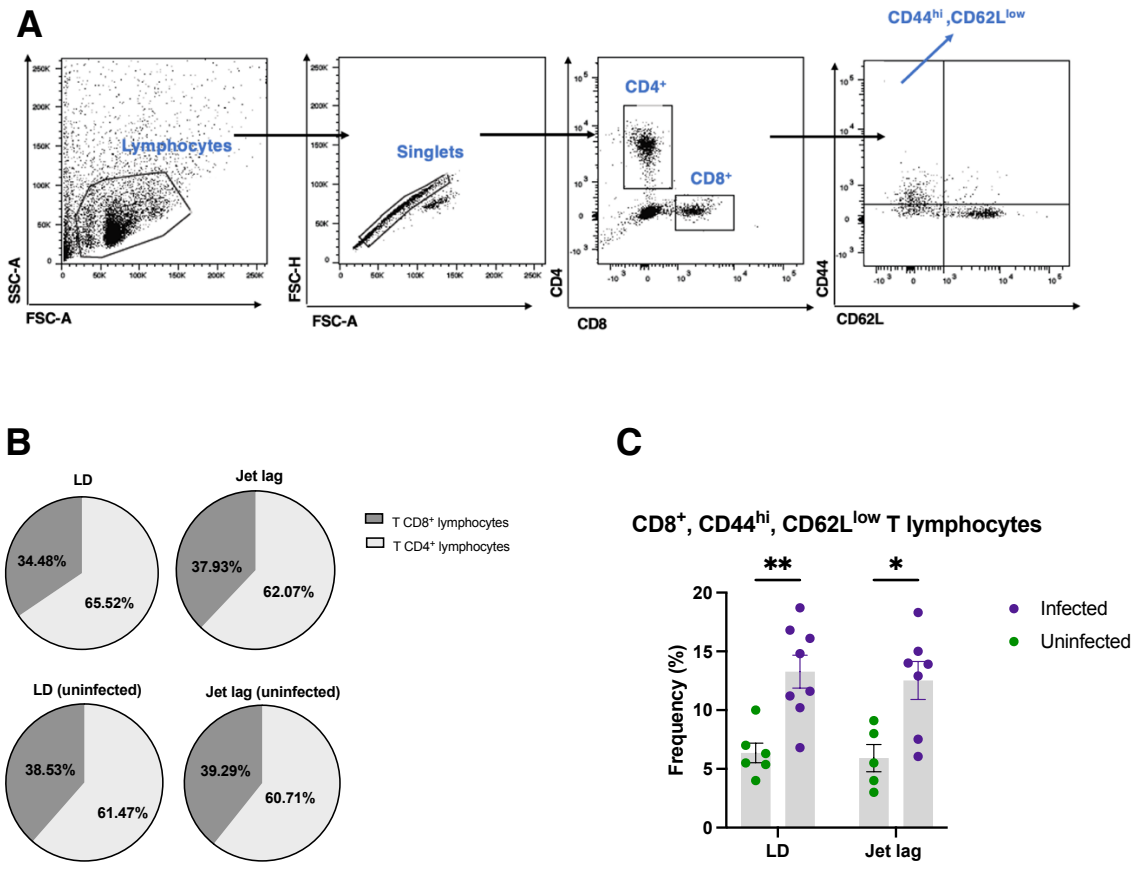

Figure S7. "Long-term" circadian disruption protocol does not affect host immune responses.

Spleen collection of mice infected with *Plasmodium berghei ANKA.* **(A)** Flow cytometer gate strategy for detection of activated T CD8$^+$ lymphocytes (CD8$^+$, CD44^{hi}, CD62L^{low} cells) obtained from tissue harvest on day 7 post-infection, from *Plasmodium berghei ANKA* infected at ZT7 (labeled as "LD") or ZT7 (jet lag), and their respective uninfected controls. "LD" is a designation for animals kept at 12 h: 12 h LD cycle. **(B, C)** Frequency of total T CD8$^+$ and T CD4$^+$ lymphocytes, and frequency of activated T CD8$^+$, CD44^{hi}, CD62L^{low} lymphocytes. Two-way ANOVA with Sidak multiple comparisons test. 6-8 mice per group, and data are shown as mean ± SEM. *p<0.05, **p<0.01.

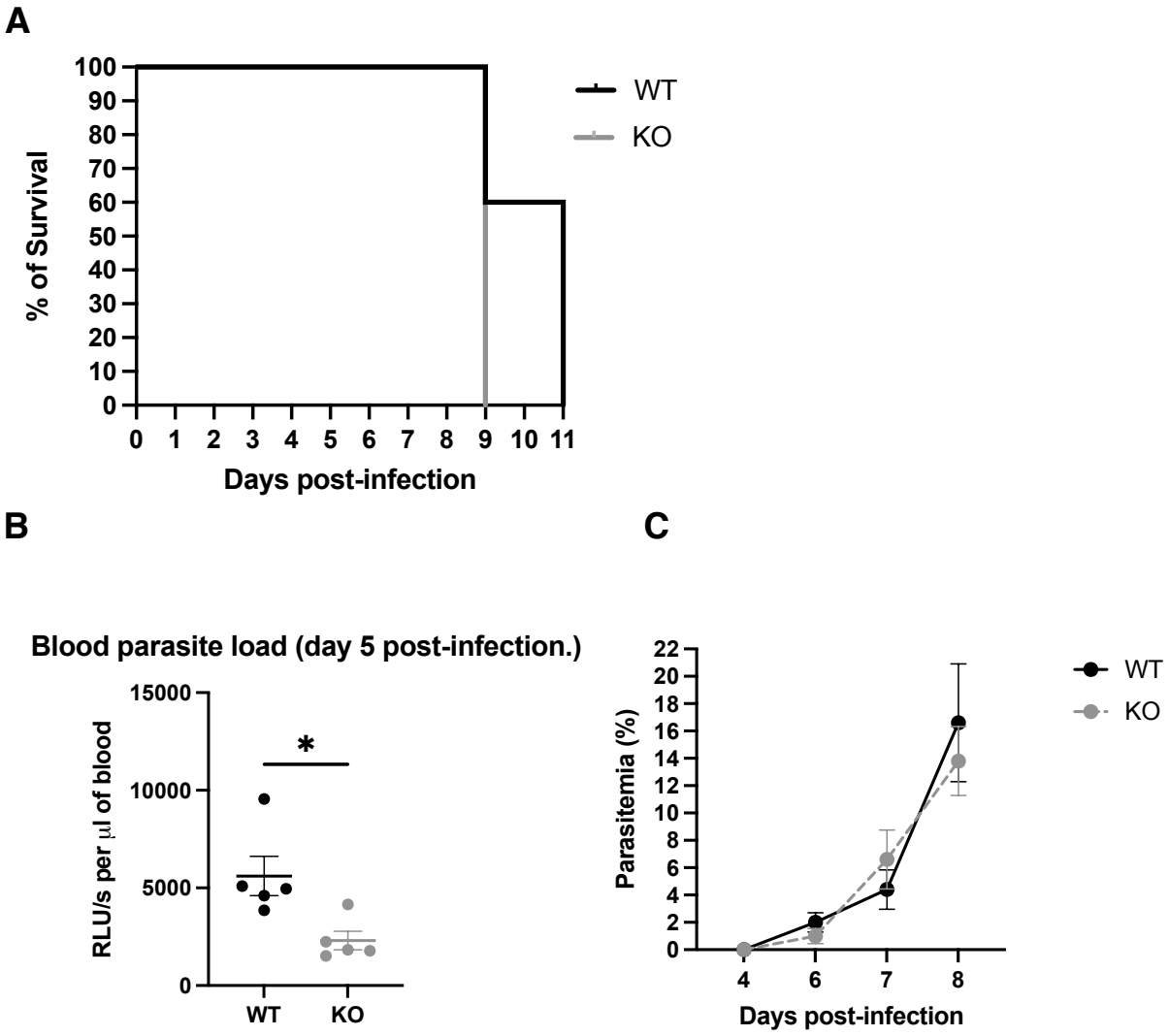

Figure S8. Parasite growth, but not host response, is reduced in circadian clock mutant mice.

Rev-erbα$^{+/+}$ and Rev-erbα$^{-/-}$ mice were injected with *Plasmodium berghei ANKA*-infected erythrocytes at ZT7 and evaluated across days post-infection. **(A)** Survival curve with Log-rank (Mantel-Cox) test analysis. **(B)** Blood parasite load of infected mice, measured by bioluminescence on day 5 post-infection. **(C)** Parasitemia across the days of infection. Two-way ANOVA with Sidak multiple comparisons test for (C) and Mann-Whitney test for (B). Data are

representative of one of the two independent experiments performed, containing 5 mice per group. Data are shown as mean ± SEM. *$p<0.05$.

Chapter 4: General Discussion and Conclusions

4.1. Specific considerations

Over the past decade, circadian rhythms have been the focus of many studies linking the immune system and host response to pathogens [163]. In the malaria field, parasite dependency on host circadian rhythms, including feeding behavior, as a tool to regulate and/or guide their synchronized developmental cycle within red blood cells has been widely demonstrated [179, 180, 231]. Although this relationship has recently been contradicted by a recent finding of endogenous circadian rhythms in malaria parasites [167, 168, 210], little is known about the true interplay between host rhythms and parasites and whether this can be applied to all *Plasmodium spp.* species. As a common factor, immune responses are particularly important during the course of this disease, more specifically by recognizing recently ruptured infected red blood cells, in a synchronized encounter [38, 207]. Up-to-the date almost all immune cells have been shown to harbor a circadian clock controlling the magnitude of immune responses [125]. Despite this, the work described in this thesis has been the first one to investigate whether the circadian clock in macrophages controls a rhythmic response upon recognition of ruptured infected red blood cells. This data was presented in **Chapter 2**, through the development of a novel *ex-vivo* stimulation model using bone-marrow-derived macrophages and *Plasmodium berghei ANKA*-infected red blood cells (iRBC) presented at 4 different time points after circadian rhythms synchronization.

We were able to identify that not only many immune response parameters were significantly affected by the time of stimulation, but they shared similarities as per the intracellular networks and cytokine/chemokine profile, as observed in studies using macrophage stimulation with *Plasmodium spp.* derived molecules, such as haemozoin. For instance, innate immune

activation through the involvement of NLRP3 inflammasome complex with consequent release of IL-1β [77, 80] was observed during haemozoin challenge. Similarly, we found a robust rhythm of IL-1β in the supernatant of cells 24 h after stimulation. Interestingly, our results showed a rhythm with similar phase for IL-1β and ROS generation. The latter is an event that not only has been widely reported in macrophages-haemozoin response [73], but it is known to be involved in the activation of the NLRP3 inflammasome pathway. Aligned with more studies in the field [69], we have also detected phosphorylation of ERK1/2, members of the MAPK signaling pathway. Moreover, the pro-inflammatory nature of this response reflects what has been shown during malaria pathogenesis, in both human and animal studies [3].

Differently from other studies in the field which have used malaria-derived isolated compounds, such as haemozoin [213], or enriched schizont-infected cells [82, 84], our model used a mix of lysed infected and non-infected red blood cells containing a large repertoire immunomodulatory molecules. Therefore, upon stimulatory assays, additional intracellular networks are likely to be involved and should not be ignored. In other words, we have generated a more realistic set-up to study iRBC-macrophages interaction, which can allow the identification of transcription factors and key proteins that can be tested for targeted therapeutically. To explore this network, we have conducted proteomics and phosphoproteomics, selecting 2 time points (22 and 34 h after cell synchronization) representing the "peak" and "trough" of most cytokines/chemokines detected, including IL-1β production and ROS production. We have also compared the effects at the cellular level specific to the presentation of iRBC (compared against control samples). As a result, we have found a striking number of proteins and phosphopeptides affected by time of stimulation (22h or 34 h post-synchronization) and iRBC administration in our proteomics/phosphoproteomics screen. Interestingly, these molecules were associated with several

immune signaling pathways, including JNK and p38, PI3K-Akt-mTOR, and IFN, with downstream implications on pro-inflammatory responses (including ROS production) and phagocytosis. Altogether, the results obtained using this novel model recapitulate the immune activation pathways and key players identified during malaria disease.

Importantly, the circadian control of ROS generation [144], and cytokine/chemokine activation [137] has been already reported, but never in the context of malaria. Since we have identified the existence of circadian control in immune responses during iRBC interaction, now it remains to be tested whether the proteins identified in our proteomics/phosphoproteomics screen, are under the direct control of macrophage's circadian clock. As others in the field have shown that clock proteins, such as BMAL1 and CLOCK, direct regulate the transcription of pro-inflammatory genes [135, 143], a potential future step for this project would be to identify if any of the molecules in our dataset has binding sites for clock proteins, such as BMAL1 and CLOCK, using wild-type and clock gene knockout BMDM. If such control exists, then the next step would be to verify if the level of the macrophages' response can be modulated when clock-targeted compounds are used, similarly to what has been shown in other studies in the field. For instance, in the study of Gibbs JE et al., human macrophages in response to LPS led to production of IL-6 directly under the control of clock protein REV-ERBα. Repression of IL-6 by REV-ERBα was confirmed by 2 ways: By using REV-ERB synthetic ligands or by *rev-erbα* knockout [137]. After identifying clock direct targets in our model, the application of synthetic ligands (i.e. GSK4112 compound used on Gibbs JE and cols study [137]) during BMDM stimulations at 4 different time points with infected RBCs would allow us to verify: First, if the rhythms in macrophages response was abolished and second, if we can modulate the intensity of the immune response acting at the activation/repression peak levels. In other words, since we know that the peak of IL-1β rhythm

happens at 22 h after cell synchronization, a repression of IL-1β activation at that time point by clock agonists/repressors would prevent a high immune activation, which is a known feature of malaria pathogenesis. Lastly, this targeted approach would require to be tested *in vivo*. By using a synchronized malaria model (e.g. *Plasmodium chabaudi* infections) by which the peak of rupture of iRBCs happens every 24 h consistent with immune activation, the application of clock activators/repressors at the maximal time of immune activation, in an attempt to shut down proinflammatory responses could potentially restrict the severity of the disease. In terms of clock activation of proinflammatory cytokines, the goal would be to suppress clock binding to target proteins. On the other hand, for molecules that are under repression of clock proteins but are involved with an anti-inflammatory response, such as the transcription factor NRF2 that regulates the expression of antioxidant proteins [144], clock activation can contribute to supress inflammation. Since immune responses are present in many different situations (e.g. infections, cancer, autoimmunity, vaccination), unravelling the clock control of immune responses would contribute with the development of chronotherapy tools that can be applied in many different scenarios. So, our findings are not exclusive to the field of malaria, but they have a much larger implication.

One limitation of our model is that we have conducted all experiments using a single cell line (a primary culture of bone marrow-derived macrophages). During malaria pathogenesis, the cells which encounter iRBCs are phenotypically more mature, characterized by patrolling monocytes or tissue-resident macrophages (i.e. splenic or liver macrophages) [212], which could potentially result in a distinct profile of response when compared to naïve bone marrow-derived macrophages. In addition to that, *ex-vivo* stimulations are isolated set-ups that do not account for the participation of other cell types (e.g. neutrophils) or molecules (e.g. complement system).

Therefore, the next step for this model would be to be tested *in vivo* with the administration of iRBCs at different circadian time points, directly at the blood-stream level for further evaluation of innate immune responses.

Apart from the circadian control of immune responses upon iRBC presentation, we decided to explore if other circadian rhythms could play a role during malaria pathogenesis, and for this purpose, we conducted studies *in vivo*. Still interested in investigating the responses at the blood stage level of the disease, in **Chapter 3** we have administered iRBCs to C57BL/6 mice. To investigate, once again, if the time where the host encounters the parasite influences disease progression, the infections were performed at one of 4 time points (ZT1, 7, 13, or 19) across 24 h. By using a highly inflammatory and lethal malaria model (ECM), our results showed, in terms of host response, that ZT19-infected mice had a lower clinical score during behavioral evaluation. The scoring system is fundamentally based on the symptoms associated with cerebral malaria [211]. In the ECM model, cerebral malaria is an event that occurs in response to adaptive immunity activation [92, 232] and sequestration at the level of the brain vessels, with active participation of innate immunity and inflammation [64]. Although the ZT19-infected mice displayed less sickness behavior on the first days of infection, as the disease progressed, they all still succumbed to cerebral malaria with high levels of pro-inflammatory cytokines in their serum. Thus, the results showed that the time of infection does not affect the development of this pathology.

However, it cannot be ruled out that physiological effects due to the time of infection could still be present, although potentially shadowed by the fast-paced nature PbA model (lethality between 7-10 days post-infection) with incredibly high levels of immune activation [66]. To further investigate if ZT19-infected mice have more prominent effects on host response, infections with non-lethal malaria models (e.g. *P. yoelli* 17XNL [93], or *P. berghei ANKA* in DBA/2 or balb/c

mice [233]) ECM preventive approaches (e.g. iron dextran [92], antimalarial drugs [234]) or knockout mouse models (e.g. IRF1$^{-/-}$ mice) [59] would have to be carried out.

On the other hand, in our model, time of infection affected parasite growth with significantly lower levels of parasite load for the ZT19-infected mice. Importantly, the lower level of parasite load in ZT19-infected mice is not due to the time of day where blood was sampled (i.e. ZT19-infected mice had their blood collected to determine daily parasite load at ZT19). Although 24-h rhythms in parasite load have been detected in both ZT7-infected and ZT19-infected mice and could influence the measurements depending on the time of the day blood is sampled, when we ran the analysis excluding "effect of time" (by calculating the sum of the averaged blood parasite load values in each time point, to determine daily levels) and compared between groups (ZT7- and ZT19-infected mice), we found that the level of parasite load on day 5 post-infection in ZT19-infected mice was about 47% lower when compared to ZT7-infected mice. In other words, a 1.47-fold change difference between groups was detected. Thus, this analysis confirmed that infection at ZT19 led to lower levels of parasite load, regardless of the blood sampling time point.

Based on these results, a few speculations as per the mechanisms involved have been proposed, all aiming at the initial hours post-infection. First, we asked whether at the middle-of-the night time point, mice displayed of a limited availability of red blood cells, in special immature forms (reticulocytes), as the target cells of infection, when compared to the middle-of-the day time point. We have confirmed this hypothesis by detecting significantly lower levels of early and late reticulocytes, at ZT19 compared to ZT7 in the blood. Although the internalized GFP^{+} reticulocytes did not show the same trend (most subsets in the blood and spleen were not significantly affected by time point), it is possible that the rare frequency of these cells in the blood-stream could have accounted for the lack of significance. That being said, further investigations are needed to confirm

if parasite growth impairments observed in ZT19 mice are due to reticulocyte availability. One way to test this could be through a tracking protocol used in Hentzschel F et al. study [97], with a few adjustments: By performing mouse inoculation of a purified culture of synchronized PbA schizonts, blood would be collected hours after to determine the frequency of ring stage-infected red blood cells. This would allow us to determine the efficiency of the infection (by counting these newly invaded cells) right after parasites release from schizont-infected cells. Newly invaded cells, mainly reticulocytes if considered the PbA tropism, would be experimentally differentiated by the presence of ring stage parasites within red blood cells. As protocol adjustments, Hentzschel F et al., study used a mCherry PbA line where the fluorescent reporter is under the control of *hsp70* promoter, increasing fluorescence as parasite matures. This allowed them to distinguish between early forms (i.e. ring stage) and late forms (i.e. schizonts) [97]. Although our model does not display of this feature, our parasites express GFP^+ throughout their entire life cycle which would allow us to still differentiate early and late forms based on flow cytometer detection of fluorescence intensity, as per protocol published already [235]. Thus, the proposed experiment could be run starting by synchronization of PbA GFP^+ cultures *in vitro* (protocol based on [236]) with injection of schizonts-infected red blood cells in a mouse at either ZT19 or ZT7. Then, collection of blood (and spleen, given the strong PbA tropism for splenic erythrocytes [97]) 1-2 h after to measure and compare between time points the frequency of ring-stage infected cells, by flow cytometry [237] or manual counting (smears). If differences between time points are observed, then it would be needed to confirm if such differences persist over time (blood collection and analysis over the course of the infection) as an indication that parasite growth was affected due to the time variations in reticulocyte abundance. However, as we have already reported a time variation in the frequency of reticulocytes, for such experiment, blood sampling would have to performed more than once

per day (every 6 h or 12 h) to confirm that regardless of the sampling time point, the effect on parasite growth over the course of the infection is resulted of the "schizont injected trial" performed either at ZT19 or ZT7.

Furthermore, in our studies it remains to be validated if the time variations in erythrocytes population are circadian-controlled. In our experiments, we have sampled blood and tissue (spleen) at 2 different ZTs (7, 19). To confirm in our model, if this is a circadian rhythm in red blood cells, including the reticulocytes subset, a minimum of 4 sampling time points over 24 h in mice kept in constant darkness would be required. In fact, literature supporting circadian rhythms in the abundance of red blood cells exists, and interestingly this rhythm is abolished in CLOCK mutant mice [238]. Thus, if we were to confirm this, a follow up experiment could be first to verify if the rhythms are abolished in full body clock gene knockout (e.g. BMAL1$^{-/-}$). Following this, to verify if the rhythms are controlled at the level of the bone-marrow, considering the known rhythm in hematopoietic stem cell (HSC) differentiation and rhythmic egress from the bone-marrow ([214], transfer of bone-marrow from BMAL1$^{-/-}$ mice into an irradiated recipient mouse, to disrupt the clock only in HSC, would proceed. As result, we would aim to verify if the rhythms in red blood cells, including reticulocytes, are once again disrupted in this approach, and if so, whether the differences observed in ZT7 and ZT19-infected mice as per parasite growth, can be reproduced.

Second, we have speculated that local immune responses at ZT19, at the peritoneal cavity site, could be responsible for parasite clearance moments after inoculation. Although we have not tested this scenario, our theories are based on the work of others. For example, our lab has demonstrated a stronger incoming of innate immune cells to the peritoneal cavity in mice inoculated with *Leishmania major* parasites during the subjective night (CT15) in comparison to subjective daytime points (CT3). This was accompanied by higher levels of chemokines such as

Mip2, *Mip1α,* and *Mip1β* [165]. Similarly, administration of LPS at the peritoneal cavity of mice at CT12 showed to result in a greater innate immune response in comparison to CT0, with the participation of pro-inflammatory cytokines and chemokines IL-6, IL-12(p40), CXCL1, CCL5 and CCL2 [137]. Interestingly, this response was shown to be regulated by the circadian clock in myeloid cells, confirmed by follow-up experiments using *LysM-bmal1*$^{-/-}$ PECs [137]. That being said, considering that circadian rhythms and the host's clock govern the intensity of immune responses in the peritoneal cavity environment, it is possible that time-dependent host responses are taking place following iRBCs injection, and could potentially influence the outcome of the infection. More specifically, whether higher immune responses are being triggered when infections are performed at ZT19 when compared to ZT7, a faster parasite clearance could be a result of this timed-controlled interaction. To test this, a few experiments could be carried out. First, innate immune responses (including the level of cell recruitment and cytokine/chemokine production) following iRBCs injection would need to be measured in the initial hours post-injection. Second, parasite tracking assays could test whether the values of parasite load at the initial hours post-inoculation are significantly reduced in ZT19-infected mice compared to ZT7.

Furthermore, to be able to confirm that the phenotype observed in our 4 time points *in vivo* experiments at later days of infection is mediated by circadian rhythms at the peritoneal cavity level, infections using *LysM-bmal1*$^{-/-}$ could be performed or alternatively, experiments using different routes of inoculation that are not influenced by local immunity (e.g. intravenous).

Still, in **Chapter 3**, we have demonstrated parasite dependency on host circadian rhythms for their growth and rhythmicity, through the execution of circadian disruption and time-restricted feeding/sucrose experiments. Interestingly, circadian disruption when administered acutely (for a short duration of time) and/or in a less disruptive protocol (6-h shift weekly) did not affect parasite

growth in our ECM model. On the other hand, parasite growth was affected upon a chronic (10 weeks) circadian disruption protocol with a more disruptive schedule (8-h shift every 2 days), suggesting that perhaps host circadian clocks require longer exposure to achieve desynchrony, or that the phenotype is mediated by "after-effects" of circadian disruption that are only present after chronic exposure. Although circadian disruption experiments using a mouse model of *Plasmodium berghei ANKA* infection have never been investigated and therefore, no literature on the topic is available, it is known that mouse exposure to an irregular lighting condition (i.e. constant light) can affect host responses, including immune responses. For instance, under 8 week-exposure to constant light, mice injected with LPS produced higher levels of pro-inflammatory cytokines IL-1β, IL-6, and TNFα [162]. However, the nature of this response is somewhat complex and transient whereas the effect was absent when tested after 24 weeks of exposure. In another study, mice subjected to 12 weeks of circadian disruption (6-h shift weekly) had their blood collected and incubated in the presence of LPS. This resulted in significantly elevated levels of IL-6 within 6 hours of stimulation which persisted after 24 h, in comparison to non-circadian disrupted mice subjected to the same challenge [239]. Similarly, mouse exposure to a month of circadian disruption (6-h shift weekly) showed to impact survival susceptibility to LPS injection, cytokine/chemokine level (blood), rhythms in peripheral tissues (i.e. liver) and more [153]. Moreover, chronic exposure to 8-h phase advance every 2 days for 8 weeks resulted in increased vulnerability to inflammation due to DSS-induced colitis in mice [160].

Nevertheless, in our model, we have not seen effects on the host response to the infection (survival, clinical scores, and immune responses) in a circadian disruption-dependent way, in any of the protocols tested. Nevertheless, chronic circadian disruption affected other host circadian rhythms, including metabolism (data on reduced amplitude and phase shift on the rhythms of

glucose over 48 h). Yet, it remains to be investigated whether more rhythms are being influenced by this protocol (e.g. hormonal production, core body temperature, sleep-wake cycle) given that many physiological processes are regulated by circadian clocks and dependent on environmental cues (e.g. light and dark cycles) [240]. As shown by Brager AJ et al., weekly exposure to circadian disruption (6-h phase advance) led to transient effects on the sleep-wake cycle of the mice, more specifically by promoting about 10% of net loss of sleep each week [239]. As several studies have linked sleep deprivation with impacts at the level of the immune system, although we have not measured sleep in our model, it is possible that the circadian disruption protocol which consisted of repeatedly 8-h shifts every 2 days for a total of 10 weeks might be impacting sleep-wake cycle of these animals. The effects of sleep on immune responses have been shown to be contradictory, where in some studies an increased frequency of circulating immune cells was observed [241] whereas in others an opposite phenotype was seen (i.e. decreased in monocytes frequency [242], neutrophils phagocytosis capacity [243] and more). Changes in the rhythms of cytokine production following sleep deprivation have also been reported [150]. Nevertheless, as the immune system has an important role in recognizing parasites and eliminating them, it should not be ignored in our model that the differences in parasite growth observed in circadian disrupted mice could be affected (or at least partially) by the sleep-wake cycle. To add to that, as feeding rhythms are also known to be influenced by light and dark cycles [228, 230] we have measured over the course of 10 weeks the body weight of circadian disrupted (and control) mice. In our model, we have not detected any statistically significant differences in body weight gain between both groups (data not shown).

Interestingly, parasite growth impairment over the days of infection was detected in mice subjected to chronic circadian disruption. When we infected mice at ZT7, 19 or 7 (jet lag) and

compared among them the parasite load levels (blood) on day 5 post-infection, we found that ZT7-infected mice (jet lag) had lower levels of parasite load over the days of infection, and that this was not due to the time of day where blood was sampled. Similar to the approach used to determine that ZT19-infected mice had impaired levels of parasite load when compared to ZT7-infected mice (by excluding the "effect of time" in the analysis), we found that ZT7-infected mice (jet lag) displayed of lower levels of blood parasite load, on day 5 post-infection, when compared to ZT7-infected mice, and when compared to ZT19-infected mice. Our fold change analysis showed that ZT7-infected mice had about 4 times more parasite load levels, and that ZT19-infected mice had about 2 times more, than ZT7-infected mice (jet lag). Thus, the results showed to us regardless of the blood sampling time point, jet lag mice had lower levels of parasite load when compared to both ZT7 and ZT19-infected mice. We have previously speculated about potential reasons why ZT19-infected mice had parasite growth impairments when compared to ZT7-infected mice. However, in our jet lag experiment, the parasite load levels obtained with this ZT7-infected mice (jet lag) were even more prominently reduced when compared to ZT7-infected mice, than the levels observed with ZT19-infected mice vs ZT7-infected mice, potentially suggesting additional mechanisms impairing parasite growth, rather than time of infection, that are taking place during circadian disruption. Although it remains unknown what are the mechanisms driving this phenotype, we have a few speculations based on our findings from circadian disruption and host rhythms (glucose) measurements, which will be discussed later.

Furthermore, in this same chapter, we showed that lower levels of parasite load in jet lag mice are not exclusive to the blood site, as we have also measured this with peripheral tissues collected on day 7 post-infection (as a read-out for iRBC sequestration) [8, 106]. We have also found that the differences in parasite load were coming from the ratio of single: multi-infected

cells. In other words, jet lag mice displayed reduced parasite load which was accompanied by a decreased frequency of multi-infected cells (i.e. red blood cells containing 2 or more rings/trophozoites). An increased frequency of multi-infected cells (observed in ZT7-infected cells) automatically leads to an increased RLU/s signal during parasite load measurements. Altogether, these findings indicate that parasite load is reduced in jet lag-subjected mice, and it is reflected by having fewer parasites entering the red blood cell, considering *Plasmodium spp.* parasites capacity of multi-invasion [215, 244]

During circadian disruption experiments, one of the most interesting observations was the rhythmicity of parasite load on ZT7 and ZT19-infected mice (and the lack of it on jet lag mice). This piece of data indicated to us that not only host circadian rhythms impact parasite growth over the course of the infection but their 24-h rhythms. We determined that parasite load rhythm peaks between ZT7 and ZT13, but the mechanism remains unknown. Given the asynchronous nature of *Plasmodium berghei ANKA* [183], it is unlikely that these rhythms are due to a 24-h parasite intra-erythrocytic division cycle, as it occurs with other *Plasmodium spp.* species [32, 206].

Furthermore, a recent study with *Plasmodium berghei ANKA* showed that their intra-erythrocytic division cycle is not influenced by host-parasite rhythms mismatch and that the proportion of each parasite stage form (ring, trophozoites and more) does not vary across 24 h [185]. It is also unlikely that the rhythms are due to sequestration events, as we have not detected a rhythm in the frequency of schizonts in the bloodstream over 24 h (data not shown). In addition to that, the same phenotype of reduced parasite load for jet lag mice in the blood was observed in the peripheral organs. If the reduced parasite load in the blood was resulted of an increased sequestration in peripheral organs, we would expect to obtain an inverted result for parasite load measurements in the organs (i.e. higher level in jet lag mice), which was not the case. Nevertheless,

despite no study has investigated this in detail, rhythms in sequestration seem to be present during *Plasmodium berghei ANKA* pathogenesis, as reported in a study conducted in 1969 [184]. As known, infected red blood cells (mainly schizont-infected) [8] (sequester in peripheral tissues such as the lung, liver, and more [63, 90]. A recent publication showed that PbA iRBC expresses a unique surface protein denominated schizont membrane-associated protein "SMAC" which binds to CD36 molecule, expressed by endothelial cells, and it is involved in sequestration events [102]. Interestingly, this protein was shown to be rhythmically expressed [169]. Nevertheless, additional experiments are required to identify in our model, why parasite load is rhythmic, and under which mechanism.

Although we have not identified the mechanisms behind parasite load rhythmicity, our follow-up experiments suggested an involvement of host metabolism, more specifically, glucose. Since jet lag affected blood parasite load rhythmicity and plasma glucose, our next steps consisted in exploring parasite rhythms' dependency on host glucose, and we have explored this in 2 different experimental ways (timed-restricted feeding and sucrose administration). Both approaches aimed to disturb host glucose rhythms, which have been successfully induced, and investigated if parasite load rhythms would be consequently affected (either with a phase shift, amplitude effects, or lack of rhythmicity). A complete lack of rhythmicity was observed in parasite load following both treatments, confirming that the rhythms are influenced by feeding rhythms and glucose availability. During *P. chabaudi* infections, parasite load rhythmicity (as per the 24-h intra-erythrocytic cycle division and schizogony) has been recently demonstrated to be guided by food intake [179]. In addition, plasma glucose showed to be essential to orchestrate this synchronized division, as diabetic mice had an absent parasite intra-erythrocytic cycle rhythm [180].

Importantly, over the course of the disease, we have not detected any statistically significant changes in the hypoglycemic state of our mice, with respect to their experimental condition (jet lag vs control). Glucose uptake by PbA parasites is a known event during malaria pathogenesis which culminates with hypoglycemia at the later stages of the disease [245]. We have confirmed that plasma glucose levels substantially dropped between day 0 and 7 post-infection, and at a similar rate in all groups.

By performing sucrose administration experiments, we have aimed to rule out confusion factors that are often carried out with timed-restricted feeding, such as an effect on peripheral clocks (e.g. located in the liver, adipose tissue) due to food entrainment [246]. Nevertheless, in our experiments, daily food intake measurements showed to be equivalent between timed-restricted feeding mice and their respective control (data not shown).

In summary, in this project, we have identified, at the cellular level, that the host circadian clock regulates the immune response to PbA iRBC, modulating signaling pathways shaping cells' proteome landscape. Moreover, we have developed a model which could be further used to screen for potential "clock-controlled proteins" to be *in vivo* tested, seeking therapeutical results. At the organismal level, we have identified that host circadian rhythms dictate host response, parasite growth, and rhythmicity in a mouse model of ECM. We have also shown parasite dependency on host circadian rhythms, indicating plasma glucose as one of the regulators of parasite load rhythmicity. Lastly, our findings have shown for the first time that the asynchronized *Plasmodium berghei ANKA* parasite relies on host circadian rhythms for its growth, and it is strongly affected by circadian disruption.

4.2. Working model, future directions and implications

During the course of this project, we have focused on addressing the role of circadian rhythms in host response to malaria, by using *Plasmodium berghei ANKA* in *ex-vivo* immune stimulations and mouse infections. More specifically, we targeted the erythrocytic stage of the disease, given its contributions to malaria pathology [66] and rhythmic host response [210]. Our findings and the proposed mechanisms are summarized in the figure 1 and 2. First, host circadian clocks are known to be entrained by environmental cues, such as light-dark cycles [116] and food intake [247]. They are responsible for ensuring that circadian rhythms (e.g. in immunity, in hematopoietic precursors, blood glucose) are generated and sustained. In the case of plasma glucose, the rhythmicity is not only circadian clock driven, but is also acutely induced by food consumption, its timing and insulin production [248, 249].

In this project, by studying the blood stage of the malaria disease (after parasites evasion of hepatocytes with consequent invasion of erythrocytes), we have identified that the encounter of these 3 rhythmic factors with *P. berghei ANKA*-infected red blood cells determined the level of host response (immune response) and the efficiency of the infection (determined by red blood cells invasion, parasite growth and rhythmicity), under homeostatic conditions (12:12 LD cycle and *ad libitum* food) (figure 1). When host circadian rhythms are desynchronized (figure 2), achieved by irregular lighting conditions or by timed-restricted feeding or sucrose administration, by using the same *P. berghei ANKA*-infected red blood cells infection model, we have observed impairments in parasite growth and rhythmicity, with association with disrupted rhythms in plasma glucose. Although we have not tested whether circadian rhythm desynchronization affected host rhythmic immune response, and time variations in red blood cells abundance (illustrated by dashed arrows and question marks in the figure 2), we speculate that both parameters are affected upon circadian

disruption given the rhythmic profile during homeostatic conditions, suggesting a circadian control involved. Therefore, a few opened questions remain.

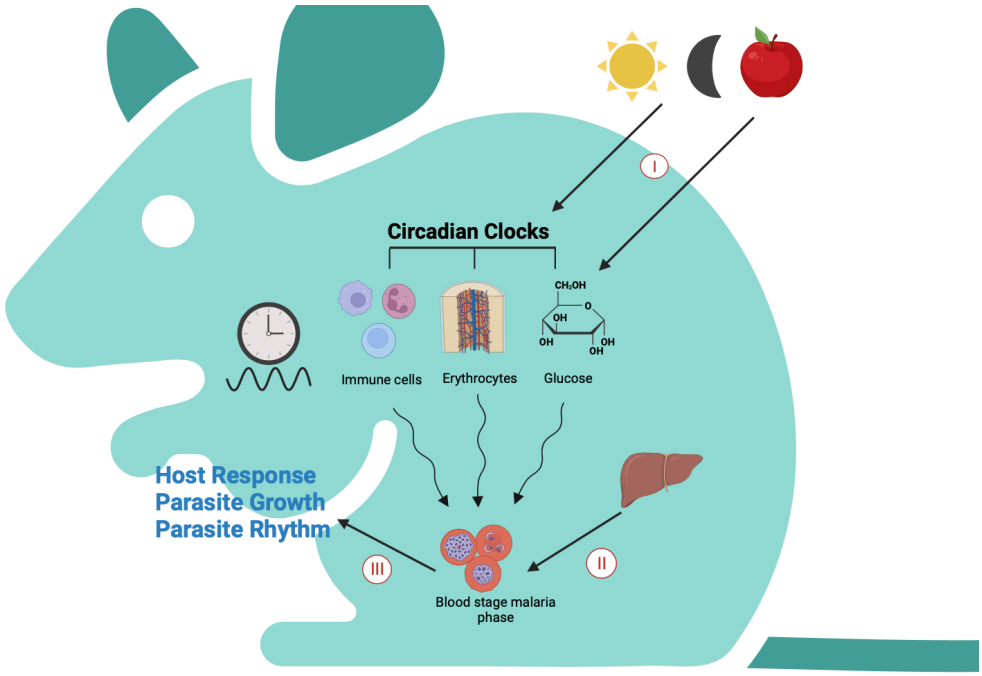

Figure 1. Working model under homeostatic conditions.

I. Host circadian clocks are entrained by light-dark cycles and feeding behavior. They are responsible for the control of rhythms in immunity, plasma glucose levels and time variations in erythrocytes abundance.

II. First, at the erythrocytic stage of the malaria disease (after parasite release from hepatocytes), the efficiency of parasite invasion of erythrocytes is dependent on time variations on erythrocyte abundance. Second, the intensity of the immune response is determined by the rhythmic encounter of immune cells and iRBCs. Finally, parasite

growth and rhythmicity are dependent on glucose availability, in a time-dependent manner.

III. The interaction of host rhythmic factors with PbA parasites at the level of the erythrocytic stage of the disease affects host response, parasite growth and parasite rhythms.

(Created with BioRender.com)

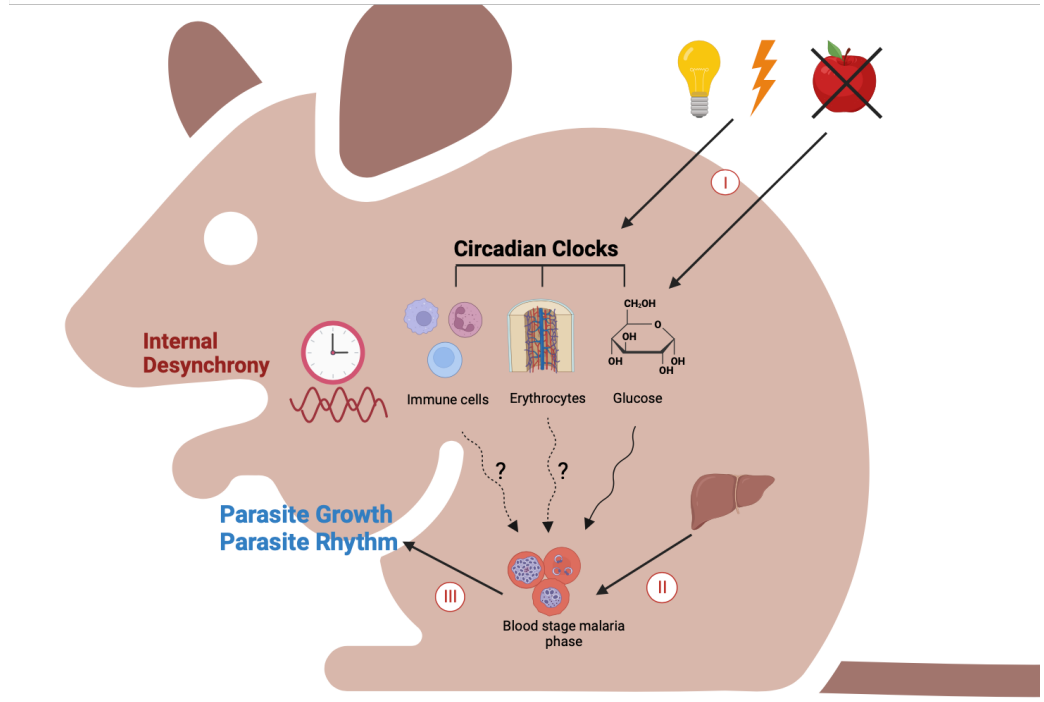

Figure 2. Working model under circadian disruption conditions.

I. Host circadian clocks are affected by irregular light-dark cycles and time-restricted feeding, leading to internal desynchronization of circadian clocks.

II. First, at the erythrocytic stage of the malaria disease (after parasite release from hepatocytes), parasite growth and rhythmicity are affected in the presence of altered glucose. It remains unknown whether the efficiency of parasite invasion of erythrocytes is

affected by internal desynchrony, as well the rhythmic encounter of immune cells and iRBCs.

III. The desynchronization of host rhythmic factors at the level of the erythrocytic stage of the disease affects parasite growth and parasite rhythms.

(Created with BioRender.com)

First question is whether circadian disruption affect the rhythmic response of innate cells upon *P. berghei ANKA*-infected red blood cells encounter? To tackle this question, peritoneal macrophages, for instance, extracted from circadian disrupted mice and stimulated *ex-vivo* with PbA iRBCs could be used. For that, stimulations at 4 different time points, in parallel with non-circadian disrupted extracted macrophages (control group), would allow us to verify if the rhythms in immune response are being affected by circadian disruption, potentially impacting the macrophages-iRBC response? We have reasons to believe that during our chronic circadian disruption model, the rhythms in innate cells-iRBC response are being affected, supported by other studies in the field. For instance, a recent study has subjected mice to a long-term circadian disruption protocol (8 h phase advance every 4 days for a total of 85 weeks) and detected an increase in the myeloid population in the blood and spleen, when compared to control LD mice [155]. Additionally, peritoneal exudate cells collected from chronic circadian disrupted mice (protocol with 6 h phase advance shifts every week for a total of 4 weeks) and subjected to LPS stimulation, led to an enhanced response when compared to cells collected from a non-circadian disrupted mice [153]. Moreover, *in vivo* injection of LPS in circadian disrupted mice led to increased values of IL-1β, IL-12, GM-CSF and IL-13 in the blood, when compared to non-circadian disrupted mice [153]. Similarly, Kupfer cells extracted from rats after circadian

disruption protocol produced significantly more TNFα in response to LPS, when compared to control rats (non-circadian disrupted) [250]. Since we have detected circadian control of BMDM response to iRBC, including IL-1β secretion, we would speculate that the levels of pro-inflammatory cytokines, upon iRBC stimulation, would be elevated in circadian disrupted macrophages when compared to non-circadian disrupted cells. As per the effects on macrophage rhythms, Castanon-Cervantes O et al. study showed effects of circadian disruption in the rhythms of clock genes (*Bmal1* and *Per2*) in peritoneal macrophages. Given clock protein control of several pro-inflammatory genes [135, 137, 142], it is possible that the rhythms in immune response detected in our model would be altered upon circadian disruption and stimulation using PbA iRBC.

A second question is, are the time variations in erythrocytes abundance observed, a true circadian rhythm? Are they being affected by circadian disruption? For a rhythm to be considered "circadian" it must persist under constant conditions (i.e. constant darkness: DD) with an endogenous period length of approximately 24 h [251]. Since our *in vivo* experiments were performed under 12:12 LD cycle, it remains to be tested if the time variations in the frequency of reticulocytes are not being influenced by light. In other words, verify if the phenotype is kept if experiments are performed under DD. Furthermore, since we have measured the levels of erythrocytes and their subsets at 2 different time points over 24 h, we cannot conclude that a rhythm in the frequency of cells is present, but rather a time variation phenotype. Interestingly, a 24-h rhythm in red blood cells counts have been reported in different species. For instance, a study with horses detected a robust rhythm with a peak at the day-night transition [252]. Similarly, in rats, the mean red blood cell count showed a 24-h rhythm with a peak during the dark phase [93].

Although most of the literature on the topic has been focusing on elucidating the rhythms in white blood cells, given their rhythmic immune properties and their role in diseases,

understanding the rhythmic control of red blood cells must be equally supported. For instance, not only this is relevant to malaria, where parasites target red blood cells and fluctuations in their abundance can contribute to the development of the disease, but for other haematological disorders, such as acute and chronic anemias. For instance, in our study, we have detected reduced frequency of early reticulocytes in the blood when animals were sampled at ZT19 time point compared to ZT7, irrespective of them being infected or not (control). As studies have shown that erythropoiesis under homeostatic conditions (healthy animals, not infected) happens at the level of the bone marrow and not much at the spleen site, whereas in scenarios under "stress erythropoiesis" (e.g. inflammation, infection, chronic hemolytic anemia) [253, 254] extra-medullary niches become the site of erythrocyte production (i.e. liver and spleen), it is possible that erythropoiesis is not the factor controlling the time variations detected. The reason behind this speculation lies on the complexity of the mechanisms governing the transition from bone-marrow to extra-medullary niches erythrocytes production. During inflammation, HSCs hematopoeisis at the level of the bone marrow, is switched to white cells generation, over erythropoiesis, allowing peripheral organs to take over production. This transition require polarization of M1 macrophages type to M2 at the level of the spleen with activation of erythropoietin (Epo) signaling and proliferation of stress erythroid progenitors [254]. That being said, it is unlikely that 2 distinct mechanisms (bone marrow production in control mice vs splenic production in infected mice) leads to the same time variation pattern (that is, reduced levels at ZT19 time point). That being said, we hypothesize that other factors, non-erythropoiesis related, are driving the time variations in erythrocytes and their subsets abundance. One possibility is a rhythmic control of erythrophagocytosis, as this is a mechanism that occurs in both homeostatic and infection/inflammatory scenarios, which could potentially explain the "conserved" low level of

erythrocytes at ZT19 time point in both control and infected mice. Splenic macrophages are key cells for sensing aged and damaged erythrocytes and for eliminating them through phagocytosis [221]. Since we have reported in this project that macrophage response to iRBC is under circadian control, and that others in the field have shown that phagocytosis is controlled by the clock [255, 256], we hypothesize that the phenotype observed for erythrocyte time variation is under the control of rhythmic phagocytosis by innate immune cells, in particular splenic macrophages, given their active participation engulfing PbA infected red blood cells during malaria [35]. Moreover, as rhythms in immunity are known to be affected by circadian disruption as discussed earlier, we believe that a lack of time variation in the frequency of erythrocytes and their subsets would be found if this parameter would be measured in our circadian disruption model. Importantly, identifying mechanisms driving the time variation in erythrocytes could help the application of targeted therapies. For instance, to induce the replenishment of the repertoire of red blood cells, the bone marrow site could be targeted to stimulate erythrocyte precursors production at a specific time of the day where it is known that the erythrocyte abundance rhythm is at its "trough". Alternatively, recent studies have shown that Epo is controlled by the circadian clock, proposing a potential target for time-controlled erythropoiesis [222]. However, reports of PbA infection supressing Epo activity [223] discourages a potential role of Epo mediating the time variations observed, otherwise we believe that the phenotype would not been carried out in both control and infected mice. Nevertheless, targeting erythropoiesis could be relevant in hematological disorders, like in the case of the genetic disorder β-talassemia, where supressing the production of erythrocytes is often a therapeutical goal, due to splenomegaly resultant from the active elimination of morphological aberrant erythrocytes [257]. Moreover, under stress conditions, clock-target therapy could be tested to supress rhythm phagocytic activity of erythrocytes,

potentially ameliorating the detrimental effects in hemolytic anemias, which are also commonly found in malaria infections [258].

A final question is, what mechanisms are driving the rhythms in blood parasite load, and how host metabolites, more specifically glucose, modulate this rhythm? Once again, as we have demonstrated a circadian control in macrophage response to iRBC, it is possible that, in our *in vivo* model, host immune responses are rhythmically eliminating iRBC and leading to rhythms in the levels of parasite load (as a result of more or less parasite burden across 24 h). As we know that rhythms in immunity are affected by chronic circadian disruption [187], this would justify why the rhythms in parasite load are abolished in jet lag mice. Interestingly, a circadian disruption study has identified effects on immunity only when mice were subjected to long-term protocols [153]. This could be a potential reason why an effect on parasite load was not observed when we used an acute circadian disruption protocol, only under a chronic exposure. Moreover, we have also seen effects on parasite load when infections were performed with *Rev-erbα*$^{-/-}$ mice, and REV-ERB*α* is known to direct control the expression of several immune genes [187]. This corroborates with a potential role of the immune system controlling parasite load levels. If confirmed that the host circadian immune rhythms are mediating the rhythms in PbA parasite load, this opens a new venue for mouse malaria studies. Most of these studies are conducted with *Plasmodium chabaudi* and they carry the difficult task of separating the rhythmic nature of the infection due to rhythms in the parasite or host circadian rhythms [210, 259].

In addition to that, up to this date, it has not been reported yet an endogenous clock in the asynchronized *P. berghei ANKA,* which makes this species an interesting model to study the isolated effect of host rhythms during malaria infection. In fact, our results support that this model is an adequate choice, as we have also demonstrated parasite load rhythm dependency on host

glucose rhythms. Mechanistically, how does this last piece of finding integrates in our working model? As Hirako IC and et al. has recently shown that *Plasmodium chabaudi* developmental cycle is synchronized by TNFα production and consequent hypoglycemia [180], we hypothesize that disturbing host metabolism (by timed-restricted feeding or sucrose administration) abolishes rhythms in parasite load due to an impairment on immune cell rhythmic response (e.g. macrophages phagocytic activity). Furthermore, reports on time-restricted feeding affecting immune responses and TNFα levels have been published [249, 260]. Interestingly, macrophage rhythmic control of TNFα is known to be regulated by REV-ERBα. To add to that, the role of REV-ERBα in maintaining metabolism is well known, and this clock protein has been appointed as a "functional integrator" of metabolic state and immune responses [261].

Furthermore, an additional future direction would be to verify a potential role of glucocorticoids (e.g. cortisol) controlling macrophages rhythmic response with consequences at the parasite load level. This is supported by studies that shown that the well-known involvement of glucocorticoids in glucose homeostasis [262], together with reports of rhythms in immunity (i.e. CXCL5 levels and neutrophils migration) being abolished in adrenalectomized mice [138].

This way, our findings in this project proposes a link between metabolic rhythms and immunity with repercussions during malaria infection. As several parasites are known to rely on host metabolism, the results of this project are relevant and applicable to future studies in the field. For instance, it is known that *T. gondii* uses host glucose as a source of energy for intracellular replication [263]. Lipids scavenger from the host is another known mechanism used by *T. gondii* [264].

4.3. Final Conclusion

The main objective of this thesis was to investigate the role of circadian rhythms in the host response to malaria. We began by hypothesizing, supported by literature research, that host circadian rhythms influence the magnitude of the response during *Plasmodium spp.* intra-erythrocytic stage of the disease, specifically upon encounter of immune cells with *Plasmodium spp*-infected red blood cells. We confirmed that this is true in a newly developed stimulation model using *Plasmodium berghei ANKA*. We have then opened our investigations to measure host responses *in vivo*, by testing if time of infection dictate the magnitude of host response. We have also measured several parameters associated with disease progression and parasite growth, and we have collected very interesting findings as per parasite rhythmicity and the role of host rhythms.

The implications of this study for the field of malaria, as a classical example of a tropical neglected disease, goes beyond simply bringing the awareness on parasite dependency on host circadian rhythms: it proposes a potential target for therapy and prevention. Since we have shown that parasite growth and the outcome of the infection can be influenced by host rhythmic factors (i.e. immunity, metabolism), our study opens venues for chronotherapy attempts, or for a more in-depth analysis of what mechanisms regulating the phenotype. This can help the understanding on the level of parasite dependency on the host, and how can this be modulated during human malaria. It was surprising to find that circadian disruption impaired parasite growth, challenging the idea of whether internal desynchrony is beneficial for a malaria infected individual. Perhaps at certain degree, an intended desynchronization of targeted cells (after identification of which cells are involved in this regulation) could also be a potential treatment venue.

Furthermore, our findings can lead to future malaria follow up studies, since we were the first ones to identify parasite load rhythms in the PbA model. For instance, a study aiming to

address whether our results are being influenced by the recently discovered rhythms in peroxiredoxin oxidation in red blood cells could be performed [265, 266]. Moreover, electrophysiological rhythms in red blood cells have been recently discovered [267]. Interestingly, the study identified that these rhythms matched the phase of parasitemia rhythms, when used a *P. chabaudi* model [267]. That being said, it remains a possibility to study: 1. Whether red blood cells rhythms are responsible for parasite load rhythmicity and the efficiency of invasion in the PbA model. 2. Whether red blood cells rhythms are regulated or influenced by host rhythms (and the circadian disruption)? 3. Whether this can determine the level of parasite-RBC invasion (single vs multi-infection)?

Lastly, we confirmed the existence of an autonomous circadian clock in macrophages regulating immune responses, as shown by others in the field [140]. We have also contributed to the field by generating a comprehensive database of proteins and phosphoproteins that are under the influence of time and treatment. These data serve as a great ally on future research, for example, on the case of studies focusing on unravelling intracellular networks regulated by the clock and their response upon an immunogenic stimulus.

References

1. Organization, G.W.H., *World malaria report 2022*. 2022.
2. Gazzinelli, R.T., et al., *Innate sensing of malaria parasites.* Nat Rev Immunol, 2014. **14**(11): p. 744-57.
3. Dunst, J., F. Kamena, and K. Matuschewski, *Cytokines and Chemokines in Cerebral Malaria Pathogenesis.* Front Cell Infect Microbiol, 2017. **7**: p. 324.
4. Ghazanfari, N., S.N. Mueller, and W.R. Heath, *Cerebral Malaria in Mouse and Man.* Front Immunol, 2018. **9**: p. 2016.
5. Goodman, A.L., et al., *The utility of Plasmodium berghei as a rodent model for anti-merozoite malaria vaccine assessment.* Sci Rep, 2013. **3**: p. 1706.
6. Scorza, T., et al., *Vaccination with a Plasmodium chabaudi adami multivalent DNA vaccine cross-protects A/J mice against challenge with P. c. adami DK and virulent Plasmodium chabaudi chabaudi AS parasites.* Int J Parasitol, 2008. **38**(7): p. 819-27.
7. Stephens, R., R.L. Culleton, and T.J. Lamb, *The contribution of Plasmodium chabaudi to our understanding of malaria.* Trends Parasitol, 2012. **28**(2): p. 73-82.
8. Franke-Fayard, B., et al., *Sequestration and tissue accumulation of human malaria parasites: can we learn anything from rodent models of malaria?* PLoS Pathog, 2010. **6**(9): p. e1001032.
9. Greenwood, B., *The molecular epidemiology of malaria.* Trop Med Int Health, 2002. **7**(12): p. 1012-21.
10. Phillips, M.A., et al., *Malaria.* Nat Rev Dis Primers, 2017. **3**: p. 17050.
11. Faye, F.B., et al., *Diagnostic criteria and risk factors for Plasmodium ovale malaria.* J Infect Dis, 2002. **186**(5): p. 690-5.

12. Mueller, I., P.A. Zimmerman, and J.C. Reeder, *Plasmodium malariae and Plasmodium ovale--the "bashful" malaria parasites.* Trends Parasitol, 2007. **23**(6): p. 278-83.

13. Antinori, S., et al., *Plasmodium knowlesi: the emerging zoonotic malaria parasite.* Acta Trop, 2013. **125**(2): p. 191-201.

14. Cowman, A.F., et al., *Malaria: Biology and Disease.* Cell, 2016. **167**(3): p. 610-624.

15. Cowman, A.F. and B.S. Crabb, *Invasion of red blood cells by malaria parasites.* Cell, 2006. **124**(4): p. 755-66.

16. Iyer, J., et al., *Invasion of host cells by malaria parasites: a tale of two protein families.* Mol Microbiol, 2007. **65**(2): p. 231-49.

17. McCullough, J., *RBCs as target of the infection.* Hematology Am Soc Hematol Educ Program, 2014. **2014**(1).

18. Kaur, H., R. Sehgal, and S. Rani, *Duffy antigen receptor for chemokines (DARC) and susceptibility to Plasmodium vivax malaria.* Parasitol Int, 2019. **71**: p. 73-75.

19. Shakya, B., et al., *Erythrocyte CD55 mediates the internalization of Plasmodium falciparum parasites.* Elife, 2021. **10**.

20. Leong, Y.W., et al., *Erythrocyte tropism of malarial parasites: The reticulocyte appeal.* Front Microbiol, 2022. **13**: p. 1022828.

21. Willyard, C., *The slow roll-out of the world's first malaria vaccine.* Nature, 2022. **612**(7941): p. S48-S49.

22. Gilson, P.R. and B.S. Crabb, *Morphology and kinetics of the three distinct phases of red blood cell invasion by Plasmodium falciparum merozoites.* Int J Parasitol, 2009. **39**(1): p. 91-6.

23. Counihan, N.A., J.K. Modak, and T.F. de Koning-Ward, *How Malaria Parasites Acquire Nutrients From Their Host.* Front Cell Dev Biol, 2021. **9**: p. 649184.

24. Piro, F., et al., *An Uninvited Seat at the Dinner Table: How Apicomplexan Parasites Scavenge Nutrients from the Host.* Microorganisms, 2021. **9**(12).

25. Martin, R.E. and K. Kirk, *Transport of the essential nutrient isoleucine in human erythrocytes infected with the malaria parasite Plasmodium falciparum.* Blood, 2007. **109**(5): p. 2217-24.

26. Rager, N., et al., *Localization of the Plasmodium falciparum PfNT1 nucleoside transporter to the parasite plasma membrane.* J Biol Chem, 2001. **276**(44): p. 41095-9.

27. Counihan, N.A., et al., *Plasmodium falciparum parasites deploy RhopH2 into the host erythrocyte to obtain nutrients, grow and replicate.* Elife, 2017. **6**.

28. Staines, H.M., et al., *Exploiting the therapeutic potential of Plasmodium falciparum solute transporters.* Trends Parasitol, 2010. **26**(6): p. 284-96.

29. Slavic, K., et al., *Life cycle studies of the hexose transporter of Plasmodium species and genetic validation of their essentiality.* Mol Microbiol, 2010. **75**(6): p. 1402-13.

30. Jiang, X., et al., *Structural Basis for Blocking Sugar Uptake into the Malaria Parasite Plasmodium falciparum.* Cell, 2020. **183**(1): p. 258-268 e12.

31. Joet, T., et al., *Validation of the hexose transporter of Plasmodium falciparum as a novel drug target.* Proc Natl Acad Sci U S A, 2003. **100**(13): p. 7476-9.

32. Mideo, N., et al., *The Cinderella syndrome: why do malaria-infected cells burst at midnight?* Trends Parasitol, 2013. **29**(1): p. 10-6.

33. Joice, R., et al., *Plasmodium falciparum transmission stages accumulate in the human bone marrow.* Sci Transl Med, 2014. **6**(244): p. 244re5.

34. Drugs., I.o.M.U.C.o.t.E.o.A., *The Parasite, the Mosquito, and the Disease*, in *Saving Lives, Buying Time: Economics of Malaria Drugs in an Age of Resistance*, K.J. Arrow, C. Panosian, and H. Gelband, Editors. 2004: Washington (DC).

35. Chua, C.L., et al., *Monocytes and macrophages in malaria: protection or pathology?* Trends Parasitol, 2013. **29**(1): p. 26-34.

36. Karunaweera, N.D., et al., *The paroxysm of Plasmodium vivax malaria.* Trends Parasitol, 2003. **19**(4): p. 188-93.

37. Cox, F.E., *History of human parasitology.* Clin Microbiol Rev, 2002. **15**(4): p. 595-612.

38. Karunaweera, N.D., et al., *Dynamics of fever and serum levels of tumor necrosis factor are closely associated during clinical paroxysms in Plasmodium vivax malaria.* Proc Natl Acad Sci U S A, 1992. **89**(8): p. 3200-3.

39. D. Kwiatkowski, B.M.G., *Why is Malaria Fever Periodic? A Hypothesis.* 1989. **5**(8): p. 264-266.

40. Goncalves, R.M., et al., *Cytokine balance in human malaria: does Plasmodium vivax elicit more inflammatory responses than Plasmodium falciparum?* PLoS One, 2012. **7**(9): p. e44394.

41. Peter Kern, C.J.H., Harald Gallati, Stefan Neifer, Peter Kremsner, Manfred Dietrich and Franz Porzsolt, *Soluble Tumor Necrosis Factor Receptors Correlate with Parasitemia and Disease Severity in Human Malaria.* The Journal of Infectious Diseases, 1992. **166**(4): p. 930-934.

42. Stevenson, M.M. and E.M. Riley, *Innate immunity to malaria.* Nat Rev Immunol, 2004. **4**(3): p. 169-80.

43. Shi, Y.P., et al., *Fcgamma receptor IIa (CD32) polymorphism is associated with protection of infants against high-density Plasmodium falciparum infection. VII. Asembo Bay Cohort Project.* J Infect Dis, 2001. **184**(1): p. 107-11.

44. Ty, M., et al., *Malaria-driven expansion of adaptive-like functional CD56-negative NK cells correlates with clinical immunity to malaria.* Sci Transl Med, 2023. **15**(680): p. eadd9012.

45. Pivkin, I.V., et al., *Biomechanics of red blood cells in human spleen and consequences for physiology and disease.* Proc Natl Acad Sci U S A, 2016. **113**(28): p. 7804-9.

46. Ghosh, D. and J.S. Stumhofer, *The spleen: "epicenter" in malaria infection and immunity.* J Leukoc Biol, 2021. **110**(4): p. 753-769.

47. Urban, B.C., et al., *Fatal Plasmodium falciparum malaria causes specific patterns of splenic architectural disorganization.* Infect Immun, 2005. **73**(4): p. 1986-94.

48. Gupta, P., et al., *Tissue-Resident CD169(+) Macrophages Form a Crucial Front Line against Plasmodium Infection.* Cell Rep, 2016. **16**(6): p. 1749-1761.

49. Borges da Silva, H., et al., *In vivo approaches reveal a key role for DCs in CD4+ T cell activation and parasite clearance during the acute phase of experimental blood-stage malaria.* PLoS Pathog, 2015. **11**(2): p. e1004598.

50. Amigorena, C.T.a.S., *The cell biology of antigen presentation in dendritic cells.* Current Opinion in Immunology, 2001. **13**: p. 45-51.

51. Hirako, I.C., et al., *Splenic differentiation and emergence of CCR5(+)CXCL9(+)CXCL10(+) monocyte-derived dendritic cells in the brain during cerebral malaria.* Nat Commun, 2016. **7**: p. 13277.

52. Jagannathan, P., et al., *IFNgamma/IL-10 co-producing cells dominate the CD4 response to malaria in highly exposed children.* PLoS Pathog, 2014. **10**(1): p. e1003864.

53. Berretta, F., C.A. Piccirillo, and M.M. Stevenson, *Plasmodium chabaudi AS Infection Induces CD4(+) Th1 Cells and Foxp3(+)T-bet(+) Regulatory T Cells That Express CXCR3 and Migrate to CXCR3 Ligands.* Front Immunol, 2019. **10**: p. 425.

54. Oakley, M.S., et al., *The transcription factor T-bet regulates parasitemia and promotes pathogenesis during Plasmodium berghei ANKA murine malaria.* J Immunol, 2013. **191**(9): p. 4699-708.

55. da Silva, H.B., et al., *IFN-gamma-induced priming maintains long-term strain-transcending immunity against blood-stage Plasmodium chabaudi malaria.* J Immunol, 2013. **191**(10): p. 5160-9.

56. Kumar, R., et al., *The regulation of CD4(+) T cells during malaria.* Immunol Rev, 2020. **293**(1): p. 70-87.

57. Goncalves, R.M., et al., *CD4+ CD25+ Foxp3+ regulatory T cells, dendritic cells, and circulating cytokines in uncomplicated malaria: do different parasite species elicit similar host responses?* Infect Immun, 2010. **78**(11): p. 4763-72.

58. Riggle, B.A., et al., *CD8+ T cells target cerebrovasculature in children with cerebral malaria.* J Clin Invest, 2020. **130**(3): p. 1128-1138.

59. Gun, S.Y., et al., *Interferon regulatory factor 1 is essential for pathogenic CD8+ T cell migration and retention in the brain during experimental cerebral malaria.* Cell Microbiol, 2018. **20**(5): p. e12819.

60. Howland, S.W., et al., *Brain microvessel cross-presentation is a hallmark of experimental cerebral malaria.* EMBO Mol Med, 2013. **5**(7): p. 984-99.

61. Imai, T., et al., *CD8(+) T cell activation by murine erythroblasts infected with malaria parasites.* Sci Rep, 2013. **3**: p. 1572.

62. Claser, C., et al., *Lung endothelial cell antigen cross-presentation to CD8(+)T cells drives malaria-associated lung injury.* Nat Commun, 2019. **10**(1): p. 4241.

63. El-Assaad, F., et al., *Cytoadherence of Plasmodium berghei-infected red blood cells to murine brain and lung microvascular endothelial cells in vitro.* Infect Immun, 2013. **81**(11): p. 3984-91.

64. Pais, T.F. and C. Penha-Goncalves, *Brain Endothelium: The "Innate Immunity Response Hypothesis" in Cerebral Malaria Pathogenesis.* Front Immunol, 2018. **9**: p. 3100.

65. Baptista, F.G., et al., *Accumulation of Plasmodium berghei-infected red blood cells in the brain is crucial for the development of cerebral malaria in mice.* Infect Immun, 2010. **78**(9): p. 4033-9.

66. Coban, C., M.S.J. Lee, and K.J. Ishii, *Tissue-specific immunopathology during malaria infection.* Nat Rev Immunol, 2018. **18**(4): p. 266-278.

67. Prada, J., Grau, G.E., Kremsner, P.G., *Ring-stage malaria antigens induce high levels of tumor necrosis factor-independent interleukin 6 secretion in blood cells from patients with severe malaria.* Mitt. Österr. Ges.Tropenmed. Parasitol., 1996. **18**: p. 247 - 252.

68. Prada, J., et al., *Production of Interleukin-6 by Human and Murine Mononuclear Leukocytes Stimulated with Plasmodium Antigens Is Enhanced by Pentoxifylline, and Tumor Necrosis Factor Secretion Is Reduced.* Infection and Immunity, 1993. **61**(6): p. 2737-2740.

69. Jaramillo, M., et al., *Hemozoin increases IFN-gamma-inducible macrophage nitric oxide generation through extracellular signal-regulated kinase- and NF-kappa B-dependent pathways.* J Immunol, 2003. **171**(8): p. 4243-53.

70. Khadjavi, A., et al., *Involvement of p38 MAPK in haemozoin-dependent MMP-9 enhancement in human monocytes.* Cell Biochem Funct, 2014. **32**(1): p. 5-15.

71. Parroche, P., et al., *Malaria hemozoin is immunologically inert but radically enhances innate responses by presenting malaria DNA to Toll-like receptor 9.* Proc Natl Acad Sci U S A, 2007. **104**(6): p. 1919-24.

72. Kalantari, P., et al., *Dual engagement of the NLRP3 and AIM2 inflammasomes by plasmodium-derived hemozoin and DNA during malaria.* Cell Rep, 2014. **6**(1): p. 196-210.

73. Jaramillo, M., M. Godbout, and M. Olivier, *Hemozoin induces macrophage chemokine expression through oxidative stress-dependent and -independent mechanisms.* J Immunol, 2005. **174**(1): p. 475-84.

74. Polimeni, M., et al., *Haemozoin induces early cytokine-mediated lysozyme release from human monocytes through p38 MAPK- and NF-kappaB-dependent mechanisms.* PLoS One, 2012. **7**(6): p. e39497.

75. Jaramillo, M., et al., *Hemozoin-inducible proinflammatory events in vivo: potential role in malaria infection.* J Immunol, 2004. **172**(5): p. 3101-10.

76. Hornung, V., et al., *Silica crystals and aluminum salts activate the NALP3 inflammasome through phagosomal destabilization.* Nat Immunol, 2008. **9**(8): p. 847-56.

77. Shio, M.T., et al., *Malarial hemozoin activates the NLRP3 inflammasome through Lyn and Syk kinases.* PLoS Pathog, 2009. **5**(8): p. e1000559.

78. He, J., et al., *Lysosome is a primary organelle in B cell receptor-mediated apoptosis: an indispensable role of Syk in lysosomal function.* Genes Cells, 2005. **10**(1): p. 23-35.

79. Arese, P. and E. Schwarzer, *Malarial pigment (haemozoin): a very active 'inert' substance.* Ann Trop Med Parasitol, 1997. **91**(5): p. 501-16.

80. Shio, M.T., et al., *PKC/ROS-Mediated NLRP3 Inflammasome Activation Is Attenuated by Leishmania Zinc-Metalloprotease during Infection.* PLoS Negl Trop Dis, 2015. **9**(6): p. e0003868.

81. Olivier, M., et al., *Malarial pigment hemozoin and the innate inflammatory response.* Front Immunol, 2014. **5**: p. 25.

82. Bettiol, E., et al., *Dual effect of Plasmodium-infected erythrocytes on dendritic cell maturation.* Malar J, 2010. **9**: p. 64.

83. Couper, K.N., et al., *Parasite-derived plasma microparticles contribute significantly to malaria infection-induced inflammation through potent macrophage stimulation.* PLoS Pathog, 2010. **6**(1): p. e1000744.

84. Terkawi, M.A., et al., *Involvement of beta-defensin 130 (DEFB130) in the macrophage microbicidal mechanisms for killing Plasmodium falciparum.* Sci Rep, 2017. **7**: p. 41772.

85. Schwarzer, E. and P. Arese, *Phagocytosis of malarial pigment hemozoin inhibits NADPH-oxidase activity in human monocyte-derived macrophages.* Biochim Biophys Acta, 1996. **1316**(3): p. 169-75.

86. Reiner, N.E., *Altered cell signaling and mononuclear phagocyte deactivation during intracellular infection.* Immunol Today, 1994. **15**(8): p. 374-81.

87. Wolf, E.J, et al., *Alterations in Murine Macrophage Arachidonic Acid Metabolism following Ingestion of Nonviable Histoplasma capsulatum.* Infection and Immunity, 1992. **60**(7): p. 2559-2564.

88. Ball, E.A., et al., *IFNAR1 controls progression to cerebral malaria in children and CD8+ T cell brain pathology in Plasmodium berghei-infected mice.* J Immunol, 2013. **190**(10): p. 5118-27.

89. Belnoue, E., et al., *On the pathogenic role of brain-sequestered alphabeta CD8+ T cells in experimental cerebral malaria.* J Immunol, 2002. **169**(11): p. 6369-75.

90. Amante, F.H., et al., *Immune-mediated mechanisms of parasite tissue sequestration during experimental cerebral malaria.* J Immunol, 2010. **185**(6): p. 3632-42.

91. Van den Steen, P.E., et al., *CXCR3 determines strain susceptibility to murine cerebral malaria by mediating T lymphocyte migration toward IFN-gamma-induced chemokines.* Eur J Immunol, 2008. **38**(4): p. 1082-95.

92. Van Den Ham, K.M., et al., *Iron prevents the development of experimental cerebral malaria by attenuating CXCR3-mediated T cell chemotaxis.* PLoS One, 2015. **10**(3): p. e0118451.

93. Latifu A. Sanni, L.F.F.a.J.L., *Mouse Models for Erythrocytic Stage Malaria.* Methods Mol Biol, 2002. **72**(5): p. 57-76.

94. Wu, J., et al., *Strain-specific innate immune signaling pathways determine malaria parasitemia dynamics and host mortality.* Proc Natl Acad Sci U S A, 2014. **111**(4): p. E511-20.

95. Randall, L.M., et al., *Common strategies to prevent and modulate experimental cerebral malaria in mouse strains with different susceptibilities.* Infect Immun, 2008. **76**(7): p. 3312-20.

96. Denny, J.E., et al., *Differential Sensitivity to Plasmodium yoelii Infection in C57BL/6 Mice Impacts Gut-Liver Axis Homeostasis.* Sci Rep, 2019. **9**(1): p. 3472.

97. Hentzschel, F., et al., *Host cell maturation modulates parasite invasion and sexual differentiation in Plasmodium berghei.* Sci Adv, 2022. **8**(17): p. eabm7348.

98. Huang, B.W., E. Pearman, and C.C. Kim, *Mouse Models of Uncomplicated and Fatal Malaria.* Bio Protoc, 2015. **5**(13).

99. Janse, C.J. and A.P. Waters, *Plasmodium berghei: the application of cultivation and purification techniques to molecular studies of malaria parasites.* Parasitol Today, 1995. **11**(4): p. 138-43.

100. Cooke, B.M., et al., *A Maurer's cleft-associated protein is essential for expression of the major malaria virulence antigen on the surface of infected red blood cells.* J Cell Biol, 2006. **172**(6): p. 899-908.

101. Lou, J., R. Lucas, and G.E. Grau, *Pathogenesis of cerebral malaria: recent experimental data and possible applications for humans.* Clin Microbiol Rev, 2001. **14**(4): p. 810-20.

102. Fonager, J., et al., *Reduced CD36-dependent tissue sequestration of Plasmodium-infected erythrocytes is detrimental to malaria parasite growth in vivo.* J Exp Med, 2012. **209**(1): p. 93-107.

103. De Niz, M., et al., *The machinery underlying malaria parasite virulence is conserved between rodent and human malaria parasites.* Nat Commun, 2016. **7**: p. 11659.

104. Possemiers, H., et al., *Experimental malaria-associated acute kidney injury is independent of parasite sequestration and resolves upon antimalarial treatment.* Front Cell Infect Microbiol, 2022. **12**: p. 915792.

105. Pongponratn, E., et al., *An ultrastructural study of the brain in fatal Plasmodium falciparum malaria.* Am J Trop Med Hyg, 2003. **69**(4): p. 345-59.

106. Blandine Franke-Fayard, C.J.J., Margarida Cunha-Rodrigues, *Murine malaria parasite sequestration: CD36 is the major receptor, but cerebral pathology is unlinked to sequestration.* PNAS, 2005. **102**(32): p. 11468-11473.

107. White, N.J., et al., *The murine cerebral malaria phenomenon.* Trends Parasitol, 2010. **26**(1): p. 11-5.

108. Royo, J., et al., *Changes in monocyte subsets are associated with clinical outcomes in severe malarial anaemia and cerebral malaria.* Sci Rep, 2019. **9**(1): p. 17545.

109. Jud, C., et al., *A guideline for analyzing circadian wheel-running behavior in rodents under different lighting conditions.* Biol Proced Online, 2005. **7**: p. 101-16.

110. Mohawk, J.A., C.B. Green, and J.S. Takahashi, *Central and peripheral circadian clocks in mammals.* Annu Rev Neurosci, 2012. **35**: p. 445-62.

111. Hergenhan, S., S. Holtkamp, and C. Scheiermann, *Molecular Interactions Between Components of the Circadian Clock and the Immune System.* J Mol Biol, 2020. **432**(12): p. 3700-3713.

112. Vitaterna, M.H., et al., *Mutagenesis and mapping of a mouse gene, Clock, essential for circadian behavior.* Science, 1994. **264**(5159): p. 719-25.

113. Konopka, R.J. and S. Benzer, *Clock mutants of Drosophila melanogaster.* Proc Natl Acad Sci U S A, 1971. **68**(9): p. 2112-6.

114. Engelmann, C.H.a.W., *Evidences for Circadian Rhythmicity in the per° Mutant of Drosophila melanogaster.* Z. Naturforsch, 1987. **42**: p. 1335-1338.

115. Masahiro Ishiura, S.K., *Expression of a Gene Cluster kaiABC as a Circadian Feedback Process in Cyanobacteria.* Science, 1998. **281**: p. 1519-1523.

116. Ashton, A., R.G. Foster, and A. Jagannath, *Photic Entrainment of the Circadian System.* Int J Mol Sci, 2022. **23**(2).

117. Richards, J. and M.L. Gumz, *Advances in understanding the peripheral circadian clocks.* FASEB J, 2012. **26**(9): p. 3602-13.

118. Lowrey, P.L. and J.S. Takahashi, *Mammalian circadian biology: elucidating genome-wide levels of temporal organization.* Annu Rev Genomics Hum Genet, 2004. **5**: p. 407-41.

119. Kornmann, B., et al., *System-driven and oscillator-dependent circadian transcription in mice with a conditionally active liver clock.* PLoS Biol, 2007. **5**(2): p. e34.

120. Welsh, D.K., J.S. Takahashi, and S.A. Kay, *Suprachiasmatic nucleus: cell autonomy and network properties.* Annu Rev Physiol, 2010. **72**: p. 551-77.

121. Takahashi, J.S., *Transcriptional architecture of the mammalian circadian clock.* Nat Rev Genet, 2017. **18**(3): p. 164-179.

122. Mavroudis, P.D. and W.J. Jusko, *Mathematical modeling of mammalian circadian clocks affecting drug and disease responses.* J Pharmacokinet Pharmacodyn, 2021. **48**(3): p. 375-386.

123. Bozek, K., et al., *Regulation of clock-controlled genes in mammals.* PLoS One, 2009. **4**(3): p. e4882.

124. Vieira, E., et al., *Clock Genes, Inflammation and the Immune System-Implications for Diabetes, Obesity and Neurodegenerative Diseases.* Int J Mol Sci, 2020. **21**(24).

125. Scheiermann, C., et al., *Clocking in to immunity.* Nat Rev Immunol, 2018. **18**(7): p. 423-437.

126. Holtkamp, S.J., et al., *Circadian clocks guide dendritic cells into skin lymphatics.* Nat Immunol, 2021. **22**(11): p. 1375-1381.

127. Scheiermann, C., et al., *Adrenergic nerves govern circadian leukocyte recruitment to tissues.* Immunity, 2012. **37**(2): p. 290-301.

128. Druzd, D., et al., *Lymphocyte Circadian Clocks Control Lymph Node Trafficking and Adaptive Immune Responses.* Immunity, 2017. **46**(1): p. 120-132.

129. Collins, E.J., et al., *Post-transcriptional circadian regulation in macrophages organizes temporally distinct immunometabolic states.* Genome Res, 2021. **31**(2): p. 171-85.

130. Mendez-Ferrer, S., et al., *Haematopoietic stem cell release is regulated by circadian oscillations.* Nature, 2008. **452**(7186): p. 442-7.

131. Lucas, D., et al., *Mobilized hematopoietic stem cell yield depends on species-specific circadian timing.* Cell Stem Cell, 2008. **3**(4): p. 364-6.

132. Nguyen, K.D., et al., *Circadian gene Bmal1 regulates diurnal oscillations of Ly6C(hi) inflammatory monocytes.* Science, 2013. **341**(6153): p. 1483-8.

133. Halberg, F., et al., *Susceptibility rhythm to E. coli endotoxin and bioassay.* Proc Soc Exp Biol Med, 1960. **103**: p. 142-4.

134. Curtis, A.M., et al., *Circadian control of innate immunity in macrophages by miR-155 targeting Bmal1.* Proc Natl Acad Sci U S A, 2015. **112**(23): p. 7231-6.

135. Spengler, M.L., et al., *Core circadian protein CLOCK is a positive regulator of NF-kappaB-mediated transcription.* Proc Natl Acad Sci U S A, 2012. **109**(37): p. E2457-65.

136. Marpegan, L., et al., *Diurnal variation in endotoxin-induced mortality in mice: correlation with proinflammatory factors.* Chronobiol Int, 2009. **26**(7): p. 1430-42.

137. Gibbs, J.E., et al., *The nuclear receptor REV-ERBalpha mediates circadian regulation of innate immunity through selective regulation of inflammatory cytokines.* Proc Natl Acad Sci U S A, 2012. **109**(2): p. 582-7.

138. Gibbs, J., et al., *An epithelial circadian clock controls pulmonary inflammation and glucocorticoid action.* Nat Med, 2014. **20**(8): p. 919-26.

139. Cox, S.L., et al., *Circadian disruption in lung fibroblasts enhances NF-kappaB activity to exacerbate neutrophil recruitment.* FASEB J, 2023. **37**(2): p. e22753.

140. Keller, M., et al., *A circadian clock in macrophages controls inflammatory immune responses.* Proc Natl Acad Sci U S A, 2009. **106**(50): p. 21407-12.

141. Bellet, M.M., et al., *Circadian clock regulates the host response to Salmonella.* Proc Natl Acad Sci U S A, 2013. **110**(24): p. 9897-902.

142. Pourcet, B., et al., *Nuclear Receptor Subfamily 1 Group D Member 1 Regulates Circadian Activity of NLRP3 Inflammasome to Reduce the Severity of Fulminant Hepatitis in Mice.* Gastroenterology, 2018. **154**(5): p. 1449-1464 e20.

143. Oishi, Y., et al., *Bmal1 regulates inflammatory responses in macrophages by modulating enhancer RNA transcription.* Sci Rep, 2017. **7**(1): p. 7086.

144. Early, J.O., et al., *Circadian clock protein BMAL1 regulates IL-1beta in macrophages via NRF2.* Proc Natl Acad Sci U S A, 2018. **115**(36): p. E8460-E8468.

145. Evans, J.A. and A.J. Davidson, *Health consequences of circadian disruption in humans and animal models.* Prog Mol Biol Transl Sci, 2013. **119**: p. 283-323.

146. *Night work, 2022*. 2023, Statistics Canada.

147. Wong, I.S., C.B. McLeod, and P.A. Demers, *Shift work trends and risk of work injury among Canadian workers.* Scand J Work Environ Health, 2011. **37**(1): p. 54-61.

148. Sletten, T.L., et al., *Health consequences of circadian disruption.* Sleep, 2020. **43**(1).

149. Atwater, A.Q., et al., *Shift Work Predicts Increases in Lipopolysaccharide-Binding Protein, Interleukin-10, and Leukocyte Counts in a Cross-Sectional Study of Healthy Volunteers Carrying Low-Grade Systemic Inflammation.* Int J Environ Res Public Health, 2021. **18**(24).

150. Cuesta, M., et al., *Simulated Night Shift Disrupts Circadian Rhythms of Immune Functions in Humans.* J Immunol, 2016. **196**(6): p. 2466-75.

151. Cho, K., *Chronic 'jet lag' produces temporal lobe atrophy and spatial cognitive deficits.* Nature, 2001. **4**(6): p. 567-568.

152. Davidson, A.J., et al., *Chronic jet-lag increases mortality in aged mice.* Curr Biol, 2006. **16**(21): p. R914-6.

153. Castanon-Cervantes, O., et al., *Dysregulation of inflammatory responses by chronic circadian disruption.* J Immunol, 2010. **185**(10): p. 5796-805.

154. Hill, A.M., et al., *Environmental circadian disruption suppresses rhythms in kidney function and accelerates excretion of renal injury markers in urine of male hypertensive rats.* Am J Physiol Renal Physiol, 2021. **320**(2): p. F224-F233.

155. Inokawa, H., et al., *Chronic circadian misalignment accelerates immune senescence and abbreviates lifespan in mice.* Sci Rep, 2020. **10**(1): p. 2569.

156. Papagiannakopoulos, T., et al., *Circadian Rhythm Disruption Promotes Lung Tumorigenesis.* Cell Metab, 2016. **24**(2): p. 324-31.

157. Casiraghi, L.P., et al., *Forced desynchronization of activity rhythms in a model of chronic jet lag in mice.* J Biol Rhythms, 2012. **27**(1): p. 59-69.

158. Elisabeth Filipski, F.D., Verdun M. King,, *Effects of Chronic Jet Lag on Tumor Progression in Mice.* Cancer Research, 2004. **64**: p. 7879-7885.

159. Kettner, N.M., et al., *Circadian Dysfunction Induces Leptin Resistance in Mice.* Cell Metab, 2015. **22**(3): p. 448-59.

160. Wang, S., et al., *REV-ERBalpha integrates colon clock with experimental colitis through regulation of NF-kappaB/NLRP3 axis.* Nat Commun, 2018. **9**(1): p. 4246.

161. Adams, K.L., et al., *Environmental circadian disruption elevates the IL-6 response to lipopolysaccharide in blood.* J Biol Rhythms, 2013. **28**(4): p. 272-7.

162. Lucassen, E.A., et al., *Environmental 24-hr Cycles Are Essential for Health.* Curr Biol, 2016. **26**(14): p. 1843-53.

163. Carvalho Cabral, P., et al., *The involvement of host circadian clocks in the regulation of the immune response to parasitic infections in mammals.* Parasite Immunol, 2022. **44**(3): p. e12903.

164. Hopwood, T.W., et al., *The circadian regulator BMAL1 programmes responses to parasitic worm infection via a dendritic cell clock.* Sci Rep, 2018. **8**(1): p. 3782.

165. Kiessling, S., et al., *The circadian clock in immune cells controls the magnitude of Leishmania parasite infection.* Sci Rep, 2017. **7**(1): p. 10892.

166. Carvalho Cabral, P., M. Olivier, and N. Cermakian, *The Complex Interplay of Parasites, Their Hosts, and Circadian Clocks.* Front Cell Infect Microbiol, 2019. **9**: p. 425.

167. Lauren M. Smith, M.F., *An intrinsic oscillator drives the blood stage cycle of the malaria parasite Plasmodium falciparum.* Science, 2020. **368**: p. 754-759.

168. Subudhi, A.K., et al., *Malaria parasites regulate intra-erythrocytic development duration via serpentine receptor 10 to coordinate with host rhythms.* Nat Commun, 2020. **11**(1): p. 2763.

169. Rijo-Ferreira, F., Acosta-Rodriguez VA, *Malaria has an intrinsic clock.* Science, 2020. **368**: p. 746-753.

170. Rijo-Ferreira, F., et al., *Trypanosoma brucei metabolism is under circadian control.* Nat Microbiol, 2017. **2**: p. 17032.

171. Rawlinson, K.A., et al., *Daily rhythms in gene expression of the human parasite Schistosoma mansoni.* BMC Biol, 2021. **19**(1): p. 255.

172. Hawking, F., *The 24-hour periodicity of microfilariae: biological mechanisms responsible for its production and control.* Proceedings of the Royal Society of London. Series B. Biological Sciences, 1997. **169**(1014): p. 59-76.

173. Otranto, D., et al., *Cutaneous distribution and circadian rhythm of Onchocerca lupi microfilariae in dogs.* PLoS Negl Trop Dis, 2013. **7**(12): p. e2585.

174. Rund, S.S., et al., *Daily Rhythms in Mosquitoes and Their Consequences for Malaria Transmission.* Insects, 2016. **7**(2).

175. Schneider, P., et al., *Adaptive periodicity in the infectivity of malaria gametocytes to mosquitoes.* Proc Biol Sci, 2018. **285**(1888).

176. Hawking, F. and K. Gammage, *The periodic migration of microfilariae of Brugia malayi and its response to various stimuli.* Am J Trop Med Hyg, 1968. **17**(5): p. 724-9.

177. Carlos T Hotta, M.L.G., *Calcium-dependent modulation by melatonin of the circadian rhythm in malarial parasites.* Nature Cell Biology, 2000. **2**: p. 466-468.

178. Korf, H.W. and C. von Gall, *Mice, melatonin and the circadian system.* Mol Cell Endocrinol, 2006. **252**(1-2): p. 57-68.

179. Prior, K.F., et al., *Timing of host feeding drives rhythms in parasite replication.* PLoS Pathog, 2018. **14**(2): p. e1006900.

180. Hirako, I.C., et al., *Daily Rhythms of TNFalpha Expression and Food Intake Regulate Synchrony of Plasmodium Stages with the Host Circadian Cycle.* Cell Host Microbe, 2018. **23**(6): p. 796-808 e6.

181. O'Donnell, A.J., M.A. Greischar, and S.E. Reece, *Mistimed malaria parasites re-synchronize with host feeding-fasting rhythms by shortening the duration of intra-erythrocytic development.* Parasite Immunol, 2022. **44**(3): p. e12898.

182. O'Donnell, A.J., et al., *Fitness costs of disrupting circadian rhythms in malaria parasites.* Proc Biol Sci, 2011. **278**(1717): p. 2429-36.

183. Mons B, J.C., *Synchronized erythrocytic schizogony and gametocytogenesis of Plasmodium berghei in vivo and in vitro.* Parasitology, 1985. **91**: p. 423-430.

184. John D Arnold, F.L., *Augmentation of growth and division synchrony and of vascular sequestration of Plasmodium berghei by the photoperiodic rhythm.* The Journal of Parasitology, 1969. **55**(3): p. 597-608.

185. O'Donnell, A.J. and S.E. Reece, *Ecology of asynchronous asexual replication: the intraerythrocytic development cycle of Plasmodium berghei is resistant to host rhythms.* Malar J, 2021. **20**(1): p. 105.

186. Collins, W.E. and G.M. Jeffery, *Plasmodium malariae: parasite and disease.* Clin Microbiol Rev, 2007. **20**(4): p. 579-92.

187. Carter, S.J., et al., *A matter of time: study of circadian clocks and their role in inflammation.* J Leukoc Biol, 2016. **99**(4): p. 549-60.

188. Nobis, C.C., N. Labrecque, and N. Cermakian, *From immune homeostasis to inflammation, a question of rhythms.* Current Opinion in Physiology, 2018. **5**: p. 90-98.

189. Cermakian, N. and N. Labrecque, *Regulation of Cytotoxic CD8+ T Cells by the Circadian Clock.* J Immunol, 2023. **210**(1): p. 12-18.

190. Arjona, A. and D.K. Sarkar, *Circadian oscillations of clock genes, cytolytic factors, and cytokines in rat NK cells.* J Immunol, 2005. **174**(12): p. 7618-24.

191. Balsalobre, A., *A Serum Shock Induces Circadian Gene Expression in Mammalian Tissue Culture Cells.* 1998.

192. Soni, R., et al., *Signaling Strategies of Malaria Parasite for Its Survival, Proliferation, and Infection during Erythrocytic Stage.* Front Immunol, 2017. **8**: p. 349.

193. Brown, A.E., P. Teja-Isavadharm, and H.K. Webster, *Macrophage activation in vivax malaria: fever is associated with increased levels of neopterin and interferon-gamma.* Parasite Immunol, 1991. **13**(6): p. 673-9.

194. Wang, H., et al., *Activation of Rap1 inhibits NADPH oxidase-dependent ROS generation in retinal pigment epithelium and reduces choroidal neovascularization.* FASEB J, 2014. **28**(1): p. 265-74.

195. Wang, X.L., et al., *Microglia-specific knock-down of Bmal1 improves memory and protects mice from high fat diet-induced obesity.* Mol Psychiatry, 2021. **26**(11): p. 6336-6349.

196. Shen, Y., et al., *NF-kappaB modifies the mammalian circadian clock through interaction with the core clock protein BMAL1.* PLoS Genet, 2021. **17**(11): p. e1009933.

197. Rankawat, S., et al., *A comprehensive rhythmicity analysis of host proteins and immune factors involved in malaria pathogenesis to decipher the importance of host circadian clock in malaria.* Front Immunol, 2023. **14**: p. 1210299.

198. Goldsmith, C.S. and D. Bell-Pedersen, *Diverse roles for MAPK signaling in circadian clocks.* Adv Genet, 2013. **84**: p. 1-39.

199. Petrzilka, S., et al., *Clock gene modulation by TNF-alpha depends on calcium and p38 MAP kinase signaling.* J Biol Rhythms, 2009. **24**(4): p. 283-94.

200. Alkhoury, C., et al., *Class 3 PI3K coactivates the circadian clock to promote rhythmic de novo purine synthesis.* Nat Cell Biol, 2023. **25**(7): p. 975-988.

201. Beker, M.C., et al., *Interaction of melatonin and Bmal1 in the regulation of PI3K/AKT pathway components and cellular survival.* Sci Rep, 2019. **9**(1): p. 19082.

202. Qualmann, B. and Mellor, H., *Regulation of endocytic traffic by Rho GTPases.* Biochem J, 2003. **371** (Pt 2): p. 233-241.

203. Kitchen, G.B., et al., *The clock gene Bmal1 inhibits macrophage motility, phagocytosis, and impairs defense against pneumonia.* Proc Natl Acad Sci U S A, 2020. **117**(3): p. 1543-1551.

204. Geiger, S.S., Fagundes, C.T., and Siegel, R.M., *Chrono-immunology: progress and challenges in understanding links between the circadian and immune systems.* Immunology, 2015. **146**(3): p. 349-58.

205. Zhuang, X., et al., *The circadian clock components BMAL1 and REV-ERBalpha regulate flavivirus replication.* Nat Commun, 2019. **10**(1): p. 377.

206. Hawking, F., *The clock of the malaria parasite.* Sci Am, 1970. **222**(6): p. 123-31.

207. Neva, F.A., et al., *Relationship of serum complement levels to events of the malarial paroxysm.* J Clin Invest, 1974. **54**(2): p. 451-60.

208. Pigeault, R., et al., *Timing malaria transmission with mosquito fluctuations.* Evol Lett, 2018. **2**(4): p. 378-389.

209. O'Donnell, A.J., N. Mideo, and S.E. Reece, *Disrupting rhythms in Plasmodium chabaudi: costs accrue quickly and independently of how infections are initiated.* Malar J, 2013. **12**: p. 372.

210. Prior, K.F., et al., *Periodic Parasites and Daily Host Rhythms.* Cell Host Microbe, 2020. **27**(2): p. 176-187.

211. Carroll, R.W., et al., *A rapid murine coma and behavior scale for quantitative assessment of murine cerebral malaria.* PLoS One, 2010. **5**(10).

212. Dobbs, K.R., J.N. Crabtree, and A.E. Dent, *Innate immunity to malaria-The role of monocytes.* Immunol Rev, 2020. **293**(1): p. 8-24.

213. Shio, M.T., et al., *Innate inflammatory response to the malarial pigment hemozoin.* Microbes Infect, 2010. **12**(12-13): p. 889-99.

214. Golan, K., et al., *Daily Onset of Light and Darkness Differentially Controls Hematopoietic Stem Cell Differentiation and Maintenance.* Cell Stem Cell, 2018. **23**(4): p. 572-585 e7.

215. Chotivanich, K., et al., *Parasite multiplication potential and the severity of Falciparum malaria.* J Infect Dis, 2000. **181**(3): p. 1206-9.

216. Ounjaijean, S., Chachiyo, S., and Somsak, V., *Hypoglycemia induced by Plasmodium berghei infection is prevented by treatment with Tinospora crispa stem extract.* Parasitol Int, 2019. **68**(1): p. 57-59.

217. Nguyen, K.D., *Circadian Gene Bmal1 Regulates Diurnal Oscillations of Ly6Chi Inflammatory Monocytes.* Science, 2013.

218. Sengupta, A., et al., *Impact of autophagic regulation on splenic red pulp macrophages during cerebral malarial infection.* Parasitol Int, 2019. **71**: p. 18-26.

219. Silver, A.C., et al., *The circadian clock controls toll-like receptor 9-mediated innate and adaptive immunity.* Immunity, 2012. **36**(2): p. 251-61.

220. Hentzschel, F. and F. Frischknecht, *Still enigmatic: Plasmodium oocysts 125 years after their discovery.* Trends Parasitol, 2022. **38**(8): p. 610-613.

221. Sengupta, S., et al., *Circadian control of lung inflammation in influenza infection.* Nat Commun, 2019. **10**(1): p. 4107.

222. Sciesielski, L.K., et al., *The circadian clock regulates rhythmic erythropoietin expression in the murine kidney.* Kidney Int, 2021. **100**(5): p. 1071-1080.

223. Thawani, N., et al., *Plasmodium products contribute to severe malarial anemia by inhibiting erythropoietin-induced proliferation of erythroid precursors.* J Infect Dis, 2014. **209**(1): p. 140-9.

224. Orban, A., et al., *Efficient monitoring of the blood-stage infection in a malaria rodent model by the rotating-crystal magneto-optical method.* Sci Rep, 2016. **6**: p. 23218.

225. Khoury, D.S., et al., *Host-mediated impairment of parasite maturation during blood-stage Plasmodium infection.* Proc Natl Acad Sci U S A, 2017. **114**(29): p. 7701-7706.

226. Gordon, E.B., et al., *Targeting glutamine metabolism rescues mice from late-stage cerebral malaria.* Proc Natl Acad Sci U S A, 2015. **112**(42): p. 13075-80.

227. Ke, H., et al., *Genetic investigation of tricarboxylic acid metabolism during the Plasmodium falciparum life cycle.* Cell Rep, 2015. **11**(1): p. 164-74.

228. la Fleur, S.E., et al., *A daily rhythm in glucose tolerance: a role for the suprachiasmatic nucleus.* Diabetes, 2001. **50**(6): p. 1237-43.

229. Bowe, J.E., et al., *Metabolic phenotyping guidelines: assessing glucose homeostasis in rodent models.* J Endocrinol, 2014. **222**(3): p. G13-25.

230. Jensen, T.L., et al., *Fasting of mice: a review.* Lab Anim, 2013. **47**(4): p. 225-40.

231. Reece, S.E. and K.F. Prior, *Malaria Makes the Most of Mealtimes.* Cell Host Microbe, 2018. **23**(6): p. 695-697.

232. Van Den Ham, K.M., et al., *Protein Tyrosine Phosphatase Inhibition Prevents Experimental Cerebral Malaria by Precluding CXCR3 Expression on T Cells.* Sci Rep, 2017. **7**(1): p. 5478.

233. Epiphanio, S., et al., *VEGF promotes malaria-associated acute lung injury in mice.* PLoS Pathog, 2010. **6**(5): p. e1000916.

234. Strangward, P., et al., *Targeting the IL33-NLRP3 axis improves therapy for experimental cerebral malaria.* Proc Natl Acad Sci U S A, 2018. **115**(28): p. 7404-7409.

235. Franke-Fayard, B., et al., *A Plasmodium berghei reference line that constitutively expresses GFP at a high level throughout the complete life cycle.* Mol Biochem Parasitol, 2004. **137**(1): p. 23-33.

236. Somsak, V. et al., *Small-scale in vitro culture and purification of Plasmodium berghei for transfection experiment.* Mol Biochem Parasitol, 2011. **177**(2): p. 156-9.

237. Janse, C.J., J. Ramesar, and A.P. Waters, *High-efficiency transfection and drug selection of genetically transformed blood stages of the rodent malaria parasite Plasmodium berghei.* Nat Protoc, 2006. **1**(1): p. 346-56.

238. Oishi, K., et al., *Clock mutation affects circadian regulation of circulating blood cells.* J Circadian Rhythms, 2006. **4**: p. 13.

239. Brager, A.J., et al., *Sleep loss and the inflammatory response in mice under chronic environmental circadian disruption.* PLoS One, 2013. **8**(5): p. e63752.

240. Bass, J. and J.S. Takahashi, *Circadian integration of metabolism and energetics.* Science, 2010. **330**(6009): p. 1349-54.

241. Dinges, D.F., et al., *Leukocytosis and natural killer cell function parallel neurobehavioral fatigue induced by 64 hours of sleep deprivation.* J Clin Invest, 1994. **93**(5): p. 1930-9.

242. Stoyan Dimitrov, T.L., *Number and Function of Circulating Human Antigen Presenting Cells Regulated by Sleep.* Sleep. **30**(4): p. 401-411.

243. Said, E.A., et al., *Sleep deprivation alters neutrophil functions and levels of Th1-related chemokines and CD4(+) T cells in the blood.* Sleep Breath, 2019. **23**(4): p. 1331-1339.

244. Mentzer, W.C. and S.L. Schrier, *Extrinsic Nonimmune Hemolytic Anemias*, in *Hematology*. 2018. p. 663-672.

245. Paul A. H. Holloway, S.K., *Plasmodium berghei: Lactic Acidosis and Hypoglycaemia in a Rodent Model of Severe Malaria; Effects of Glucose, Quinine and Dichloroacetate.* Experimental Pathology. **72**: p. 123-133.

246. Pickel, L. and H.K. Sung, *Feeding Rhythms and the Circadian Regulation of Metabolism.* Front Nutr, 2020. **7**: p. 39.

247. Challet, E., *The circadian regulation of food intake.* Nat Rev Endocrinol, 2019. **15**(7): p. 393-405.

248. Grant, C.L., et al., *Timing of food intake during simulated night shift impacts glucose metabolism: A controlled study.* Chronobiol Int, 2017. **34**(8): p. 1003-1013.

249. Panda, S., *Circadian physiology of metabolism.* Science, 2016. **354**(6315): p. 1008-1015.

250. Guerrero-Vargas, N.N., et al., *Shift Work in Rats Results in Increased Inflammatory Response after Lipopolysaccharide Administration: A Role for Food Consumption.* J Biol Rhythms, 2015. **30**(4): p. 318-30.

251. Gillette, M.U. and S.M. Abbott, *Biological Timekeeping.* Sleep Med Clin, 2009. **4**(2): p. 99-110.

252. Piccione, G., et al., *Nycthemeral change of some haematological parameters in horses.* Journal of Applied Biomedicine, 2005. **3**(3): p. 123-128.

253. Liu, J., et al., *Quantitative analysis of murine terminal erythroid differentiation in vivo: novel method to study normal and disordered erythropoiesis.* Blood, 2013. **121**(8): p. e43-9.

254. Ruan, B. and R.F. Paulson, *Metabolic regulation of stress erythropoiesis, outstanding questions, and possible paradigms.* Front Physiol, 2022. **13**: p. 1063294.

255. Oliva-Ramirez, J., et al., *Crosstalk between circadian rhythmicity, mitochondrial dynamics and macrophage bactericidal activity.* Immunology, 2014. **143**(3): p. 490-7.

256. Mitsuaki Hayashi, S.S., *Characterization of the Molecular Clock in Mouse Peritoneal Macrophages.* Biol Pharm Bull, 2007. **30**(4): p. 621-626.

257. Origa, R., *beta-Thalassemia.* Genet Med, 2017. **19**(6): p. 609-619.

258. White, N.J., *Anaemia and malaria.* Malar J, 2018. **17**(1): p. 371.

259. Sarah E. Reece, K.F.P.a.N.M., *The Life and Times of Parasites: Rhythms in Strategies for Within-host Survival and Between-host Transmission.* Journal of Biological Rhythms, 2017. **32**(6): p. 516-533.

260. Deota, S., et al., *Diurnal transcriptome landscape of a multi-tissue response to time-restricted feeding in mammals.* Cell Metab, 2023. **35**(1): p. 150-165 e4.

261. Cisse, Y.M., et al., *Time-Restricted Feeding Alters the Innate Immune Response to Bacterial Endotoxin.* J Immunol, 2018. **200**(2): p. 681-687.

262. Granner, D.K., J.C. Wang, and K.R. Yamamoto, *Regulatory Actions of Glucocorticoid Hormones: From Organisms to Mechanisms.* Adv Exp Med Biol, 2015. **872**: p. 3-31.

263. Blume, M., et al., *A Toxoplasma gondii Gluconeogenic Enzyme Contributes to Robust Central Carbon Metabolism and Is Essential for Replication and Virulence.* Cell Host Microbe, 2015. **18**(2): p. 210-20.

264. Charron, A.J. and L.D. Sibley, *Host cells: mobilizable lipid resources for the intracellular parasite Toxoplasma gondii.* J Cell Sci, 2002. **115**(Pt 15): p. 3049-59.

265. O'Neill, J.S., et al., *Circadian rhythms persist without transcription in a eukaryote.* Nature, 2011. **469**(7331): p. 554-8.

266. Ch, R., et al., *Rhythmic glucose metabolism regulates the redox circadian clockwork in human red blood cells.* Nat Commun, 2021. **12**(1): p. 377.

267. Labeed, F.H., et al., *Circadian rhythmicity in murine blood: Electrical effects of malaria infection and anemia.* Front Bioeng Biotechnol, 2022. **10**: p. 994487.

Copyright

ELSEVIER LICENSE
TERMS AND CONDITIONS

May 14, 2023

This Agreement between Ms. Priscilla Cabral ("You") and Elsevier ("Elsevier") consists of your license details and the terms and conditions provided by Elsevier and Copyright Clearance Center.

License Number	5547901178578
License date	May 14, 2023
Licensed Content Publisher	Elsevier
Licensed Content Publication	Microbes and Infection
Licensed Content Title	Innate inflammatory response to the malarial pigment hemozoin
Licensed Content Author	Marina T. Shio,Fikregabrail A. Kassa,Marie-Josée Bellemare,Martin Olivier
Licensed Content Date	Nov 1, 2010
Licensed Content Volume	12
Licensed Content Issue	12-13
Licensed Content Pages	11
Start Page	889